Performance and Design of Space-Time Trellis Codes for Wireless Channels

by

Salam Adel Hassan Zummo

A Thesis Presented to the

FACULTY OF THE COLLEGE OF GRADUATE STUDIES

KING FAHD UNIVERSITY OF PETROLEUM & MINERALS

DHAHRAN, SAUDI ARABIA

In Partial Fulfillment of the
Requirements for the Degree of

MASTER OF SCIENCE

In

ELECTRICAL ENGINEERING

December, 1999

INFORMATION TO USERS

This manuscript has been reproduced from the microfilm master. UMI films the text directly from the original or copy submitted. Thus, some thesis and dissertation copies are in typewriter face, while others may be from any type of computer printer.

The quality of this reproduction is dependent upon the quality of the copy submitted. Broken or indistinct print, colored or poor quality illustrations and photographs, print bleedthrough, substandard margins, and improper alignment can adversely affect reproduction.

In the unlikely event that the author did not send UMI a complete manuscript and there are missing pages, these will be noted. Also, if unauthorized copyright material had to be removed, a note will indicate the deletion.

Oversize materials (e.g., maps, drawings, charts) are reproduced by sectioning the original, beginning at the upper left-hand corner and continuing from left to right in equal sections with small overlaps.

Photographs included in the original manuscript have been reproduced xerographically in this copy. Higher quality 6" x 9" black and white photographic prints are available for any photographs or illustrations appearing in this copy for an additional charge. Contact UMI directly to order.

Bell & Howell Information and Learning
300 North Zeeb Road, Ann Arbor, MI 48106-1346 USA
800-521-0600

Performance and Design of Space-Time Trellis Codes for Wireless Channels

BY

SALAM ADEL HASSAN ZUMMO

A Thesis Presented to the

DEANSHIP OF GRADUATE STUDIES

KING FAHD UNIVERSITY OF PETROLEUM & MINERALS

DHAHRAN, SAUDI ARABIA

In Partial Fulfillment of the
Requirements for the Degree of

MASTER OF SCIENCE

In

ELECTRICAL ENGINEERING

December 1999

KING FAHD UNIVERSITY OF PETROLEUM AND MINERALS
DHAHRAN, SAUDI ARABIA

DEANSHIP OF GRADUATE STUDIES

This thesis, written by **Salam Adel Hassan Zummo** under the direction of his Thesis advisor and approved by his Thesis Committee, has been presented to and accepted by the Dean of Graduate Studies, in partial fulfillment of the requirements for the degree of **MASTER OF SCIENCE IN ELECTRICAL ENGINEERING**

Thesis Committee

Dr. Saud A. Al-Semari, **Chairman**

Dr. Maamar Bettayeb, **Member**

Dr. Mahmoud Dawoud, **Member**

Dr. Maan A. Kousa, **Member**

Dr. Samir Al-Baiyat
Chairman, Department of Electrical Engineering

Dr. Abdallah M. Al-Shehri
Dean, Graduate Studies

عمادة الدراسات العليا
DEANSHIP OF GRADUATE STUDIES

31-01-2000
Date

All praises goes to Allah,

Then,

To my father

and

In memory of my mother

Acknowledgements

First thankfulness and praises are for Allah, the Most Merciful, and Most Compassionate. He blesses me with his ever-enduring mercies.

I acknowledge the support and facilities provided by the Electrical Engineering Department and the Deanship of Graduate Studies at King Fahd University of Petroleum and Minerals.

My great and deep appreciation go to my thesis advisor Dr. Saud Al-Semari for his unlimited help, guidance and time devoted to my thesis completion and research development.

I also remain grateful and thankful to Dr. Maan Kousa for his constructive advices that guided me to the continuation in the research area. Throughout my academic life, he strengthened my skills and understanding of the communication area.

I would like to thank the other thesis committee members Dr. Maamar Bettayeb and Dr. Mahmoud Dawoud for their valuable time and effort devoted in reviewing and correcting my thesis. Their helpful suggestions and comments are also appreciated.

My heartful thanks go to my father for his prayers and encouragement. Also, I wish to thank my brother Hakam for his great help and support throughout my academic life. The unflinching support of my family made difficult tasks achievable, may Allah reward them for their patience.

Contents

List of Figures

THESIS ABSTRACT

Name: Zummo, Salam Adel

Title: Performance and Design of Space-Time Trellis Codes for Wireless Channels

Degree: Master of Science

Major Field: Electrical Engineering

Date of Degree: December, 1999

The very advancing theory of Space-Time (ST) codes has attracted many researchers to study their performance and design criteria. In this thesis, the existing upper bound on the bit error probability of ST codes over rapid fading channels was evaluated. A very tight upper bound is proposed and derived.

This thesis also contributes towards the design of good ST codes for rapid fading channels. Codes based on QPSK and 16-QAM signal constellations are designed using design criteria developed from the performance analysis. Two encoding schemes are used to design ST codes. The first one is based on multiple trellis codes and the second one uses the I-Q encoding scheme. Two decoding algorithms are proposed to decode I-Q ST codes: the optimal and suboptimal decoding algorithms.

The designed codes are tested over correlated fading channels with proper and improper interleaving. They are also compared when the Channel State Information are estimated at the receiver using orthogonal pilot symbol insertion technique.

KING FAHD UNIVERSITY OF PETROLEUM AND MINERALS,

DHAHRAN, SAUDI ARABIA

خلاصة الرسالة

الاسم: سلام عادل حسن زمو

العنوان: أداء وتصميم الترميزات الفراغية الوقتية الشبكية للاتصالات اللاسلكية

التخصص: هندسة كهربائية

التاريخ: ديسمبر ١٩٩٩ م

لقد جذب تطور نظرية الترميزات الفراغية الوقتية (Space-Time Codes) كثيراً من الباحثين لدراسة أدائها وتصميمها. يحسب هذا البحث حداً أعلى (Upper Bound) لاحتمال الخطأ في البتات (BER) اعتماداً على الحد المطور من قبل. كما أنه يطرح ويشتق حداً أعلى أدق من الحد السابق.

يساهم هذا البحث في تصميم ترميزات فراغية وقتية جيدة ومناسبة للقنوات اللاسلكية السريعة التغير. لقد تم تصميم ترميزات تعتمد على إشارات رباعية (QPSK) وسداسية عشر (16-QAM) باستخدام معايير التصميم المستنتجة من تحليل الأداء. ويستخدم هذا البحث طريقتين للترميز. تعتمد أولاهما على الترميزات الشبكية المتعددة (MTCM)، بينما تعتمد الأخرى على الترميز الموازي–العمودي (I-Q). كما يطرح هذا البحث طريقتين لفك الترميزات الفراغية الوقتية الموازية–العمودية (I-Q ST Codes) وهما: المثلى والأقل مثالية.

لقد تم اختبار الترميزات المصممة على القنوات اللاسلكية ذات الذاكرة مع استخدام مخلخلين أحدهما مناسب والآخر غير مناسب. كما تم مقارنة الترميزات في حالة تقدير حالة القناة (Channel State Information) عند المستقبل باستخدام طريقة إدخال إشارات طيارة متعامدة (Orthogonal Pilot Signal Insertion).

درجة الماجستير في العلوم

جامعة الملك فهد للبترول والمعادن

الظهران، المملكة العربية السعودية

ديسمبر ١٩٩٩م / رمضان ١٤٢٠ هـ

CHAPTER 1

INTRODUCTION

1.1 General Overview

Mobile communication is emerging in almost all fields and applications. As technology advances, wireless communication systems are required to provide services such as voice, data transfer and multimedia applications. Since mobility is encountered during a mobile communication session, such systems suffer from the multipath effect and the time-varying channel characteristics. Multipath fading causes the reception of the current signal in addition to other delayed samples of previous signals. This is known as the Inter-symbol-interference (ISI) phenomenon, which causes a significant degradation in the system's performance and an error floor at high signal-to-noise ratio (SNR).

As the transmission rate is increased, the ISI becomes worse and advanced equalization techniques are used at the receiver. Moreover, error correction codes are used to improve the system reliability. The recently proposed Space-Time (ST) Codes in [1,2] provide high transmission rate, error correction coding and diversity gain without the need for complex equalizers.

In this introductory chapter, fading channels are described and their mitigation techniques are then discussed. After that, trellis codes are presented with their performance analysis. Then, ST codes are introduced and their design criteria over quasi-static fading channels are briefly described. An up-to-date literature survey about ST codes is presented. The I-Q trellis encoding scheme is then introduced. The thesis contribution and organization are finally stated.

1.2 Fading Channels

In wireless communications, the channel is usually random and time-variant. Its response changes within a communication session, either rapidly or slowly. Hence, depending on the rate of change, it is considered to be either slow fading (SF), or fast fading (FF) channel.

In order to describe the variation of fading channels in time, the Spaced-time correlation function is used [3]. It gives the correlation of channel gains versus time. The period of time in which the correlation function is almost constant defines the coherence time $(\Delta t)_c$. This is the time over which the channel treats signals invariantly. The frequency representation of this function is called the Scattering function. It indicates how the

spectrum is spread if a pure sine wave is transmitted. The maximum spread in the spectrum is called the Doppler spread f_D.

In FF environments, the channel changes its gain at a rate (f_DT) larger than the symbol transmission rate so that one symbol exhibits different attenuation gains. In SF environments, the channel gain changes in a much slower rate than the symbol rate. The rapidity of the channel variations depends mainly on the speed of movement of the mobile handset. As it increases, the channel changes faster and hence the fade samples become less correlated in time.

Multipath reception results from reflections of the transmitted signal at different reflectors and scatterers. In this case, the signal is received via different paths, each with a different delay. Fading channels can also be classified according to the maximum delay between signals received via different paths (called multipath spread T_m). They can be either frequency-selective (FS) channels, or frequency-nonselective (FNS) (flat) fading channels [3]. Multipath spread can be found from the multipath profile that represents the output of the channel at relative path delay τ. In frequency domain, the spaced-frequency correlation function represents the correlation between channel gains at different frequencies. The maximum frequency, beyond which the channel output is uncorrelated, is called the coherence bandwidth $(\Delta f)_c$. FS Channels treat different frequency components differently whereas FNS channels treat them in the same way.

Fading channels are statistically modeled using different probabilistic methods. Referring to [4], the distribution of the samples of a fading channel is generally modeled by a

Rayleigh distribution. Therefore, the probability density function (pdf) of the channel fade amplitude samples ($|a|$) is:

$$f_a(|a|) = |a|/\sigma^2 \exp(-|a|^2/2\sigma^2), \quad a>0, \tag{1.1}$$

Where $2\sigma^2$ is the average power of the fading samples, and the phase is uniformly distributed on the period $[0,2\pi]$. When a direct path exists at the receiver, the pdf of the channel fade samples is Rician distributed. There are various mitigation techniques to reduce the effects of fading channels as described in the following.

1.3 Fading Mitigation Techniques

To reduce the effect of multipath fading channels, several mitigation techniques are used. Equalization is used to cancel the ISI at the receiver resulting from the multipath phenomenon. It is simply a filter that performs the inverse effect of the channel. In order to know the effect of the channel on the transmitted signal, a training sequence known to the receiver is transmitted. This sequence is used to train the equalizer for the underlying channel so that it can cancel out the channel effects when the data is transmitted. There are various kinds of equalizers: the linear equalizer and the Decision Feedback equalizer (DFE). When channel state information (CSI) is known at the receiver, Maximum Likelihood Sequence Estimation (MLSE) provides the best performance.

When the fade values happen to be very small, the received signal can be affected easily by the noise. To reduce the probability of having the channel at deep fades, the receiver can utilize diversity to get different versions of the transmitted signal. This can be done using either receive diversity or transmit diversity.

The most popular diversity method is space diversity at the receiver [4]. It is implemented by having more than one antenna at the receiver in order to receive uncorrelated versions of the transmitted signal. It is necessary for the received versions at the receiver to be uncorrelated in order to maximize the probability of not having them all at deep fades. Hence, receive antennas should be separated by a minimum distance that depends on the wavelength of the transmitted carrier. Systems with space diversity at the receiver perform better than systems without diversity with the advantage of no bandwidth penalty. In such systems, a combining algorithm should be used at the receiver to combine signals received over different branches. Some of the known combining methods are the equal-gain combining (EGC), maximal-ratio combining (MRC) and selection combining (SC). They vary in terms of performance and implementation complexity [4].

On the other hand, diversity can be provided from the transmitter side. In this case, the transmitter is responsible for providing the receiver by uncorrelated versions of the transmitted signal. This is done by transmitting the same signal more than one time resulting in bandwidth penalty and more transmission power. When space transmit diversity is used, the same signal is transmitted at the same time and frequency over multiple transmit antennas. In this case, no bandwidth expansion is required on the cost of having many transmit antennas. This is proved to perform better than systems using space diversity at the receiver [5].

In frequency diversity, the same signal is transmitted in more than one frequency-division multiplexed (FDM) channels. The same concept can be applied in time domain. In time diversity, the same signal is transmitted over more than one interleaved time-division multiplexed (TDM) channels. Interleaving is required in order to provide time diversity

and convert slow fading channels into independent fading ones, so that the received signals undergo independent fades.

Sending the same signal more than one time can be viewed as a repetition code. A more sophisticated approach is to use error correction codes in conjunction with interleaving at the transmitter and send the resulting signals using one antenna. This provides the receiver with replicas of the original signal in the form of redundancy. Trellis codes can be used to provide the required time diversity from the transmitter side.

1.4 Trellis Codes

The main idea behind developing bandwidth-efficient trellis codes is to transmit at the required symbol rate in addition to providing error correction and time diversity in the case of fading channels. The general block diagram of a trellis-coded system is shown in Figure 1.1. It generally consists of a (k/k+1) convolutional encoder that receives k bits. From the Figure, only k bits are encoded where the rest k_l bit are not encoded and the a total of (k+1+k_l) bits are mapped onto a signal constellation of size $2^{(k+1+kl)}$. The existence of the uncoded bits results in parallel transitions when departing from each state in the encoder, that reduces the Euclidean and Hamming distances between mapped symbols at these transitions. In general, using trellis codes increases the constellation size of the output signal that reduces the Euclidean distance between symbols. [6]

Ungerbeock proposed the set partitioning method to solve this problem [6]. He partitioned the resulting signal constellation into non-overlapping sets of symbols so that the Euclidean distance between symbols in the same set is larger than that of the original

constellation. So, upon leaving one state, not all symbols in the constellation are allowed to appear at the encoder's output. Only symbols from the same set can appear when the encoder leaves or merge in the same state. The set partitioning is performed until the maximum Euclidean distance is reached. For additive white Gaussian noise (AWGN) channels, the pairwise error probability of trellis codes is [6]:

$$P(s_l, \hat{s}_l) = \tfrac{1}{2} \operatorname{erfc}(-d^2_E(s_l, \hat{s}_l) / 4N_o), \qquad (1.2)$$

Where s_l and $\hat{s}_l$ are the correct and erroneous sequences of length l, respectively, i.e: $s_l=(s_1,s_2,...,s_l)$ and $\hat{s}_l=(\hat{s}_1,\hat{s}_2,...,\hat{s}_l)$. The factor $d^2_E(s_l, \hat{s}_l)$ is the free squared Euclidean distance between sequences s_l and $\hat{s}_l$. For AWGN channels, the free squared Euclidean distance is the limiting factor of the performance of the trellis code. As the number of encoder's states is increased, the free squared Euclidean distance between two possible error events increases. There is an upper limit for the number of states for which the free distance increases [6]. This limit depends on the number of branches leaving each state and the encoder's constraint length. Also, as the constellation size increases, set partitioning becomes more difficult and the required free squared Euclidean distance decreases. For AWGN channels, the optimal set partitioning is the one proposed by Ungerboeck [6].

The performance of trellis codes over Rayleigh and Rician fading channels was evaluated in [6]. It is shown that significant improvement can be achieved by interleaving the outputs of the encoder, which randomizes the error distribution by destroying the memory of the channel. For Rayleigh fading channels, the pairwise error probability is upper bounded by:

$$P(s_l, \hat{s}_l) \le \prod_{i \in \eta} 1/(1+|s_i-\hat{s}_i|^2/(4N_o)),$$

$$\le 1/[(1/4N_o)^{l_\eta} d^2_P(l_\eta)] \quad (1.3)$$

Where s_i and $\hat{s}_i$ are the i^{th} symbol in the correct sequence and the error event, respectively. The symbol η denotes the set of all i's for which $s_i \neq \hat{s}_i$. Defining l_η as the length of the error event η, and $d^2_P(l_\eta) = \prod_{i \in \eta} |s_i-\hat{s}_i|^2$ is the squared product distance (SPD) between symbols in the error event, then the Minimum Time Diversity (MTD) is L=min(l_η) and the minimum squared product distance (MSPD) is d^2_P = min($d^2_P(l_\eta)$). The MTD of the trellis code (L) is upper bounded by a value that depends on the number of states in the encoder as follows [6]:

$$L \le \lfloor \nu/k \rfloor + 1, \quad (1.4)$$

where ν is the number of memory elements of the encoder and k is the number of input bits to the encoder.

In general, a trellis code designed to be optimal for AWGN channels may not be optimal for fading channels. Equation (1.3) shows that the code's MTD and MSPD are the main performance criteria. The MTD is defined to be the minimum number of different symbols between all possible error events and the correct path. It is a symbol-wise Hamming distance, which represents the time diversity of the code. It is equivalent to the free distance in the convolutional codes with bits outputs. The MSPD distance is defined to be the product of differences between each symbol in the shortest error event and that in the correct path. The design criterion for fading channels is to maximize L and d^2_P. Maximizing L is equivalent to increasing the diversity offered by the coded system.

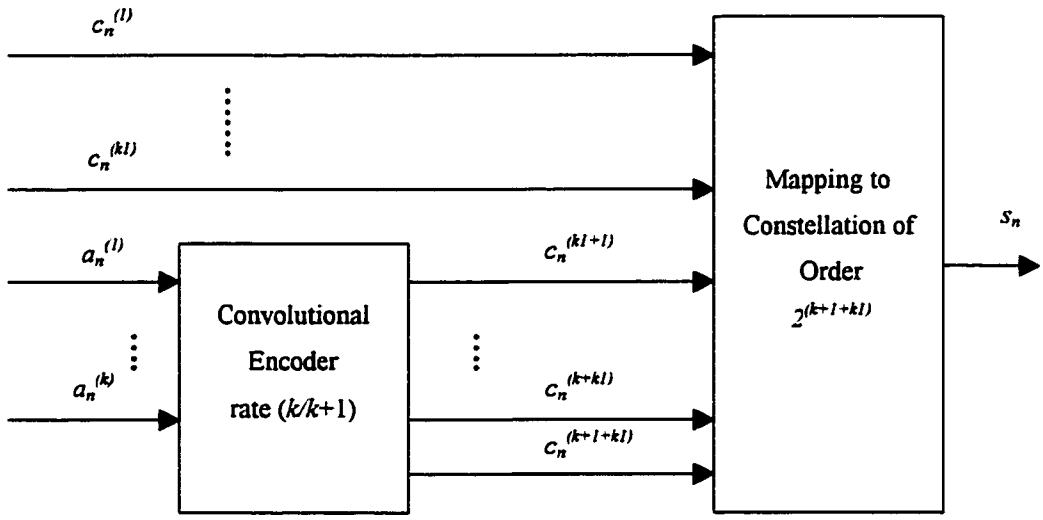

Figure 1.1: General block diagram of Trellis Coded system.

Trellis codes can be combined with space diversity to obtain improved performance. In [7], this idea is implemented and analyzed for the case of MPSK constellation over Rayleigh fading channels. The MRC method is used to combine signals at different receive antennas. In [8], trellis codes with sufficient interleaving depth, combined with space diversity are analyzed and simulated. It is shown that they perform better than systems with more complex codes (without diversity) and systems with higher-order diversity (without coding). Moreover, the performance of coded systems with different combining methods is analyzed in [8]. Tight bounds on the bit error probability are presented.

Simulation results for the 8-state Ungerboeck 8PSK trellis code are plotted in Figure 1.2, for AWGN and independent Rayleigh channel. For the Rayleigh channel case, the CSI is assumed to be known at the receiver. From the Figure, it is clear that the system's performance over AWGN is much better than that over fading channels.

The idea of combining space diversity and time diversity to provide better performance was proposed in [9]. It is referred to as the delay diversity, where two transmit antennas are used and the same information signal is transmitted from both antennas with a delay of one symbol interval between them.

$$c^1_t = c_{t-1}, \qquad c^2_t = c_t$$

Where c^i_t is the transmitted signal at the i^{th} transmit antenna at time t. Here, c_t and c_{t-1} are the output symbols of the encoder at time instances t and (t-1). This system can be viewed as a rate-½ repetition code whose symbols are transmitted one after the other in consecutive time intervals instead of transmitting the two at the same time. Full study of this system dictates that it does not require any bandwidth expansion and can provide a

diversity advantage of two. The concept of ST codes is a generalization to the delay diversity system presented in [9].

1.5 Space-Time (ST) Codes

1.5.1 Motivation

Motivations behind the development of this new class of codes are the need of transmitting at higher bit rate, and to enhance performance by providing transmit and receive diversity along with error correcting capabilities [1]. As mentioned before, the need for more sophisticated equalization techniques becomes more essential as the transmission rate increases. To avoid increasing the bandwidth in addition to supplying error correction and time diversity, ST codes are used to transmit N different signals at the same time.

By this method, space and time diversity can be combined to achieve better performance and to increase bandwidth efficiency. In such systems, the input sequence is input into a channel encoder to produce N signals that are transmitted at the same time via N transmit antennas. In this case, the bit rate achieved is that of system without diversity multiplied by N. In the following, the structure of a typical ST encoder/decoder, the performance criteria of ST codes and a detailed literature survey of ST code are presented.

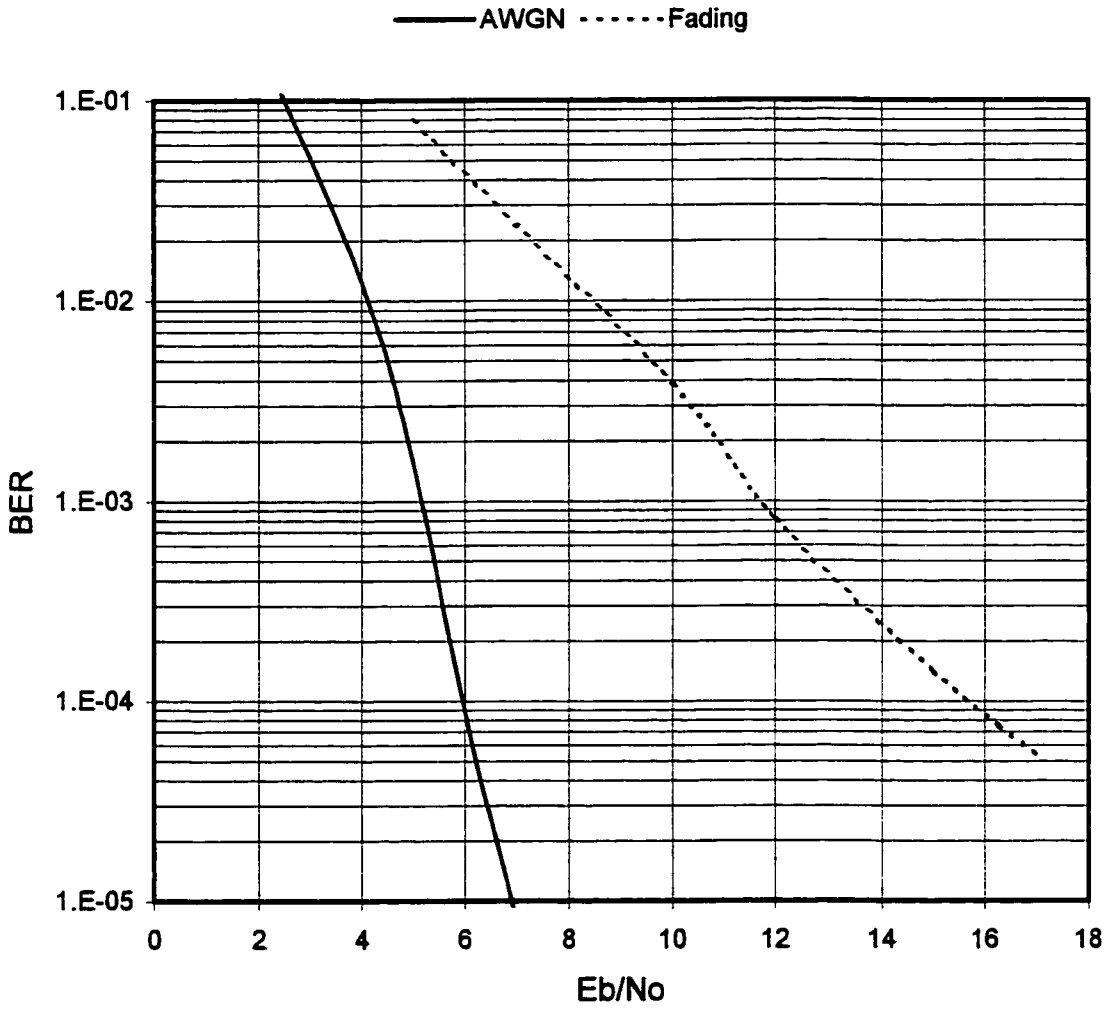

Figure 1.2: Performance of the 8-state 8PSK Ungerboeck trellis code.

1.5.2 Encoder/Decoder of ST Systems

A typical ST encoder/decoder system is shown in Figure 1.3. The encoder consists of a Multiple trellis coded modulation (MTCM) encoder, N modulators and N transmit antennas, while the decoder consists of M receive antennas, M demodulators and a Viterbi decoder that can provide diversity as well as error correction capabilities. As a result, the combination of high bit transmission rate, error correction capability and both time and space diversity advantages are achieved when ST codes are used.

The signal d_t received at the j^{th} antenna at time t is a noisy superposition of all transmitted symbols over all transmit antennas and is given by:

$$d_t = \sum_{i=1}^{N} \alpha_{ij,t}\, c^i_t + \eta_t \qquad (1.5)$$

where η_t is an AWGN modeled as independent samples of a zero-mean complex Gaussian random process with variance $N_o/2$ per dimension. The coefficient $\alpha_{ij,t}$ is the path gain from the i^{th} transmit antenna to the j^{th} receive antenna at time t and c^i_t is the transmitted symbol from the i^{th} transmit antenna at time t.

At the receiver side, the Viterbi decoder computes a branch metric defined by the following:

$$\sum_{j=1}^{M} | d_t - \sum_{i=1}^{N} \alpha_{i,j,t}\, c^i_t |^2 \qquad (1.6)$$

An example of a typical QPSK ST code presented in [1] is illustrated in Figure 1.4. The trellis diagrams of the 4 and 8-state codes are shown in Figure 1.4-a, where the QPSK signal constellation used in the code is shown in Figure 1.4-b. In each row in the trellis diagrams, four signal pairs are the labels of the four branches diverging from each state.

Having four branches at each transition is due to having two input bits to the encoder resulting in four different combinations and hence four branches departing from each state. At each branch, the two numbers in the corresponding signal pair indicate the signals to be transmitted over the first and second transmit antennas. For example, upon the transition from the state 0 to state2, the branch label (02) indicates the transmission of s_0 over the first antenna and s_2 over the second antenna. Here, s_i indicates the signal with label i in the signal constellation.

The 4-state code can be viewed as a delay diversity system. From its trellis diagram, the symbol to be transmitted over the first antenna when a transition happens from an old state to a new state, is the same as the old state. Similarly, the symbol to be transmitted over the second antenna is the new state. In the next transition, the old state becomes the new state in the previous transition. So, the symbol transmitted over the first antenna in this time is the same symbol transmitted over the second antenna in the previous transition. Moreover, the symbol at the second antenna at this time is the current state after the second transition. Hence, symbols transmitted over the second antenna will be transmitted over the first antenna with a delay of one symbol duration, which dictates the delay diversity system. This is illustrated in Figure 1.4-c for the case of three transitions from the zero state to the following states in sequence: (132). A delay of one symbol duration between the transmitted symbols over the two transmit antennas is observed from the order of transmitted symbols over the two antennas.

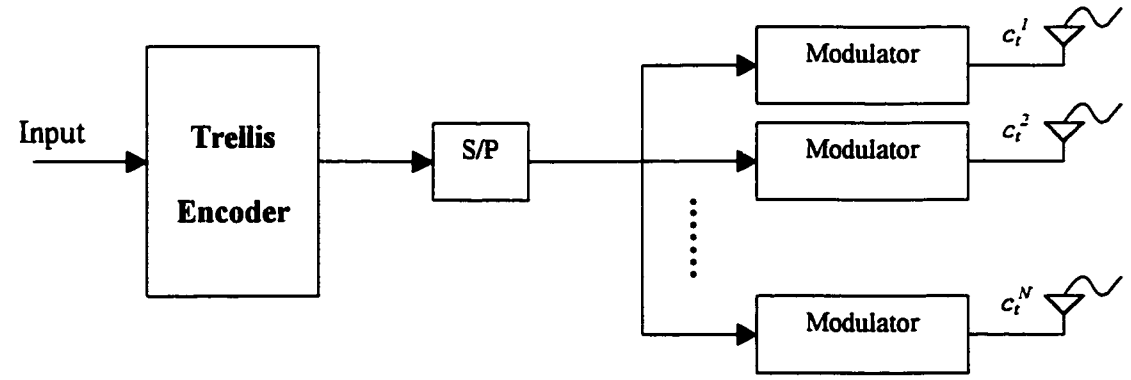

(a)

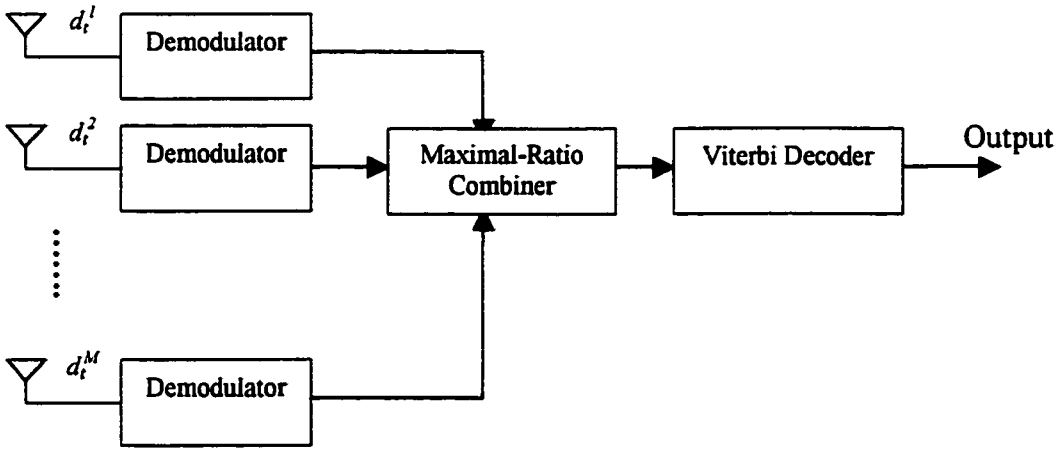

(b)

Figure 1.3: ST system (a) Encoder, (b) Decoder. S/P: Serial-to-Parallel converter.

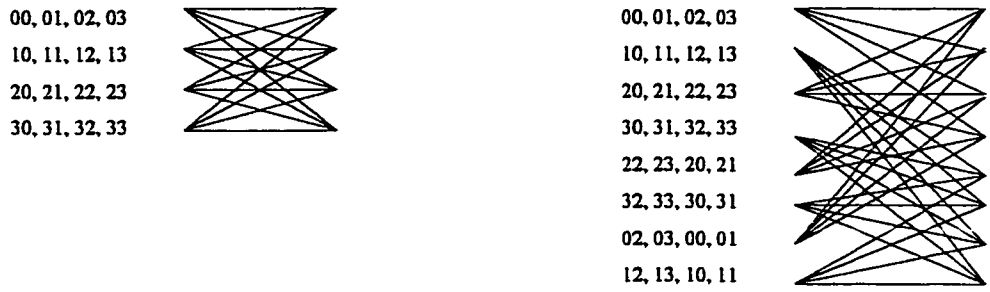

(a)

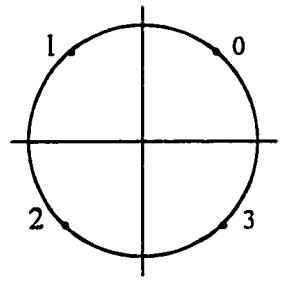

(b)

Input Sequence:

10 11 01

t

Symbols at 1st Tx antenna: $s_3\ s_1\ s_0$

Symbols at 2nd Tx antenna: $s_2\ s_3\ s_1$

t

(c)

Figure 1.4: (a) QPSK ST code designed in [1], 4 and 8-state with 2 bit/s/Hz, (b) QPSK constellation, (c) Example of input/output for the 4-state code in (a).

1.5.3 Performance Criteria of ST Systems

In [1] and [10], performance criteria for ST codes are derived for the cases of rapid and quasi-static fading channels. In quasi-static fading channels, the fade samples are assumed to be constant for the period of one frame and independent from one frame to the other. On the other hand, the fade samples in rapid fading channels change independently from one symbol to the other within the frame. It should be clear that these definitions are different from the SF and FF channels. In SF channels, the fading samples are correlated for adjacent symbols, not constant for one frame as in the quasi-static case. However, the fades samples in the FF channels change within one symbol, resulting in different fades affecting the same symbol.

The performance of ST codes over quasi-static channels is briefly presented in the following. Consider a codeword C_l that has been transmitted over l time intervals and was erroneously decoded as $\hat{C}_l$ where:

$$C_l = c^1{}_1\, c^2{}_1 \ldots c^N{}_1\, c^1{}_2 \ldots c^N{}_2 \ldots\ldots c^1{}_l \ldots\ldots c^N{}_l$$

$$\hat{C}_l = \hat{c}^1{}_1\, \hat{c}^2{}_1 \ldots \hat{c}^N{}_1\, \hat{c}^1{}_2 \ldots \hat{c}^N{}_2 \ldots\ldots \hat{c}^1{}_l \ldots\ldots \hat{c}^N{}_l$$

Here, l is the length of the sequence in time and N is the number of transmit antennas, resulting in a total of Nl symbols in the codeword C_l. The pairwise error probability of deciding $\hat{C}_l$ in favor of C_l using maximum liklihood decoding is upper bounded by the Chernoff bound [1] as:

$$P(C_l,\hat{C}_l \,|\, \alpha_{ij},\ i=1,\ldots,N,\ j=1,\ldots,M) \le \exp(-d^2{}_E(C_l,\hat{C}_l)/4N_o), \tag{1.7}$$

where

$$d^2{}_E(C_l,\hat{C}_l) = \sum_{t=1}^{l}\sum_{j=1}^{M} E_s\Big|\sum_{i=1}^{N} \alpha_{ij}\,(c^i{}_t - \hat{c}^i{}_t)\Big|^2 \tag{1.8}$$

The quantity in the inner summation represents Euclidean distance between the i^{th} symbol in the correct sequence and that in the decoded one. The quantity inside the middle summation is the metric computed for a transition between two states in the encoder. As mentioned for quasi-static channels, the fades samples are assumed to be constant for one frame period of length l and hence the time subscript is omitted. The total expression $d^2_E(C_l,\hat{C}_l)$ is the accumulated path metric between the two sequences.

A similar manipulation to the squared Euclidean distance, done in the Appendix for rapid fading channels, can be applied here for the quasi-static case. After that, the conditional pairwise error probability $P(C_l,\hat{C}_l|\alpha_{ij})$ is averaged with respect to the fades Rayleigh distribution and an upper bound on $P(C_l,\hat{C}_l)$ is found to be:

$$P(C_l,\hat{C}_l|\beta_{ij}) \leq \{ (\prod_{i=1}^{r} \lambda_i)^{1/r} E_s/4N_o \}^{-rM} \qquad (1.9)$$

Where r is the number of nonzero eigenvalues of the matrix A, where A is an NxN matrix with:

$$A_{pq}(c,\hat{c}) = \sum_{t=1}^{l} (c^p{}_t - \hat{c}^p{}_t).(c^q{}_t - \hat{c}^q{}_t), \qquad (1.10)$$

Note that the remaining $(N-r)$ eigenvalues do not contribute to the above inequality.

The diversity advantage of the ST code is defined to be the gain in the SNR over system without diversity, and the coding gain is the gain in SNR over uncoded systems when operating at the same diversity advantage. From equation (1.10), the diversity advantage is rM, and the coding gain is $(\prod_{i=1}^{r} \lambda_i)^{1/r}$. According to these parameters, the code design

must satisfy some conditions that maximize both the diversity and coding advantages. These are summarized by the rank and determinant criteria.

The rank criterion tells that the matrix A must be full rank (i.e: its rank equals N) in order to achieve maximum diversity order NM. If a diversity order of rM is the target, then the rank of that matrix must be at least equal to r. The determinant criterion says that a coding gain is maximized if the product of all nonzero eigenvalues λ_i's is maximized. This is equivalent to maximizing the minimum determinant of A for all pairs of distinct possible codewords.

The same criteria with some changes are applied when the fading samples of the transmit branches are correlated. Performance of ST codes over quasi-static fading channels with correlated branches is worse than that over quasi-static channels with independent branches due to the dependency between the fading coefficients from one transmit branch to another one.

For the rapid fading case, in which the fading process changes from one sampling time to the other, the rank criterion is called the distance criterion that maximizes the diversity advantage. Moreover, the determinant criterion is called product criterion and it should be maximized in order to achieve the maximum coding advantage [1]. The performance analysis of this case is treated in details in Chapter 2.

In [1] and [10], performance criteria developed above are used to set rules for the design of ST codes over quasi-static fading channels. For the case of 2 transmit antennas and fully connected trellises, transitions departing from the same state should differ in the second symbol while transitions arriving at the same state should differ in the first

symbol. Some codes satisfying these rules are designed and simulated in [1] and [2] for quasi-static channels.

1.5.4 Literature Survey on Existing ST Systems

In [11], hybrid design criteria for both rapid and quasi-static fading channels are proposed and some codes are designed for illustration. These codes are powerful when the channel varies slowly or rapidly. This is a more practical case because wireless channels are generally time-varying with different rates.

Reasons behind the development of ST coded systems are not the need for higher transmission rate only, but also the need for transmission at the current rates (or lower) with same quality at much lower SNR. One application of this idea is a better frequency reuse in cellular systems where this factor is mostly dependent upon the transmission power. In dense populated areas, it is required to reuse the same frequency as much as possible in order to increase the system capacity and to service as much calls as possible. This need introduces a new class of codes called Low-rate multi-dimensional ST codes or Smart-Greedy codes.

The basic idea behind these codes is the use of concatenated codes to provide more error correction capability at the cost of having more bandwidth requirement than basic ST coded systems described above. In [11], some designed codes using hybrid design criteria are illustrated and simulated. In these codes, each symbol corresponding to each transmit antenna is transmitted over two consecutive intervals. As expected, their performance is much better than codes designed in [2].

Examples using concatenated codes are presented in [11]. Codes designed in the same paper are used as the inner codes to correct most occurring errors and a Reed-Solomon (RS) code is used as an outer code. Since at high SNR, most of the erroneous frames contain few bit errors, the outer code is used to correct the remaining errors that the inner code was not able to correct. By this method, better frame error rate (FER) is obtained in addition to diversity gain and coding gain without any bandwidth expansion.

All the work on the ST codes described above assumes perfect CSI at the receiver. To know the CSI, some estimation techniques that depend on advanced digital signal processing theory must be used. Therefore, Naguib and others in [12] and [13] proposed the use of orthogonal pilot signal insertion (OPSI). The idea is based on the pilot symbol assisted modulation (PSAM) technique used to estimate the CSI in single transmit antenna systems. This is done by inserting periodic orthogonal known pilot sequences in each of the simultaneously transmitted bursts. At the receiver side, a well designed interpolation filter is used to estimate channel state accurately enough. Using this approach, simulation results for FER vs. SNR, using different interpolation filters for a reference model, are obtained. Also, results relating SNR vs. Doppler spread f_D of the same model are obtained for the same types of filters. The reference model is a narrowband TDM system that uses ST coded modem with two transmit and one receive antennas. After symbols are output from the encoder, they are split into 2 streams that are interleaved using symbol-by-symbol block interleaver. After that, orthogonal pilot sequences are inserted and the resulting bursts are transmitted simultaneously over the transmit antennas. This system is explained in more details in Chapter 4.

A more practical case to be considered in mobile communication is when there is a small mismatch in the estimation of the CSI. Analysis of such case is carried out in [14] where a mathematical model is derived and simulation results are obtained for different ST coded systems. It is shown that the performance of these codes degrades by a negligible amount when compared to the assumption of ideal CSI. The degradation is approximately 1 dB for the PSK and QAM systems.

In addition to the use of ST coded systems in providing high or low transmission rates with good quality at low SNR, it can be used to implement an orthogonal frequency division multiplexed (OFDM) physical layer. In [15], an OFDM channel is implemented using N transmit antennas to service l users. The input to the encoder is a block of the users' bits that is used to modulate N signals for each user. This results in lN signals, with N of them are for one user and they are transmitted simultaneously via the N transmit antennas. Some coding examples that use ST coded, RS coded and concatenated RS/ST-coded systems are simulated and discussed.

ST codes have been used in combination with array processing in order to produce better bandwidth efficiency with reasonable FER. In [16], N transmit antennas are used and divided into k groups. So, there will be k independent space-time encoders with each of them using N/k transmit antennas to transmit the symbols at their outputs. At the receiver, there is N/k added symbols that can be separated using trellis-based decoder. These symbols are added to the outputs of other groups' outputs that can be separated using some interference suppression algorithms. This method is called combined array processing with space-time codes. No simulation results for this approach were presented

but it seems to have an advantage of better bandwidth efficiency on the cost of some degradation in performance and more complexity at the receiver side.

The performance of ST coded systems in the presence of mobility conditions and multipath reception was derived in [17]. The design criteria developed before in [1,2] have been examined for the frequency-selective fading channels. The concept of ST transmission has been deeply investigated and more sophisticated system architectures were proposed in [18,19]. In [18], the idea of layered ST (LST) codes was proposed. Two kinds of such layering were proposed: the horizontally LST and diagonally LST codes. Simulation results showed that the diagonally LST codes outperform the horizontally LST codes. The concatenation of ST codes with turbo codes was proposed in [19]. A symbol-by-symbol maximum a posteriori probability (MAP) decoding rule for the proposed system was derived. Significant coding gains were observed in such systems.

The idea of ST block codes (STBC) has appeared recently in [20]. It exploits the ST diversity in order to enhance the performance of the channel, rather than increasing the transmission rate. It uses 2 transmit antennas to transmit two output symbols from the encoder at the first time instance. At the next time instance, the two antennas transmit the same two symbols but after manipulating them so that the transmitted codeword at the second instance is orthogonal to the codeword at the first instance. This idea was compared to the conventional diversity combining schemes, and its performance was comparable to the MRC. A detection algorithm was also proposed in [20] to detect the received signal in this system. A new detection scheme for this system was then proposed in [21]. The beauty of the new scheme is its simplicity, such that its computational requirements is very small compared to the previously proposed one in [20]. The

performance criteria and code design rules for the STBC systems were developed in [22]. The performance was investigated for quasi-static fading channels with full CSI at the receiver.

A generalization of the idea of STBC systems was developed for a general number of transmit antennas in [23]. The generalization is based on composing orthogonal sequences or codewords at each time instance, and these codewords are derived from a basic codeword that is transmitted at the first time instance. Also, many coding examples were introduced and explained to clarify the generalization idea. In [24], the performance evaluation was derived for the generalized STBC system for any number of transmit antenna. Also, many simulation cases for different coding examples were discussed and compared to each others. The idea of STBC was used for interference cancellation in wireless networks in [25]. A minimum mean square error (MMSE) interference suppression algorithm was also derived and examined.

1.6 I-Q Trellis Codes

As mentioned earlier, the transmit time diversity can be achieved by repeating the transmission of each symbol in different time slots. Such system can be viewed as a repetition code and consumes higher bandwidth. Therefore, it is expected that using more sophisticated codes with large MTD will yield large gains over uncoded systems. Also, the coded systems can use higher rate encoders resulting in less bandwidth expansion than the repetition code.

Unfortunately, the MTD of a trellis code is inversely proportional to the number of input bits and proportional to the number of memory elements in the encoder. So, the MTD can be increased either by reducing the number of input bits or adding more memory elements to the encoder. But reducing the number of input bits reduces the encoder's rate and hence reduces the transmitted bit rate. Also, adding more memory elements to the encoders requires more decoding memory and increases the complexity of the Viterbi algorithm used at the decoder. This suggests that using different independent encoders in parallel, each encodes part of the input bits, can increase the MTD of the resulting code. Such a scheme is called I-Q trellis coded system.

The performance criterion of the I-Q trellis codes over Rayleigh fading channels was investigated and an upper bound of the bit error rate with diversity combining was derived in [8]. Also, some I-Q codes with throughputs of 1, 2 and 3 bits/s/Hz were designed in [26] using QPSK and 16-QAM constellations. The designed codes show significant gains over the convolutional codes having the same complexity. The complexity of a convolutional code is measured by the total number of nonparallel paths leaving all the states divided by the number of information bits associated with a transition through the trellis. The I-Q encoding approach is applied to design good ST codes for rapid fading channels.

1.7 Thesis Contribution

The objective of this work is to contribute in this rapidly advancing theory, i.e: Space-Time coding. All work done in the literature in deriving upper bounds on the bit error

probability of the ST systems considers the pairwise error probability without trying to evaluate the bit error probability. In this thesis, the bit error probability of the derived pairwise error probability for rapid fading channels is evaluated. This bound is shown to be very loose. A much tighter bound is proposed and derived. The two bounds are compared and the new bound is shown to be very tight to the simulation results.

Throughout the work done in the literature on ST codes, all codes are designed for quasi-static fading channels. Since the case of rapid fading channels is very common in wireless systems, the design of good ST codes in such environments is considered. The designed codes are based on QPSK and 16-QAM constellations.

The I-Q encoding scheme is well known to increase the MTD of the code with lower trellis complexity [26]. Hence, this idea is used to design good ST codes, which are referred to as the I-Q ST codes. Two techniques for detecting and decoding the I-Q ST coded systems are proposed and compared. The first one is the super-trellis optimal decoding technique and the second one is the suboptimal decoding technique. Again, both QPSK and 16-QAM constellations are used in the design. All designed codes are tested for non-ideal interleaving conditions and estimated CSI at the receiver.

1.7.1 Thesis Organization

The next chapter is devoted for evaluating the existing bound on the bit error probability and deriving the proposed tighter bound. The upper bounds are derived using the error weight distribution and the modified transfer function of the code.

In Chapter 3, the design aspects of good ST codes for rapid fading channel are explained in details. ST codes using QPSK and 16-QAM constellations are designed for rapid

fading channels. After that, the performance of the designed codes is compared with the existing codes in the literature via simulation. The decoding techniques for the I-Q ST codes are introduced and discussed. The effect of having non-ideal interleaving is studied via simulation techniques.

The effect of having CSI estimated at the receiver is considered in Chapter 4. This is done based on the OPSI technique and using a Wiener interpolation filter. The performance of the designed codes is compared with that of the existing codes.

The main conclusions, findings, and extension of this work are then summarized in Chapter 5.

CHAPTER 2

PERFORMANCE EVALUATION OF ST CODES OVER RAPID FADING CHANNELS

2.1 Introduction

As mentioned earlier in chapter 1, the performance criteria for ST codes over quasi-static and rapid fading channels were derived in [1]. These criteria were used to infer the design criteria of ST codes over quasi-static and rapid fading channels. The performance was investigated using the pairwise error probability and no attempts to compute an upper

bound on the bit error probability were done. The evaluation of the bit error probability will be accomplished using the error weight profile and the transfer function of the code. In this chapter, the upper bound on the pairwise error probability, derived in [1] for rapid fading channels, is reviewed. After that, an upper bound on the bit error probability is evaluated from the pairwise error probability. A proposed tighter bound on the pairwise error probability is then derived and the resulting bit error probability is evaluated. The tighter bound is compared to the existing bound. The two bounds are applied to the existing QPSK ST codes presented in [1].

2.2 Weight Profile and Transfer Function

The weight profile of a trellis code is a function that describes the weight distribution of the code. It is derived from the characteristics of the code as follows. Consider a trellis encoder that encodes k input bits into n output bits that are grouped into N groups with $m=n/N$ bits in each group. Each group is mapped to a symbol in a signal constellation of size 2^m by a one-to-one mapping function G, such that:

$$c^1_t = G(b_0, b_1, \ldots, b_{m-1}) = G(\underline{b}^1)$$

and $$c^i_t = G(b_{(i-1)m}, b_{1+(i-1)m}, \ldots, b_{m-1+(i-1)m}) = G(\underline{b}^i) \quad , \text{ for } i=1,2,\ldots,N$$

Where c^i_t is the mapped signal to be transmitted via the i^{th} transmit antenna, b_i is the i^{th} output bit, and $\underline{b}^i$ is the m-bit word to be mapped onto the symbol on the i^{th} transmit antenna. Define g_j as the j^{th} k-bit possible input sequence to the encoder and $\underline{b}_j$ and $\underline{e}_j$ are the corresponding n-bit correct and error bit sequences out of the trellis encoder, respectively. Also, the corresponding j^{th} m-bit word that is mapped into the i^{th} symbol at

the output of the encoder is denoted as $\underline{b}^i_j$, where the corresponding m-bit error sequence is denoted as $\underline{e}^i_j$. Then the error weight profile function is defined to be the function that gives the distance distribution of the output of the encoder due to all input sequences g_j's when the decoder decodes a possible error sequence $\underline{e}_j$. It is defined as [6]:

$$F(\underline{e}_j,D) = \sum_{\underline{g}_j} P(g_j) D^{d_E^2[G(\underline{b}_j),G(\underline{b}_j \oplus \underline{e}_j)]}$$

$$= \sum_{\underline{g}_j} P(g_j) D^{\sum_{i=1}^{N} d_E^2[G(\underline{b}^i_j),G(\underline{b}^i_j \oplus \underline{e}^i_j)]} \qquad (2.1)$$

Here D is a variable indicating the distance due to any error sequence in its exponent and it is found by averaging over the pdf of the channel. When all input sequences have equal probability of occurrence, then $P(g_j)$ is replaced by $1/2^k$, where k is the number of input bits to the encoder. In the second expression in (2.1), the Euclidean distance between the N-symbol codewords was replaced by the sum of all the Euclidean distances between the N distinct symbol pairs, where this is the case in ST codes as it is proved in the next section. For fading channel, the Euclidean distance is averaged with respect to the pdf of the fading random process α:

$$F(\underline{e}_j,D) = \sum_{\underline{g}_j} \frac{1}{2^k} E_\alpha [D^{d_E^2[G(\underline{b}_j),G(\underline{b}_j \oplus \underline{e}_j)]}] \qquad (2.2)$$

After performing the expectation in (2.2) and replacing the total Euclidean distance by the summation in (2.1), equation (2.2) can be simplified to the following:

$$F(\underline{e}_j,D) = \sum_{\underline{g}_j} \frac{1/2^k}{1 + \frac{1}{4No} \sum_{i=1}^{N} d_E^2[G(\underline{b}^i_j),(G(\underline{b}^i_j \oplus \underline{e}^i_j)]} \qquad (2.3)$$

Define $\delta_j^2 = \sum_{i=1}^{N} d_E^2[G(\underline{b}_j^i), G(\underline{b}_j^i, \underline{e}_j^i)]$, and $F(\underline{e}_j, D) = f(\delta_j^2) = D_j$. Then,

$$F(\underline{e}_j, D) = \sum_{\underline{g}_j} \frac{1/2^k}{1 + \frac{1}{4No}\delta_j^2} \tag{2.4}$$

Using (2.4), the weight distribution of the trellis code, when used as a ST code, can be evaluated and hence the bit error probability is calculated as to be explained in the next sections. The transfer function of the trellis code is found from the error weight profile by averaging it over all possible error events of lengths l, and for all possible sequence lengths. Hence, the transfer function is defined as:

$$T(D) = \sum_{l=1}^{\infty} \sum_{E_l \neq 0} \prod_{j=1}^{l} F(\underline{e}_j, D) \tag{2.5}$$

Where E_l is an error sequence consisting of l time intervals, i.e: the sequence consists of l codewords each of n bits resulting in a total of nl bits. The transfer function is a function of the variable D, which enumerates the distance of an error sequence from the correct one. Hence, the transfer function is modified by adding a new variable I^r, where the exponent r indicates the Hamming weight of the input sequence causing the encoder to deviate from the all-zero sequence.

The modified transfer function is formed by considering the trellis encoder as a linear system with the zero-state as its input and output at the same time. The other states of the encoder are considered as the states of the system. It is found by finding the state transition matrix for the states different from the zero state. For an encoder with ν memory elements and hence 2^ν states, the state transition matrix H is a $(2^\nu\text{-}1)\text{x}(2^\nu\text{-}1)$ square matrix. The element in the i^{th} row and j^{th} column of the H matrix, (H_{ij}) is the gain

of the output compared to the all-zero sequence when the encoder makes a transition from the i^{th} to the j^{th} states. This gain is a product of the form $I^r D_k$, indicating the Hamming weight of the input sequence causing the transition (r) and the distance profile of the output sequence from the all-zero sequence (D_k) due to the input sequence g_k. The state transition equations of the trellis code [6] is:

$$\underline{S} = \underline{H}.\underline{S} + \underline{B} \quad \text{and} \quad \underline{S} = (\underline{I}-\underline{H})^{-1}\underline{B} \tag{2.6}$$

Where $\underline{S}$ is the $(2^{\nu}-1)$-length column vector having the states of the encoder other than the zero state, $\underline{H}$ is the transition matrix, $\underline{B}$ is a $(2^{\nu}-1)$-length column vector describing the input to the system from the zero-state, and $\underline{I}$ is a $(2^{\nu}-1)\times(2^{\nu}-1)$ identity matrix. The modified transfer function $T(I,D)$ is found by realizing the zero-state as the output of the system. Hence, the modified transfer function is a function of the variables I^r, distance variable D and all states except the zero state, i.e:

$$T(I,D) = f(I^r, D, S_i), \quad i=1,2,3,\ldots,2^{(2\nu-1)} \tag{2.7}$$

Where S_i is the i^{th} state of the encoder. Examples of finding the modified transfer function of the QPSK ST code presented in Chapter 1 are illustrated in section 2.5.

In many trellis codes, the weight profile from the correct sequence depends on the correct sequence chosen [6]. Such codes are said to be nonlinear and the state diagram, required to define the error weight profile in this case, consists of $2^{2\nu}$ states instead of 2^{ν} states only. However, if the code satisfies the criteria of Zehavi and Wolf for isometric codes, it is possible to describe it by a 2^{ν}-state state diagram [27]. All the codes described in this chapter satisfy these conditions, and hence their weight profile can be described using the above approach. The modified transfer function is used in the proceeding sections to

compute the bit error probability from the pairwise error probability, which is derived in the next section.

2.3 Existing Upper Bound

2.3.1 Pairwise Error Probability

Pairwise error probability is defined in section 1.5.3 as the probability of decoding a received signal sequence C_l as an error sequence $\hat{C}_l$, $P(C_l,\hat{C}_l)$. Referring to the ST system described in Chapter 1, the pairwise error probability of that system over rapid fading channel was derived in [1] as follows. Consider the notations C_l and $\hat{C}_l$ defined in section 1.5.3, the probability of deciding on the sequence $\hat{C}_l$ in favor of the sequence C_l using maximum liklihood sequence decoding is upper bounded by the Chernoff bound [1]:

$$P(C_l,\hat{C}_l \mid \alpha_{ij,t},\ i=1,\ldots,N,\ j=1,\ldots,M,t=1,\ldots,l) \le \exp\left(-d^2_E(C_l,\hat{C}_l)/4N_o\right),$$

where
$$d^2_E(C_l,\hat{C}_l) = \sum_{t=1}^{l}\sum_{j=1}^{M} E_s\left|\sum_{i=1}^{N} \alpha_{ij,t}\,(c^i_t - \hat{c}^i_t)\right|^2, \qquad (2.8)$$

and E_s is the average transmitted signal energy at each transmit antenna. The quantity in the inner summation represents Euclidean distance between the i^{th} symbol in the correct sequence and that in the decoded one. The quantity inside the middle summation is the metric computed for a transition between two states in the encoder. The fades samples are assumed to be independent from one time interval to the other, satisfting the rapid fading channel assumption. The received signals at the different receive antennas are combined using MRC scheme. The total expression $d^2_E(C_l,\ \hat{C}_l)$ is the accumulated path metric

between the two sequences for the l time intervals. The detailed derivation of the performance criteria of ST codes over rapid fading channels is presented in the Appendix. The expression in (A.11) is rewritten by defining the minimum number of time intervals in the set η as L. Hence, the pairwise error probability can be upper bounded by:

$$P(C_l,\hat{C}_l) \le \prod_{t=1}^{L} \left[1+ |c_t - \hat{c}_t|^2 (E_s/4N_o)\right]^{-M} \tag{2.9}$$

The parameter L, which is the length of the shortest error event with L time intervals, can be referred to as Space-Time MTD (ST-MTD) of the ST code. It can be visualized as the "branch-wise" Hamming distance or the MTD in conventional trellis codes, by considering the whole codeword c_t as one symbol.

The diversity advantage of the ST code is defined in Chapter 1 to be the gain in the SNR over systems without diversity, i.e: the exponent of $(E_s/4N_o)$, and the coding gain is the gain in SNR over uncoded systems when operating at the same diversity advantage, i.e: quantity multiplied by $(E_s/4N_o)$ [1]. From the last equation, a diversity advantage of LM is achieved if the ST-MTD of the code is L and the coding gain is the quantity multiplied by $(E_s/4N_o)$ which is $|c_t - \hat{c}_t|^2$.

So, in order to design good ST codes suitable for rapid fading channels, two parameters should be maximized. The first one is the branch-wise Hamming distance or the ST-MTD between codewords transmitted from all antennas for the period of the shortest error event, i.e: L. The second one is the quantity:

$$\prod_{t\in\eta} |c_t - \hat{c}_t|^2 = \prod_{t\in\eta}\sum_{i=1}^{N} |c^i_t - \hat{c}^i_t|^2 \le \prod_{t=1}^{L}\sum_{i=1}^{N} |c^i_t - \hat{c}^i_t|^2 \tag{2.10}$$

Which is the analogous to the MSPD in conventional trellis codes. It can be referred to as the Space-Time MSPD (ST-MSPD) of the ST code. The first and second parameters to be maximized are referred to in [1] as Distance and Product criteria, respectively.

One can see that ST codes can be viewed as a generalization to trellis codes used with one transmit antenna systems. This is done by replacing the concepts of MTD and MSPD in conventional trellis codes by the ST-MTD and ST-MSPD, respectively. If N=1, then the ST code is transformed into a conventional trellis code with one transmit antenna. The pairwise error probability in (2.9) is used to derive the bit error probability of ST codes in the following section.

2.3.2 Bit Error Probability

As mentioned earlier, the bit error probability was not evaluated for any ST code in the literature since the pairwise error probability was enough to derive the design criteria. In order to evaluate the bit error probability, the error event probability should be calculated. The error event probability is defined as the probability for the shortest error event to happen. It is written in terms of the pairwise error probability using the union bound that counts for all erroneous sequences with their probabilities of occurrence [6] as:

$$P_e \leq \sum_{l=1}^{\infty} \mathrm{P}(\mathbf{C}_l)\, \mathrm{P}(\boldsymbol{C}_l, \hat{\boldsymbol{C}}_l) \tag{2.11}$$

And the pairwise error probability is expressed in terms of the error weight distribution [6] as:

$$\mathrm{P}(\boldsymbol{C}_l, \hat{\boldsymbol{C}}_l) \leq \tfrac{1}{2} \sum_{l=1}^{\infty} \sum_{E_l \neq 0} \prod_{i=1}^{l} F(\underline{e}_i, D) \tag{2.12}$$

Combining (2.5) and (2.11), then the error event probability becomes [6]:

$$P_e \leq \tfrac{1}{2}\, \mathrm{T}(I,D) \tag{2.13}$$

The bit error probability can be found from the error event probability by dividing by the number of input bits to the encoder and taking the derivative of the transfer function with respect to the input bits enumerating variable I [6], and hence can be expressed as:

$$P_b \leq \frac{1}{2k} \frac{\partial T(I,D)}{\partial I}\Big|_{I=1} \tag{2.14}$$

This expression is rewritten as:

$$P_b \leq \frac{1}{2k} \lim_{\varepsilon \to 0} \frac{T(I+\varepsilon,D) - T(I,D)}{\varepsilon}\Big|_{I=1} \tag{2.15}$$

The expression in (2.15) can be approximated by choosing ε to be very small number (e.g. $\varepsilon = 10^{-6}$).

2.4 Tighter Upper Bound

2.4.1 Pairwise Error Probability

The bit error probability of trellis codes with receive diversity is tightly upper bounded in [8]. The same methodology is followed here in deriving the bit error probability for ST coded systems in rapid fading environments as follows. The pairwise error probability can be tightly upper bounded by using (A.6) and the exact expression of the pairwise error probability [6] as:

$$\mathrm{P}(\boldsymbol{C}_t, \hat{\boldsymbol{C}}_t \,|\, \alpha_{ij,t}, i=1{:}N, j=1{:}M, t=1,\ldots,l) = \tfrac{1}{2}\, \mathrm{erfc}\left(\sqrt{\frac{d_E^2(C_t, \hat{C}_t \,|\, \alpha_{ij,t}, i=1{:}N, j=1{:}M, t=1{:}l)}{4N_o}} \right)$$

$$= \tfrac{1}{2}\,\mathrm{erfc}\left(\sqrt{\frac{E_s}{4N_o}\sum_{t=1}^{l}\sum_{j=1}^{M}\sum_{i=1}^{N}\lambda_{i,t}\,|\beta_{ij,t}|^2}\right)$$

$$= \tfrac{1}{2}\,\mathrm{erfc}\left(\sqrt{\sum_{t=1}^{l}\sum_{i=1}^{N} d_{i,t}\gamma_{i,t}}\right) \qquad (2.16)$$

Where $d_{i,t} = \lambda_{i,t}\dfrac{E_s}{4N_o}$ and $\gamma_{i,t} = \sum_{j=1}^{M} |\beta_{ij,t}|^2$. Since all the eigenvalues $\lambda_{i,t}$'s are zero except one, then the nonzero $d_{i,t}$ is replaced by $\dfrac{E_s}{4N_o}|\boldsymbol{c}_t - \hat{\boldsymbol{c}}_t|^2 = \dfrac{E_s}{4N_o}\sum_{i=1}^{N} |c'_t - \hat{c}'_t|^2$. So, the inner summation in (2.16) reduces to $d_t\Gamma_t$, where the quantity $d_t = \dfrac{E_s}{4N_o}|\boldsymbol{c}_t - \hat{\boldsymbol{c}}_t|^2$ and $\Gamma_t = \{\gamma_{i,t}: \lambda_{i,t} \neq 0\}$. Hence, the pairwise error probability becomes:

$$\mathrm{P}(\boldsymbol{C}_t, \hat{\boldsymbol{C}}_t \,|\, \alpha_{ij,t}, i=1{:}N, j=1{:}M, t=1,\ldots,l) = \tfrac{1}{2}\,\mathrm{erfc}\left(\sqrt{\sum_{t=1}^{l} d_t\Gamma_t}\right) \qquad (2.17)$$

Since the variables $|\beta_{ij,t}|$'s have Rayleigh distribution with mean square $\mathrm{E}[|\beta_{ij,t}|^2]=1$, then $|\beta_{ij,t}|^2$ are exponentially distributed with unity mean. Therefore, the variables Γ_t's, which are sums of exponentially distributed random variables, will have an M-Erlang distribution with parameter one. The pdf of this distribution is written [28] as:

$$f_\Gamma(\Gamma_t) = \frac{1}{(M-1)!}\Gamma_t^{(M-1)}\, e^{-\Gamma_t}, \qquad \Gamma_t \geq 0. \qquad (2.18)$$

The expression of the pairwise error probability in (2.17) is conditional on the fading coefficients. To find the unconditional probability, it has to be averaged with respect to these coefficients, resulting in:

$$P(C_l,\hat{C}_l) = \tfrac{1}{2} \int_0^{\infty} \cdots \int_0^{\infty} erfc\left(\sqrt{\sum_{t=1}^{l} \Gamma_t d_t}\right) f_\Gamma(\Gamma_1) \cdots f_\Gamma(\Gamma_l)\, d_{\Gamma_1} \ldots d_{\Gamma_l} \qquad (2.19)$$

Defining $\delta_t = \dfrac{d_t}{1+d_t}$ and $\omega_t = \Gamma_t(1+d_t)$, and replacing $f_\Gamma(\Gamma_t)$ by the corresponding $f_\omega(\omega_t)$ using pdf transformation formula [6,28], then the unconditional pairwise error probability can be written as:

$P(C_l,\hat{C}_l)=$

$$= \tfrac{1}{2} \prod_{t\in\eta} \frac{1}{(1+d_t)^M} \int_0^{\infty} \cdots \int_0^{\infty} erfc\left(\sqrt{\sum_{t=1}^{l} \delta_t \omega_t}\right) \exp\left(\sum_{t=1}^{l} \delta_t \omega_t\right) f_\omega(\omega_1) \ldots f_\omega(\omega_l)\, d_{\omega_1} \ldots d_{\omega_l} \qquad (2.20)$$

Where $\eta = \{t: c_t \neq \hat{c}_t\}$. Defining $L_\eta = |\eta|$ and $\delta_m = \min\{\delta_t, t \in \eta\}$, then it is clear that:

$$\sum_{t=1}^{l} \delta_t \omega_t \geq \delta_m \sum_{t=1}^{l} \omega_t \qquad (2.21)$$

Since the function $erfc(x)\exp(x^2)$ is a monotonically decreasing function for $x \geq 0$, then the pairwise error probability is upper bounded by:

$$P(C_l,\hat{C}_l) \leq \frac{1}{2} \prod_{t\in\eta} \frac{1}{(1+d_t)^M} \int_0^{\infty} erfc\left(\sqrt{\delta_m \Omega}\right) e^{(\delta_m \Omega)} f_\Omega(\Omega) d\Omega \qquad (2.22)$$

Where $\Omega = \sum_{t\in\eta} \omega_t$. Since each of the ω_t's is a product of an M-Erlang distributed random variable with parameter one, Γ_t and a constant quantity d_t, then the variable ω_t is also an M-Erlang random variable with pdf as in (2.18). The variable Ω is a sum of L_η M-Erlang random variables with parameter one, and hence its distribution is an ML_η-Erlang distribution with parameter equal to one. Thus, its pdf is of the form:

$$f_{\Omega}(\Omega) = \frac{1}{(ML_{\eta}-1)!}\,\Omega^{(ML_{\eta}-1)}e^{-\Omega}\,, \qquad \Omega \geq 0. \tag{2.23}$$

Substituting in the pairwise error probability expression:

$$\mathrm{P}(C_l,\hat{C}_l) \leq \frac{1}{2(ML_{\eta}-1)!}\prod_{t\in\eta}\frac{1}{(1+d_t)^M}\int_0^{\infty} erfc\left(\sqrt{\delta_m\Omega}\right)e^{(\delta_m\Omega)}\Omega^{(ML_{\eta}-1)}e^{-\Omega}d\Omega \tag{2.24}$$

The integral in the expression of the pairwise error probability is evaluated using the following equality [6]:

$$\frac{1}{2(K-1)!}\int_0^{\infty} erfc\left(\sqrt{xy}\right)e^{-y(1-x)}y^{(K-1)}dy = \frac{1}{2^{2K}}\sum_{j=1}^{K}\binom{2K-j-1}{K-1}\left(\frac{2}{1+\sqrt{x}}\right)^j \tag{2.25}$$

Then, the pairwise error probability is evaluated to be:

$$\mathrm{P}(C_l,\hat{C}_l) \leq \frac{1}{2^{2ML_{\eta}}}\sum_{j=1}^{ML_{\eta}}\binom{2ML_{\eta}-j-1}{ML_{\eta}-1}\left(\frac{2}{1+\sqrt{\delta_m}}\right)^j \times \prod_{t\in\eta}\frac{1}{(1+d_t)^M} \tag{2.26}$$

Defining the minimum time instances in which the codewords $c_t = c^1_t\ c^2_t\ \ldots\ c^N_t$ are different from the all-zero codeword to be L, and since $L \leq L_{\eta}$, then the pairwise error probability can be written as:

$$\mathrm{P}(C_l,\hat{C}_l) \leq \frac{1}{2^{2ML}}\sum_{j=1}^{ML}\binom{2ML-j-1}{ML-1}\left(\frac{2}{1+\sqrt{\delta_m}}\right)^j \times \prod_{t\in\eta}\frac{1}{(1+d_t)^M} \tag{2.27}$$

The new bound on the pairwise error probability dictates the same design criteria inferred from the existing bound. The new bound is the same as the existing bound in (2.9) with a multiplication by a tightening constant. This term is the term to the left of the product term in (2.27). For the new bound to be tighter than the existing bound, it is required that its computed value to be less than the value computed from the existing bound.

The tightening constant is a function of the number of receive antennas, the ST-MTD of the ST code and the SNR of the channel considered d_t. The value of the constant increases by reducing δ_m and hence by reducing d_t which indicates the SNR of the channel. It also increases as the product ML is reduced. In Figure 2.1, the tightening constant is plotted versus the product ML for three SNR values, 0 and 10 dB. For higher SNR values the constant becomes smaller and hence it was not plotted for higher SNR values. It is clear that the value of the constant is always less than one, proving the tightness of the new bound.

2.4.2 Bit Error Probability

Since the product term in the pairwise error probability in (2.27) defines the error weight profile of the trellis code in Rayleigh fading channels, then the modified transfer function [6] is:

$$T(I,D) = \prod_{t \in \eta} \frac{1}{(1+d_t)^M} \tag{2.28}$$

Combining (2.14), (2.27) and (2.28), the bit error probability is written as:

$$P_b \le \frac{1}{k}\left[\frac{1}{2^{2ML}}\sum_{j=1}^{ML}\binom{2ML-j-1}{ML-1}\left(\frac{2}{1+\sqrt{\delta_m}}\right)^j\right] \times \frac{\partial T(I,D)}{\partial I}\Big|_{I=1} \tag{2.29}$$

Also, it can be seen that the tighter bound on the bit error probability is the same as the existing one except for a scaling factor that tights the existing bound. Examples of evaluating the existing and new bounds are considered in the next section.

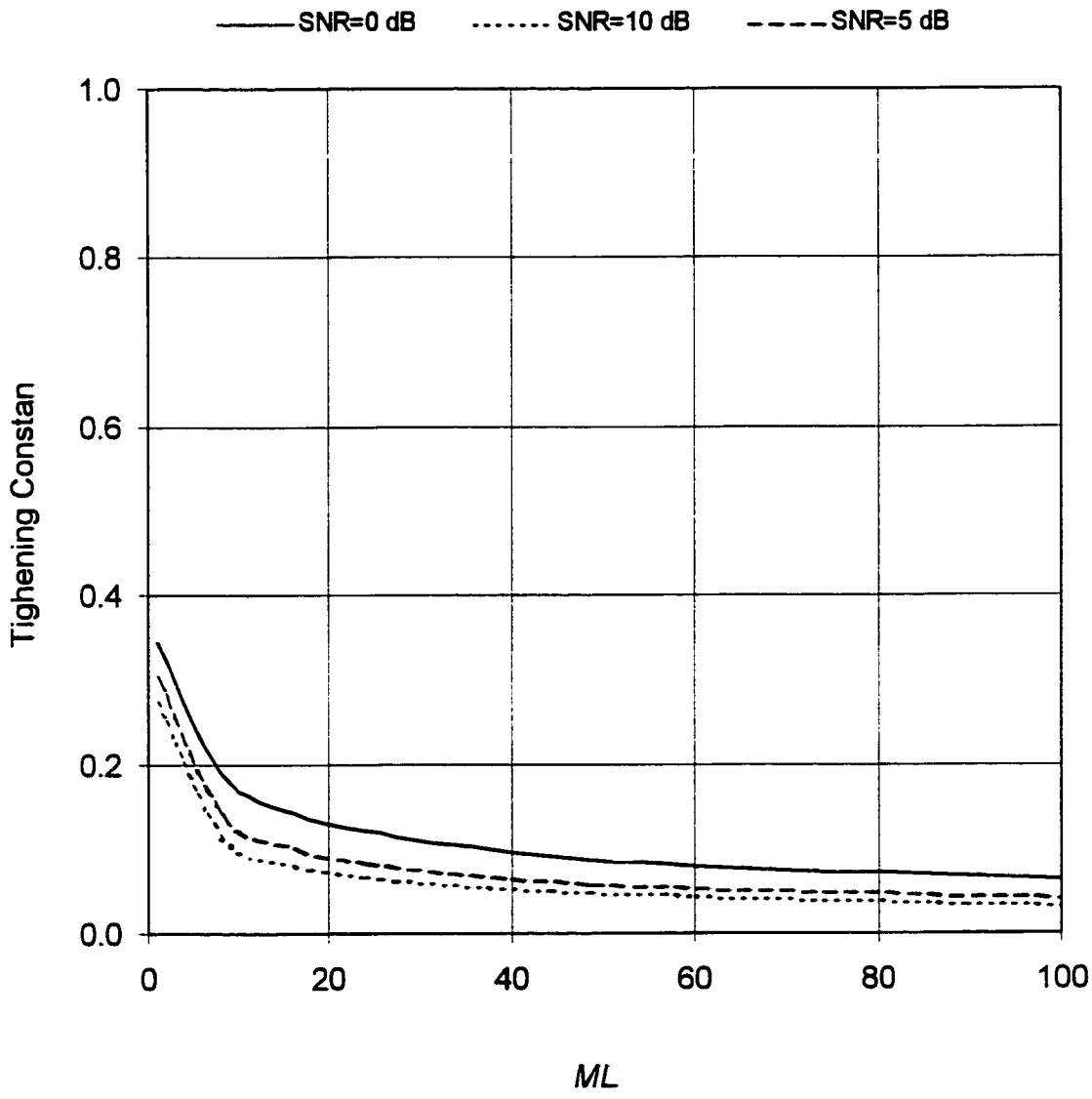

Figure 2.1: Tightening constant at the left of the product term in (2.27) versus *ML* for three SNR values.

2.5 Comparison Examples

2.5.1 Four-State QPSK ST Code

This code was presented in [1] for quasi-static fading channels. The trellis diagram of this code is shown in Figure 1.4-a. When the zero state is considered as the input and output of the system, the state transition equations can be expressed as follows:

$$\begin{bmatrix} S_1 \\ S_2 \\ S_3 \end{bmatrix} = \begin{bmatrix} ID_{11} & ID_1 & ID_1 \\ ID_2 & ID_{12} & ID_1 \\ I^2D_2 & I^2D_1 & I^2D_{12} \end{bmatrix} \begin{bmatrix} S_1 \\ S_1 \\ S_1 \end{bmatrix} + \begin{bmatrix} ID_{22} \\ ID_{11} \\ I^2D_{11} \end{bmatrix},$$

and the state vector solution is found to be:

$$\begin{bmatrix} S_1 \\ S_2 \\ S_3 \end{bmatrix} = \begin{bmatrix} I-ID_{11} & -ID_1 & -ID_1 \\ -ID_2 & I-ID_{12} & -ID_1 \\ -I^2D_2 & -I^2D_1 & I-I^2D_{12} \end{bmatrix}^{-1} \begin{bmatrix} ID_{22} \\ ID_{11} \\ I^2D_{11} \end{bmatrix}$$

As explained earlier, the element in the i^{th} row and j^{th} column of the transition matrix indicates the gain from the i^{th} to the j^{th} states of the encoder. It consists of two variables: I whose exponent indicates the Hamming weight of the input sequence causing the transition, and the D's which are the squared Euclidean distance between the output sequence resulting from the transition and the correct sequence. Without loss of generality, the all-zero sequence is considered as the correct sequence. The D's are explained in the following.

Referring to the QPSK constellation in Figure 1.4-b, define: $\delta_1^2 = d^2_E(s_0,s_1) = d^2_E(s_0,s_3)$, $\delta_2^2 = d^2_E(s_0,s_2)$, where s_i is the signal with label i in the QPSK constellation, and $f(\delta_i^2)=\frac{1}{1+\delta_i^2/4N_o}$. The parameter $f(\delta_i^2)$ is computed from the error weight profile in

Equation (2.4). Since the encoder's output consists of 4 bits, then each error sequence is a 4-bit sequence corresponding to two QPSK signals to be transmitted over the two transmit natenas. So, the above D's and the corresponding error sequences are:

$$\begin{aligned}
&D_1 = f(\delta_1^2), && \underline{e}_i = 0001 \text{ or } 0011 \text{ or } 0100 \text{ or } 1100,\\
&D_2 = f(\delta_2^2), && \underline{e}_i = 0010 \text{ or } 1000,\\
&D_{11} = f(2\delta_1^2), && \underline{e}_i = 0101 \text{ or } 0111 \text{ or } 1101 \text{ or } 1111,\\
&D_{22} = f(2\delta_2^2), && \underline{e}_i = 1010,\\
&D_{12} = f(\delta_1^2+\delta_2^2), && \underline{e}_i = 0110 \text{ or } 1110 \text{ or } 1001 \text{ or } 1011,
\end{aligned} \tag{2.30}$$

For the case of the error sequence $\underline{e}_i = 0001$, the corresponding error signals are $s_0 s_1$. The modified transfer function in terms of the states is found by adding the gains of all the merging branches into the zero state. It is found to be:

$$T(I,D) = D_{11}S_1 + D_{12}S_2 + D_{12}S_3$$

Solving the transition equation for the states and substituting in the modified transfer function equation, yields the required modified transfer function. The bit error probability is calculated from equation (2.15), where the derivative of the modified transfer function is to be evaluated around I=1. The derived bounds on the bit error probability of this code are plotted versus the NE_s/N_o in Figure 2.2. Also, the simulation results are presented on the same Figure. It is clear that the existing bound is far away from the simulation curve by almost 2 dBs. Also, it can be observed that the tighter bound is very close to the simulation curve, validating the above derivation.

2.5.2 Eight-State QPSK ST Code

This code is an extension of the previous code but with an additional memory element resulting in an 8-state code. The state diagram of the code is shown in Figure 1.4-a. The state transition matrix is found to be:

$$\begin{bmatrix} S_1 \\ S_2 \\ S_3 \\ S_4 \\ S_5 \\ S_6 \\ S_7 \end{bmatrix} = \begin{bmatrix} 0 & ID_{12} & 0 & ID_{12} & 0 & ID_1 & 0 \\ 0 & ID_{22} & 0 & ID_2 & 0 & I & 0 \\ 0 & I^2D_{12} & 0 & I^2D_{12} & 0 & I^2D_1 & 0 \\ D_1 & 0 & D_1 & 0 & D_{12} & 0 & D_1 \\ ID_{11} & 0 & ID_{11} & 0 & ID_{11} & 0 & ID_1 \\ ID_{12} & 0 & ID_{12} & 0 & ID_1 & 0 & ID_1 \\ I^2D_{11} & 0 & I^2D_{11} & 0 & I^2D_{11} & 0 & I^2D_1 \end{bmatrix} \begin{bmatrix} S_1 \\ S_2 \\ S_3 \\ S_4 \\ S_5 \\ S_6 \\ S_7 \end{bmatrix} + \begin{bmatrix} ID_1 \\ ID_2 \\ ID_1 \\ 0 \\ 0 \\ 0 \\ 0 \end{bmatrix},$$

and the state vector solution is found to be:

$$\begin{bmatrix} S_1 \\ S_2 \\ S_3 \\ S_4 \\ S_5 \\ S_6 \\ S_7 \end{bmatrix} = \begin{bmatrix} 1 & -ID_{12} & 0 & -ID_{12} & 0 & -ID_1 & 0 \\ 0 & 1-ID_{22} & 0 & -ID_2 & 0 & -I & 0 \\ 0 & -I^2D_{12} & 1 & I^2D_{12} & 0 & -I^2D_1 & 0 \\ -D_1 & 0 & -D_1 & 1 & -D_{12} & 0 & -D_1 \\ -ID_{11} & 0 & -ID_{11} & 0 & 1-ID_{11} & 0 & -ID_{11} \\ -ID_{12} & 0 & -ID_{12} & 0 & -ID_1 & 1 & -ID_1 \\ -I^2D_{11} & 0 & -I^2D_{11} & 0 & -I^2D_{11} & 0 & 1-I^2D_1 \end{bmatrix}^{-1} \begin{bmatrix} -ID_1 \\ -ID_2 \\ -ID_1 \\ 0 \\ 0 \\ 0 \\ 0 \end{bmatrix}$$

The D's are defined in equation (2.30). The modified transfer function in terms of the states is:

$$T(I,D) = D_2S_2 + D_{22}S_4 + D_2S_6$$

Solving the transition equation for the states and substituting in the bit error probability for the modified transfer function yields the existing bound. The derived bounds on the bit error probability of this code are plotted versus NE_s/N_o in Figure 2.3. Also, the simulation results are presented on the same Figure. It is clear that the existing bound is far away from the simulation curve by almost 2 dBs. Also, it can be observed that the tighter bound is very close to the simulation curve, validating the above derivation.

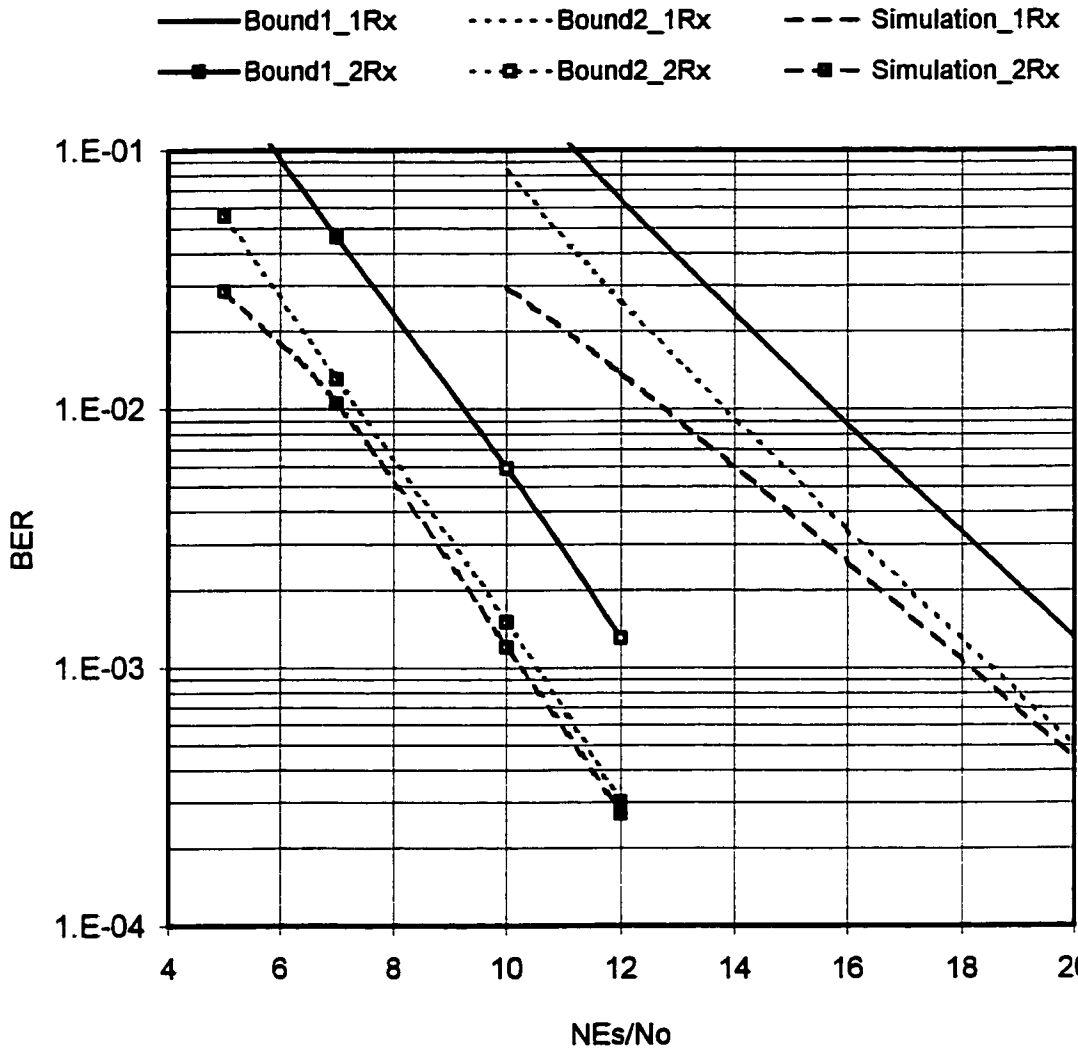

Figure 2.2: Performance of the 4-state QPSK ST code designed in [1].

2.6 Summary

Throughout this chapter, the performance of ST codes over rapid Rayleigh fading channels was discussed in details. Two upper bounds on the bit error probability were derived, evaluated and compared for QPSK ST code presented in [1]. From the expressions of the bounds, two main design criteria of ST codes over rapid fading channels can be stated. The first one is to maximize the ST-MTD of the code and the second one is to maximize the ST-MSPD of the code. In the next chapter, the design of good ST codes over rapid fading channels is considered. The above criteria are used as guidelines in the design process.

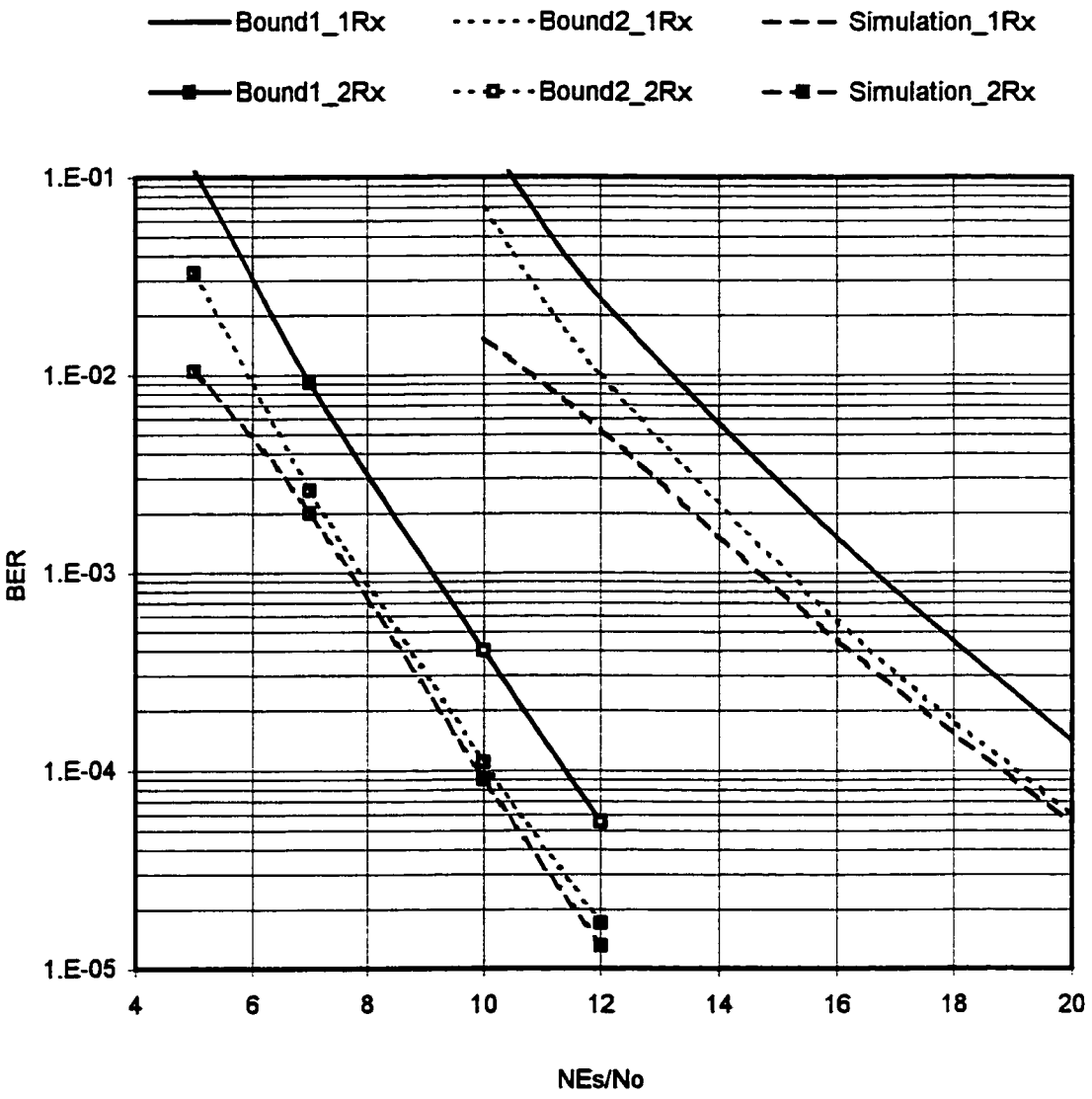

Figure 2.3: Performance of the 8-state QPSK ST code designed in [1].

CHAPTER 3

DESIGN OF ST CODES FOR RAPID FADING CHANNELS

3.1 Introduction

As mentioned in the introductory chapter, the design of ST codes for rapidly changing fading channels was not considered in the literature. However, some ST codes were designed in [1] for quasi-static fading channels for N=2, using QPSK, 8PSK and 16QAM constellations. Therefore, this chapter is devoted to the design of good ST codes to transmit signals over rapid fading channels using two transmit antennas, N=2. The design is based on choosing the branch labels of the trellis code so that the design criteria of ST

codes over rapid fading channels developed in Chapter 2 are maximized. The case of N=2 was considered because using higher number of transmit antennas does not provide large diversity gains over systems with less transmit antennas as that provided in two transmit antennas compared to the one antenna case [1].

In the next section, the designed and existing codes based on QPSK constellation are explained in details. Then, the designed codes based on the 16-QAM constellation are discussed. Following that, the decoding algorithms used to decode the I-Q ST codes are presented and illustrated. Finally, the designed codes are compared with the existing codes for channels with different fading rates.

3.2 ST Codes based on QPSK Constellation

In this section, the design of ST codes based on the QPSK signal constellation is discussed. Two ST codes with throughputs of 2bit/s/Hz for rapid fading channels are designed in the following. The first code uses single MTCM encoder to output the transmitted signals on both antennas. The second code uses the I-Q encoding scheme to maximize the design criteria developed in Chapter 2. The QPSK ST code presented in [1] is explained at the beginning.

QPSK1:

This ST code was designed in [1] for quasi-static fading channels. For simplicity of notation, it will be referred to as QPSK1 throughout the following discussion. Its throughput is 2 bit/s/Hz and it uses a rate-2/4 MTCM encoder to encode the incoming 2 bits to 4 output bits. The 4 bits at the output of the encoder are mapped onto two QPSK

signals. Since there are 2 input bits, there are four departing branches from each state. For the code to have no parallel branches, which is required in fading channels, it should have at least 2 memory elements and hence 4 states. Since this code is designed for quasi-static fading channels, it is expected to perform poorly over rapid fading channels. However, it is presented here for comparison purposes as a baseline of ST codes. So, the new designed QPSK ST codes are compared to this code since it is the only reference for comparison.

The QPSK1 codes having 4 to 32 states were presented in [1] and the trellis diagrams of the 4 and 8-state codes are shown in Figure 1.4-a. Design rules were drawn from the design criteria for the fully connected trellis codes in [1] as follows. Branches departing from the same state differ in the second symbol and branches arriving at the same state differ in the first symbol. In other words, the symbol on the first antenna specifies the current state while the symbol on the second antenna specifies the next state. As explained in section 1.5.2, this code can be viewed as the delay diversity system presented in [9]. It is stated in [1] that these design rules insure the required diversity gain in the overall performance over quasi-static fading channels. The ST-MTD of the 4-state and 8-state codes is 2. The ST-MSPD's of the 4-state and 8-state are 4 and 16, respectively. Of course, this code is not good for rapid fading channels since the ST-MTD and ST-MSPD are very small and can be improved using different design rules. Such codes are discussed in the following.

QPSK2:

This is a ST code with throughput of 2 bits/s/Hz. It is referred to as QPSK2 throughout the following sections. It uses a rate-2/4 MTCM encoder, resulting into a 2-dimensional

QPSK signal space at the output of the encoder. It is designed to maximize both the ST-MTD and the ST-MSPD of the code. To be able to do this, the 2-dimensional QPSK signal space at the output of the encoder is partitioned into subsets. At each time the partitioning is performed, it is required to increase the HD between signals in the same subset, which is referred to as inter-subset HD. If this HD can not be increased anymore, then the partitioning is performed so that the inter-subset ST squared product distance (ST-SPD) is increased. This is repeated until each subset has number of signal pairs equal to the number of departing branches at each state, which is 4 in this case. At this time, both the HD and the ST-SPD between pairs in the same subset are maximized.

This procedure is the conventional one used in designing MTCM codes for Rayleigh fading channels [29], except for the replacement of the MTD and MSPD by the ST-MTD and ST-MSPD, respectively. By doing this, the design criteria for rapid fading channels are satisfied. The set partitioning of a 2-dimensional QPSK signal space is shown in Figure 3.1. The design rules used to design this code are the following. The signals that appear as the labels of branches that diverge from the same state are drawn from the same subset. Moreover, signal labels of branches that emerge at the same state have HD maximized to two. By following these rules, it is insured that the designed code gives the maximum ST-MTD and ST-MSPD as desired by insuring the maximum HD and ST-SPD between the possible encoded symbols.

The trellis diagram of this code is shown in Figure 3.2. The ST-MTD is 2 for both the 4-state and 8-state codes. In these codes, the mentioned design rules are applied. The ST-MSPD for both the 4-stste and 8-state codes is 24, which is much higher than that of the

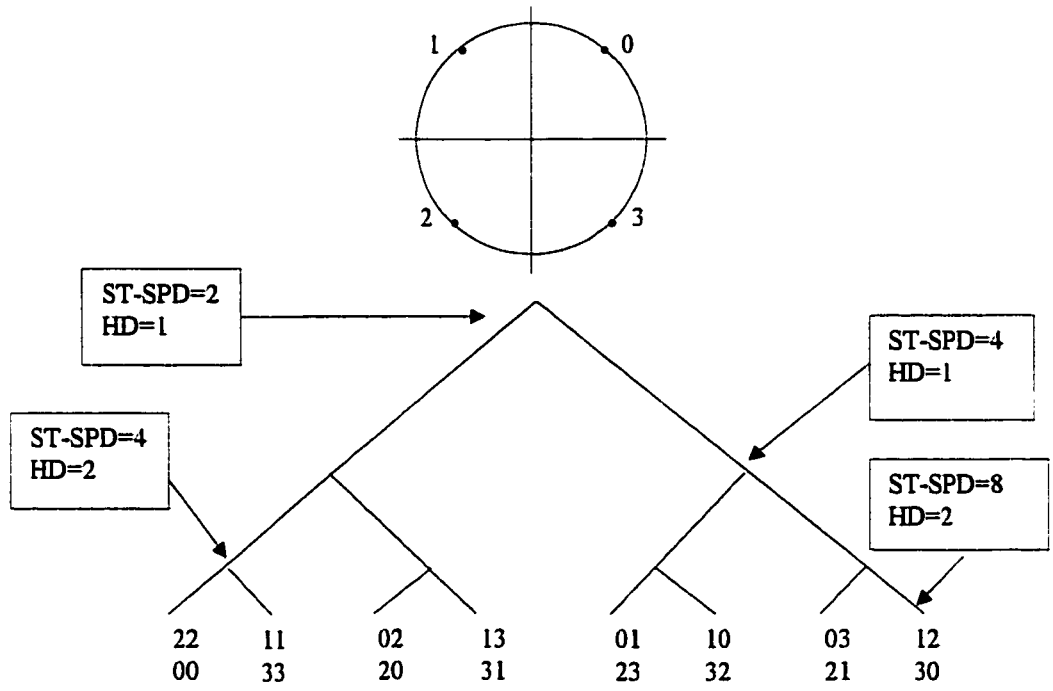

Figure 3.1: 2-dimensional QPSK set partitioning.

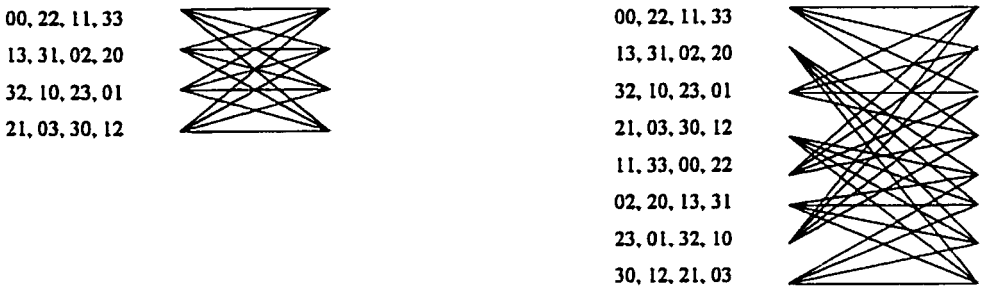

Figure 3.2: QPSK2 ST code, 4 and 8-state, 2 b/s/Hz.

QPSK1 codes. Since the multiplicity of the shortest error event path is reduced in the case of 8-state code, the 8-state code outperforms the 4-state code.

I-Q:

This is a ST code with throughput of 2 bits/s/Hz. It is designed using the I-Q encoding scheme. The structure of the encoder/decoder employing the ST concept, that is used to produce this code, is shown in Figure 3.3. It uses two rate ½ encoders, where each one encodes one bit per signaling interval. Each encoder outputs two bits: the first two bits from both encoders are mapped into a QPSK signal to be transmitted over the first antenna. The second two bits are mapped into the second QPSK symbol and transmitted over the second antenna. The codes used were designed in [26] but were used with one transmit antenna. However, they are used here with two transmit antennas and, hence they are used to transmit the encoded symbols from both encoders at the same time. In I-Q ST encoders, each encoder encodes one component of the two transmitted signals, i.e: either the I or the Q components. So, if the MTD and MSPD of each encoder are maximized, then the ST-MTD and ST-MSPD of the overall code are also maximized.

The trellis diagrams of the 4-state and 8-state codes are shown in Figure 3.4. It can be observed that the labels of branches departing or emerging at the same state differ in both bits. This maximizes the MTD of the 4-state and 8-state codes to be 5 and 6, respectively. Hence, the ST-MTD's of the 4-state and 8-state codes are 3 and 4, respectively. The ST-MSPD of the 4-state and 8-state codes is 32. The huge increase in both the ST-MTD and the ST-MSPD resulting from using the I-Q encoding scheme instead the single MTCM encoder is clear and its effect will be observed in the performance of the code.

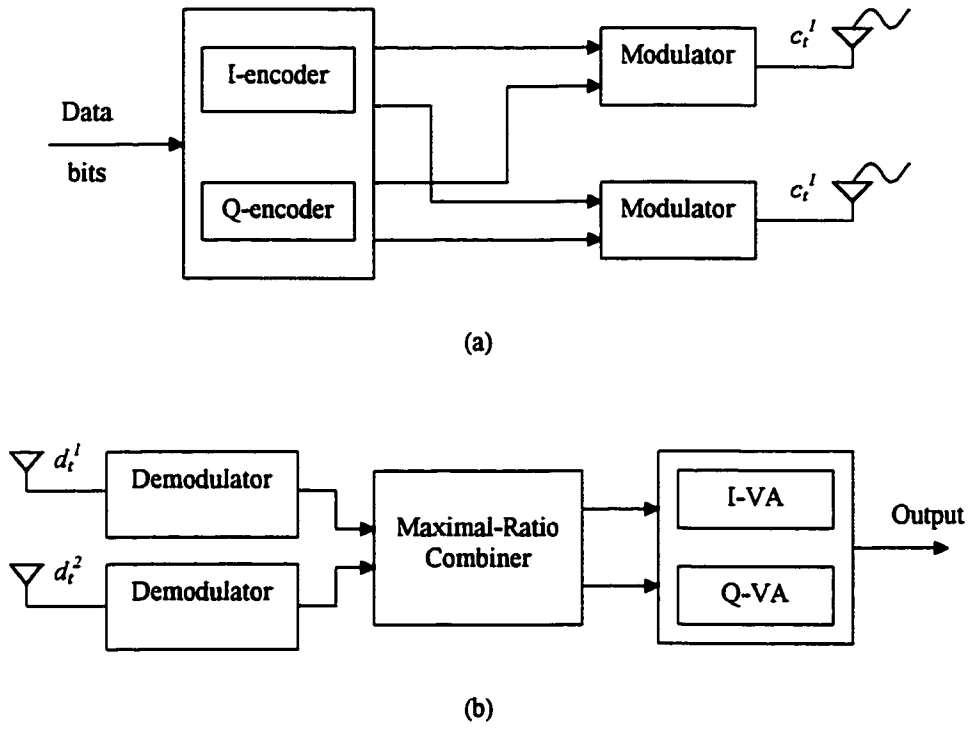

Figure 3.3: The structure of the I-Q ST system (a) Encoder, (b) Decoder.

Figure 3.4: I-Q S-T code designed in [26], 4 and 8-state, 2 b/s/Hz.

3.3 ST Codes based on 16-QAM Constellation

In the following, two ST codes that use two transmit antennas are designed based on the 16-QAM signal constellation. The first code uses single MTCM encoder to output the transmitted signals on both antennas where the second code uses the I-Q encoding scheme. The 16-QAM ST code presented in [1] is explained at the beginning.

QAM1:

This is a ST code with a throughput of 4 bit/s/Hz. It is referred to as QAM1 throughout the discussion. It uses a rate-4/8 MTCM encoder to encode the 4 input bits into 8 bits. The 8 bits at the output of the encoder are mapped into two 16-QAM signals drawn from a 2-dimensional 16-QAM signal space. The one-dimensional 16-QAM signal constellations using natural and Gray mapping are shown in Figure 3.5. This code uses the naturally mapped 16-QAM constellation. Since there are four input bits, then the number of departing branches from each state is 16, and hence the encoder should have 16 states so that the code has no parallel branches, which is an important condition for code design in fading channels. The trellis of the 16-state code was designed for quasi-static fading channel and shown in Figure 3.6. It is designed in [1] based on the corresponding design criteria for quasi-static fading channels. Hence, it is not expected to perform well over rapid fading channels but is considered as the baseline for 16-QAM ST codes. Therefore, the new designed codes in this section are compared to this code as a reference.

The code has the following properties: branches departing from the same state differ in the second symbol and branches arriving at the same state differ in the first symbol. These

properties are the design rules for the fully connected trellis codes as found in [1]. The ST-MTD and ST-MSPD of this code are 2 and 0.16, respectively. It can be seen that this code does not perform well in rapid fading channel because of its low ST-MSPD. Codes with higher ST-MTD and ST-MSPD values are designed in the following.

QAM2:

This is a ST code with throughput of 4 bits/s/Hz. It is referred to as QAM1 throughout the discussion. It also uses a rate-4/8 MTCM encoder and the Gray-mapped 16-QAM constellation. The encoder is set to choose one QAM signal pair from 16^2=256 signal pairs. It is designed to maximize both the ST-MTD and the ST-MSPD. To be able to this, the allowed pair of 16-QAM signals to appear at branches departing or emerging into the same state should be different in both symbols. This can be done by following the same permutation method used for the 2-dimensional MPSK signal space in [30] with slight modifications. The permuted vectors are formed such that the aforementioned criteria are satisfied. This maximizes the HD between subsets and hence maximizes the ST-MSPD of the code. In the following, the modified permutation method is explained.

At the beginning, all the possible 16-QAM symbols are listed in order, starting by s_0 and ending with s_{15} in a 16x1 vector. Then a 16x2 vector is formed by listing all the pairs of same first and second symbols. This vector is denoted by A_0^0. The vector, that has the second column of A_0^0 shifted by one row, is denoted by A_i^0. Similarly, when the vector A_i^0 is shifted by one row, it is denoted by A_i^j. Figure 3.7-a shows the vectors A_0^0, A_1^0 and A_0^1 as examples of the permuted vectors. The labels of branches leaving each state is taken as the rows of the vectors having the maximum HD from each other. The trellis diagram of the 16-state code designed using this method is shown in Figure 3.7-b.

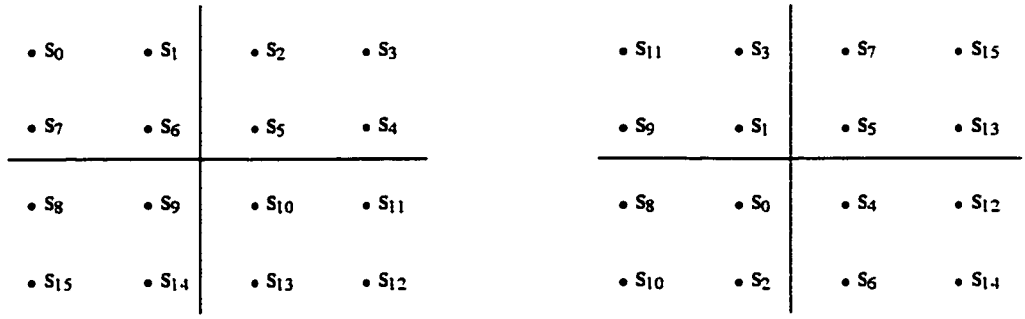

Figure 3.5: 16-QAM signal constellation (a) natural mapping (b) Gray mapping

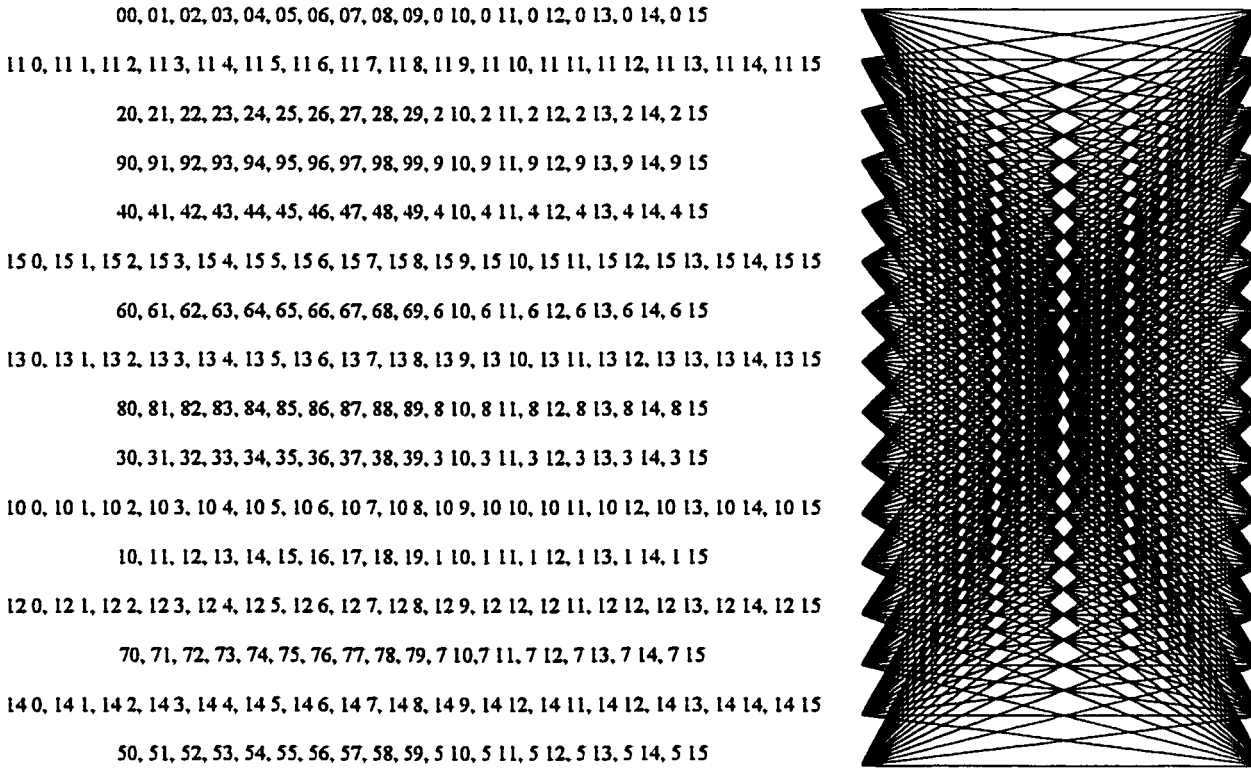

Figure 3.6: Trellis diagram of the QAM1 ST code designed in [1] 4 bits/s/Hz.

$$A_0^{\,0} = \begin{bmatrix} 0 & 0 \\ 1 & 1 \\ 2 & 2 \\ 3 & 3 \\ 4 & 4 \\ 5 & 5 \\ 6 & 6 \\ 7 & 7 \\ 8 & 8 \\ 9 & 9 \\ 10 & 10 \\ 11 & 11 \\ 12 & 12 \\ 13 & 13 \\ 14 & 14 \\ 15 & 15 \end{bmatrix} \qquad A_1^{\,0} = \begin{bmatrix} 0 & 1 \\ 1 & 2 \\ 2 & 3 \\ 3 & 4 \\ 4 & 5 \\ 5 & 6 \\ 6 & 7 \\ 7 & 8 \\ 8 & 9 \\ 9 & 10 \\ 10 & 11 \\ 11 & 12 \\ 12 & 13 \\ 13 & 14 \\ 14 & 15 \\ 15 & 0 \end{bmatrix} \qquad A_0^{\,1} = \begin{bmatrix} 1 & 1 \\ 2 & 2 \\ 3 & 3 \\ 4 & 4 \\ 5 & 5 \\ 6 & 6 \\ 7 & 7 \\ 8 & 8 \\ 9 & 9 \\ 10 & 10 \\ 11 & 11 \\ 12 & 12 \\ 13 & 13 \\ 14 & 14 \\ 15 & 15 \\ 0 & 0 \end{bmatrix}$$

(a)

$A_0^{\,0}$	00, 11, 22, 33, 44, 55, 66, 77, 88, 99, 10 10, 11 11, 12 12, 13 13, 14 14, 15 15
$A_8^{\,1}$	15 7, 08, 19, 2 10, 3 11, 4 12, 5 13, 6 14, 7 15, 80, 91, 10 2, 11 3, 12 4, 13 5, 14 6
$A_4^{\,2}$	14 2, 15 3, 04, 15, 26, 37, 48, 59, 6 10, 7 11, 8 12, 9 13, 10 14, 11 15
$A_{12}^{\,3}$	13 9, 14 10, 15 11, 0 12, 1 13, 2 14, 3 15, 40, 51, 62, 73, 84, 95, 10 6, 11 7, 12 8
$A_1^{\,4}$	12 13, 13 14, 14 15, 15 0, 01, 12, 23, 34, 45, 56, 78, 89, 9 10, 10 11, 11 12
$A_9^{\,5}$	11 4, 12 5, 13 6, 14 7, 15 8, 09, 1 10, 2 11, 3 12, 4 13, 5 14, 6 15, 70, 81, 92, 10 3
$A_5^{\,6}$	10 15, 11 0, 12 1, 13 2, 14 3, 15 4, 05, 16, 27, 38, 49, 5 10, 6 11, 7 12, 8 13, 9 14
$A_{13}^{\,7}$	96, 10 7, 11 8, 12 9, 13 10, 14 11, 15 12, 0 13, 1 14, 2 15, 30, 41, 52, 63, 74, 85
$A_2^{\,8}$	8 10, 9 11, 10 12, 11 13, 12 14, 13 15, 14 0, 15 1, 02, 13, 24, 35, 46, 57, 68, 79
$A_{10}^{\,9}$	71, 82, 93, 10 4, 11 5, 12 6, 13 7, 14 8, 15 9, 0 10, 1 11, 2 12, 3 13, 4 14, 5 15, 60
$A_6^{\,10}$	6 12, 7 13, 8 14, 9 15, 10 0, 11 1, 12 2, 13 3, 14 4, 15 5, 06, 17, 28, 39, 4 10, 5 11
$A_{14}^{\,11}$	53, 64, 75, 86, 97, 10 8, 11 9, 12 10, 13 11, 14 12, 15 13, 0 14, 1 15, 20, 31, 42
$A_4^{\,12}$	48, 59, 6 10, 7 11, 8 12, 9 13, 10 14, 11 15, 12 0, 13 1, 14 2, 15 3, 04, 15, 26, 37
$A_{11}^{\,13}$	3 14, 4 15, 50, 61, 72, 83, 94, 10 5, 11 6, 12 7, 13 8, 14 9, 15 10, 0 11, 1 12, 2 13
$A_7^{\,14}$	29, 3 10, 4 11, 5 12, 6 13, 7 14, 8 15, 90, 10 1, 11 2, 12 3, 13 4, 14 5, 15 6, 07, 18
$A_5^{\,15}$	15, 26, 37, 48, 59, 6 10, 7 11, 8 12, 9 13, 10 14, 11 15, 12 0, 13 1, 14 2, 15 3, 04

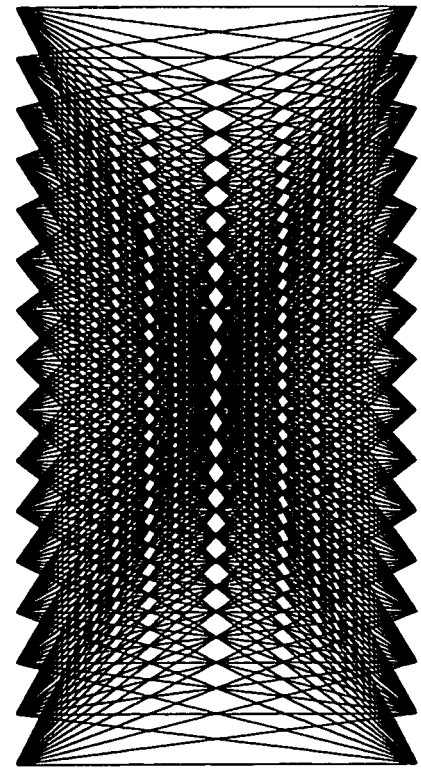

(b)

Figure 3.7: (a) Examples of vectors used in the permutation method of the 2-dimensional 16-QAM signal space, (b) Trellis diagram of the QAM2 ST code, 4 bits/s/Hz.

Using the modified permutation method enables us to choose the branch labels of the code, so that the labels of branches emerging or leaving the same states are different in both symbols. This insures the same ST-MTD and higher ST-MSPD than the previous code QAM1, by insuring the maximum HD and ST-SPD between the possible encoded symbols. The ST-MTD and the ST-MSPD of the 16-state code are 2 and 3.2, respectively. It can be seen that this code has higher ST-MSPD than QAM1 code, and hence it is expected to outperform it.

I-Q:

This is a ST code with throughput of 4 bit/s/Hz. It is designed using the I-Q encoding scheme and uses the same encoder/decoder shown in Figure 3.3. It consists of two rate 2/4 encoders, where each one encodes two bits per signaling interval. Each encoder outputs two 4-AM symbols: the first two symbols from both encoders are mapped onto a 16-QAM signal to be transmitted over the first antenna. The second two symbols are mapped into the second 16-QAM symbol and transmitted over the second antenna. So, the I-encoder outputs the I components of both signals where the Q components of both signals are taken as the outputs of the Q-encoder.

In order to design codes with the highest possible MTD and MSPD, the 2-dimensional 4-AM signal space is partitioned in the same way the 2-dimensional QPSK signal space was partitioned. The partitioning process is done so that the HD and the SPD in the generated subsets are higher each time the partitioning is performed. The partitioning process is repeated until the number of the signals in each subset is equal to the number of the branches leaving one state (i.e.: 4). The set partitioning of the 2-dimensional 4-AM signal space is shown in Figure 3.8.

The minimum number of memory elements used in each encoder is 2 (i.e.: the number of states equal to 2^2=4 states), so that there are no parallel branches from one state to another. The trellis diagrams of the 4, 8, 16 and 32-state codes are shown in Figure 3.9. It can be observed from the trellis diagrams that the labels of branches departing or emerging at the same state differ in both symbols. This maximizes the ST-MTD of the 4, and 8-state to 2 and that of the 16 and 32-state codes to 3. Note that the MTD of the 4, and 8-state is 4 and that of the 16 and 32-state is 6. The ST-MSPD is maximized if the MSPD of the code is maximized. The MSPD of the 4 and 8-state codes is 14.75 and those of the 16 and 32-state codes are 9.44, and 151, respectively. Moreover, the ST-MSPD is 16.6 for the 4 and 8-state codes, 26.6 for the 16-state code and 106 for the 32-state code. The large difference in both the ST-MTD and the ST-MSPD, compared to those of the previous 16-QAM codes, and resulting from using the I-Q encoding scheme is clearly observed.

The complexity of a trellis code is equal to the total number of branches leaving all states divided by the associated information bits with each transition. In the QAM1 and QAM2 cases, there are 16x16 total branches and 4 information bits associated with each transition, resulting in a complexity of 256/4=64. The I-Q code that has a similar complexity is the 32-state code, since the total number of branches is (4x32+4x32) and the number of associated information bits 4. Hence, the resulting complexity is 64, which is the same as the QAM1 and QAM2 codes. So, for fair comparison, the 16-state QAM1 and QAM2 codes are compared to the 32-state I-Q code. The decoding algorithms used to decode the I-Q ST codes are presented in the following section.

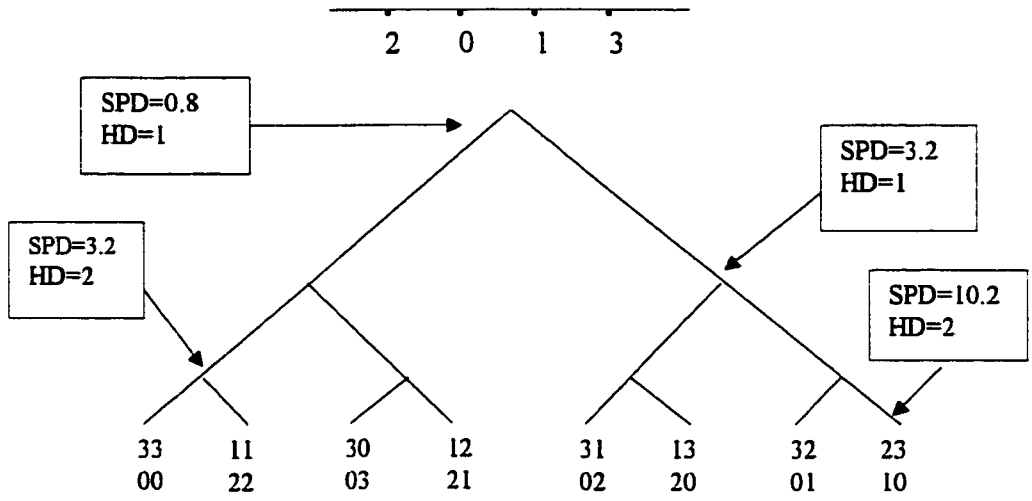

Figure 3.8: 2-dimensional 4-AM set partitioning.

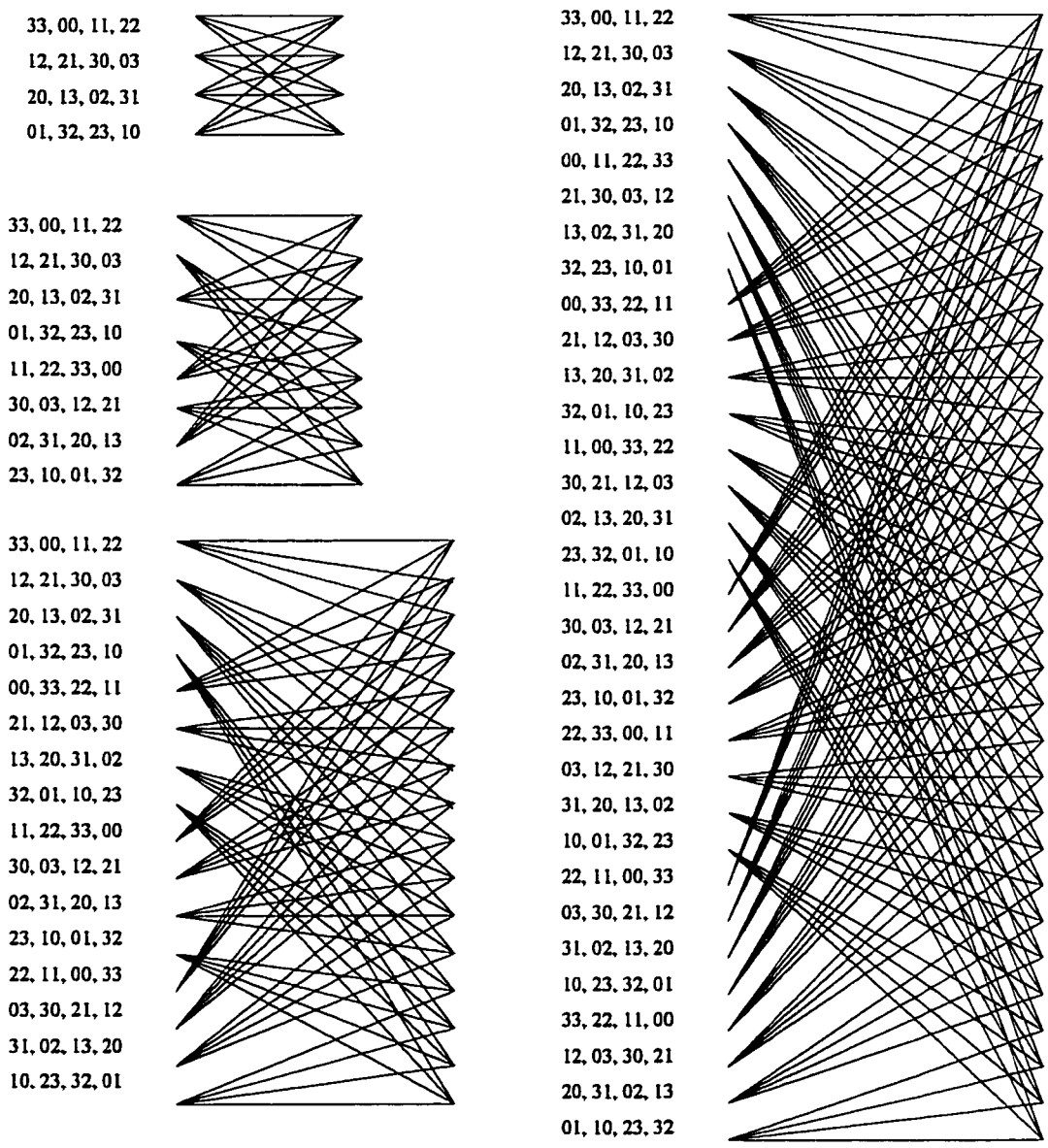

Figure 3.9: Trellis diagrams of I-Q QAM ST code (4, 8, 16 and 32-state), 4 bit/s/Hz.

3.4 Suboptimal Decoding of I-Q ST Codes

At the receiver, the received signal at the j^{th} receive antenna has the following form:

$$d_t^j = \sum_{i=1}^{N} (\alpha_{Iij,t}+j\,\alpha_{Qij,t}).(x_t^i+jy_t^i) + \eta_t^j \qquad (3.1)$$

Where $(\alpha_{Iij,t}+j\alpha_{Qij,t})$ is the path gain from the i^{th} transmit antenna to the j^{th} receive antenna at time t. It is sampled from a complex Gaussian random process with zero mean and a variance of unity in both dimensions. The symbol, $(x_t^i+jy_t^i)$ represents the complex baseband signal transmitted from the i^{th} transmit antenna at time interval t. Throughout this section, the subscript t is omitted for simplicity of notation. Equation (3.1) can be further manipulated as follows:

$$d^j = \sum_{i=1}^{N} \{ (\alpha_{Iij}\, x^i - \alpha_{Qij} y^i) + j\,(\alpha_{Iij} y^i + \alpha_{Qij} x^i) \} + \eta^j \qquad (3.2)$$

or:

$$d^j = r_I^j + jr_Q^j + \eta^j \qquad (3.3)$$

Where the subscripts I and Q in Equation (3.3) denote the in-phase and quadrature components of the received signals and the fades samples. It is clear that the received signal is a function of all in-phase and quadrature components of the transmitted signals. Since the I-decoder does not know any information about the signals at the output of the Q encoder (i.e: Q components of the transmitted signals), new detection scheme for the Q components is required to be devised.

In the regular I-Q coding, the fade phase effect can be compensated for upon the reception of each signal. Hence, it was possible to decouple the in-phase and quadrature parts from each other and decode them independently. However, it is not possible to do so

for the I-Q ST codes since the phase of each transmitted signal was affected by a fade's phase independently from other transmitted signals, and all the transmitted signals were added at the receiver. So, the phase of each transmitted signal cannot be recognized from the received sum and hence, cannot be compensated for in this case. The proposed decoding algorithm solves this problem by using a detection scheme to detect the quadrature components in the I-decoder and the in-phase components in the Q-decoder. The analysis is performed for the case of two transmit antennas and is devoted for the I-decoder case. The same algorithm is applicable to the Q-decoder.

The method is based on partitioning the signal space at the output of the transmit antennas and compute a metric for each subset. The resultant metrics are then used in the Viterbi algorithm to decode the I components. Since there are two transmitted signals at each signaling interval, there is a 2-dimesional signal space of the constellation used. In general, space partitioning is performed such that each subset has one of the possible signals at the output of the I-encoder. In the following, the mentioned set partitioning is applied to the I-Q ST codes based on both the QPSK and 16-QAM constellations.

3.4.1 I-Q ST QPSK Codes

Let S^{lk} denotes the set of the QPSK signal pairs that are transmitted from the I-Q ST encoder given that the bits at the output of the I-encoder are l and k. From this notation, the bit l is the in-phase component of the signal transmitted over the first transmit antenna, while the bit k is the in-phase component of the signal transmitted via the second transmit antenna. In addition, the signal s_j^i is the QPSK signal whose label is j, that is transmitted over the i^{th} transmit antenna. The QPSK signal constellation used here is the

Gray-mapped constellation shown in Figure 3.1. The 2-dimensional QPSK signal space is partitioned as follows.

$$S^{00} = \{(s_0^1, s_0^2), (s_0^1, s_2^2), (s_2^1, s_0^2), (s_2^1, s_2^2)\}$$

$$S^{10} = \{(s_1^1, s_0^2), (s_1^1, s_2^2), (s_3^1, s_0^2), (s_3^1, s_2^2)\}$$

$$S^{01} = \{(s_0^1, s_1^2), (s_0^1, s_3^2), (s_2^1, s_1^2), (s_2^1, s_3^2)\}$$

$$S^{11} = \{(s_1^1, s_1^2), (s_1^1, s_3^2), (s_3^1, s_1^2), (s_3^1, s_3^2)\} \tag{3.4}$$

Now, the following four metrics are computed at the I-decoder before the trellis:

$$M_{lk} = \min_{(s^1, s^2) \in S^{lk}} \sum_{j=1}^{M} \left(r_I^j - \sum_{i=1}^{N} \alpha_{Iij} x^j + \sum_{i=1}^{N} \alpha_{Qij} y^j \right)^2$$

$$+ \left(r_Q^j - \sum_{i=1}^{N} \alpha_{Qij} x^j - \sum_{i=1}^{N} \alpha_{Iij} y^j \right)^2 \tag{3.5}$$

Where x^j and y^j are the in-phase and quadrature components of the QPSK signal s_j^l. In each M_{lk}, four metrics are compared and the minimum is found accordingly, ending with four different metrics. Each of the four remaining metrics is associated with one of the four different bit combinations that may be at the output of the I-encoder. These metrics are computed before the trellis of the I-decoder and hence, their computation is considered to be in the detection stage.

At each state inside the trellis, the decoder compares two of above metrics whose subscripts l and k are the same as the labels of the branches emerging at that state. Since the encoder of this system has one input bit, there are two branches emerging at each state and hence, there are two possible metrics to be compared at each state in the trellis. It is clear that the proposed decoding algorithm does need a pre-trellis metric computation, but it does not need additional computation in the trellis, because all the computed metrics

must be computed at a time during the Viterbi decoding algorithm. So, after the metrics have been computed, the work done in trellis is a comparison of the appropriate metrics not computing any new metrics.

3.4.2 I-Q ST 16-QAM Codes

The same decoding algorithm is used for the 16-QAM encoded I-Q ST systems. For this code, the signal space to be partitioned is a 2-dimensional 16-QAM space that consists of 16^2 possible signal pairs. In the same token as the QPSK case, the partitioning is performed so that all pairs in one subset are due to the same 4-AM symbol pair at the output of the I-encoder. Hence, for each 4-AM symbol pair, there are 16 possible 16-QAM signal pairs that could be transmitted from both transmit antennas.

Again, the notation S^{lk} denotes the possible 16-QAM pairs that can appear at the output of the I-Q ST encoder given that the 4-AM symbols at the output of the I-encoder are l and k. In addition, the signal s_j^i is the 16-QAM signal whose label in the constellation is j, and is transmitted over the i^{th} transmit antenna. The 16-QAM signal constellation using Gray mapping is found in Figure 3.4. The set partitioning yields the following subsets.

$$S^{00} = \{ (s_0^1,s_0^2),(s_0^1,s_1^2),(s_0^1,s_2^2),(s_0^1,s_3^2),(s_1^1,s_0^2),(s_1^1,s_1^2),(s_1^1,s_2^2),(s_1^1,s_3^2),$$
$$(s_2^1,s_0^2),(s_2^1,s_1^2),(s_2^1,s_2^2),(s_2^1,s_3^2),(s_3^1,s_0^2),(s_3^1,s_1^2),(s_3^1,s_2^2),(s_3^1,s_3^2) \}$$

$$S^{01} = \{ (s_0^1,s_4^2),(s_0^1,s_5^2),(s_0^1,s_6^2),(s_0^1,s_7^2),(s_1^1,s_4^2),(s_1^1,s_5^2),(s_1^1,s_6^2),(s_1^1,s_7^2),$$
$$(s_2^1,s_4^2),(s_2^1,s_5^2),(s_2^1,s_6^2),(s_2^1,s_7^2),(s_3^1,s_4^2),(s_3^1,s_5^2),(s_3^1,s_6^2),(s_3^1,s_7^2) \}$$

$$S^{02} = \{ (s_0^1,s_8^2),(s_0^1,s_9^2),(s_0^1,s_{10}^2),(s_0^1,s_{11}^2),(s_1^1,s_8^2),(s_1^1,s_9^2),(s_1^1,s_{10}^2),(s_1^1,s_{11}^2),$$
$$(s_2^1,s_8^2),(s_2^1,s_9^2),(s_2^1,s_{10}^2),(s_2^1,s_{11}^2),(s_3^1,s_8^2),(s_3^1,s_9^2),(s_3^1,s_{10}^2),(s_3^1,s_{11}^2) \}$$

$$S^{03} = \{ (s_0^1,s_{12}^2),(s_0^1,s_{13}^2),(s_0^1,s_{14}^2),(s_0^1,s_{15}^2),(s_1^1,s_{12}^2),(s_1^1,s_{13}^2),(s_1^1,s_{14}^2),(s_1^1,s_{15}^2),$$
$$(s_2^1,s_{12}^2),(s_2^1,s_{13}^2),(s_2^1,s_{14}^2),(s_2^1,s_{15}^2),(s_3^1,s_{12}^2),(s_3^1,s_{13}^2),(s_3^1,s_{14}^2),(s_3^1,s_{15}^2) \}$$

$$S^{10} = \{ (s_4^1,s_0^2),(s_4^1,s_1^2),(s_4^1,s_2^2),(s_4^1,s_3^2),(s_5^1,s_0^2),(s_5^1,s_1^2),(s_5^1,s_2^2),(s_5^1,s_3^2),$$
$$(s_6^1,s_0^2),(s_6^1,s_1^2),(s_6^1,s_2^2),(s_6^1,s_3^2),(s_7^1,s_0^2),(s_7^1,s_1^2),(s_7^1,s_2^2),(s_7^1,s_3^2) \}$$

$$S^{11} = \{ (s_4^1,s_4^2),(s_4^1,s_5^2),(s_4^1,s_6^2),(s_4^1,s_7^2),(s_5^1,s_4^2),(s_5^1,s_5^2),(s_5^1,s_6^2),(s_5^1,s_7^2),$$
$$(s_6^1,s_4^2),(s_6^1,s_5^2),(s_6^1,s_6^2),(s_6^1,s_7^2),(s_7^1,s_4^2),(s_7^1,s_5^2),(s_7^1,s_6^2),(s_7^1,s_7^2) \}$$

$$S^{12} = \{ (s_4^1,s_8^2),(s_4^1,s_9^2),(s_4^1,s_{10}^2),(s_4^1,s_{11}^2),(s_5^1,s_8^2),(s_5^1,s_9^2),(s_5^1,s_{10}^2),(s_5^1,s_{11}^2),$$
$$(s_6^1,s_8^2),(s_6^1,s_9^2),(s_6^1,s_{10}^2),(s_6^1,s_{11}^2),(s_7^1,s_8^2),(s_7^1,s_9^2),(s_7^1,s_{10}^2),(s_7^1,s_{11}^2) \}$$

$$S^{13} = \{ (s_4^1,s_{12}^2),(s_4^1,s_{13}^2),(s_4^1,s_{14}^2),(s_4^1,s_{15}^2),(s_5^1,s_{12}^2),(s_5^1,s_{13}^2),(s_5^1,s_{14}^2),(s_5^1,s_{15}^2),$$
$$(s_6^1,s_{12}^2),(s_6^1,s_{13}^2),(s_6^1,s_{14}^2),(s_6^1,s_{15}^2),(s_7^1,s_{12}^2),(s_7^1,s_{13}^2),(s_7^1,s_{14}^2),(s_7^1,s_{15}^2) \}$$

$$S^{20} = \{ (s_8^1,s_0^2),(s_8^1,s_1^2),(s_8^1,s_2^2),(s_8^1,s_3^2),(s_9^1,s_0^2),(s_9^1,s_1^2),(s_9^1,s_2^2),(s_9^1,s_3^2),$$
$$(s_{10}^1,s_0^2),(s_{10}^1,s_1^2),(s_{10}^1,s_2^2),(s_{10}^1,s_3^2),(s_{11}^1,s_0^2),(s_{11}^1,s_1^2),(s_{11}^1,s_2^2),(s_{11}^1,s_3^2) \}$$

$$S^{21} = \{ (s_8^1,s_4^2),(s_8^1,s_5^2),(s_8^1,s_6^2),(s_8^1,s_7^2),(s_9^1,s_4^2),(s_9^1,s_5^2),(s_9^1,s_6^2),(s_9^1,s_7^2),$$
$$(s_{10}^1,s_4^2),(s_{10}^1,s_5^2),(s_{10}^1,s_6^2),(s_{10}^1,s_7^2),(s_{11}^1,s_4^2),(s_{11}^1,s_5^2),(s_{11}^1,s_6^2),(s_{11}^1,s_7^2) \}$$

$$S^{22} = \{ (s_8^1,s_8^2),(s_8^1,s_9^2),(s_8^1,s_{10}^2),(s_8^1,s_{11}^2),(s_9^1,s_8^2),(s_9^1,s_9^2),(s_9^1,s_{10}^2),(s_9^1,s_{11}^2),$$
$$(s_{10}^1,s_8^2),(s_{10}^1,s_9^2),(s_{10}^1,s_{10}^2),(s_{10}^1,s_{11}^2),(s_{11}^1,s_8^2),(s_{11}^1,s_9^2),(s_{11}^1,s_{10}^2),(s_{11}^1,s_{11}^2) \}$$

$$S^{23} = \{ (s_8^1,s_{12}^2),(s_8^1,s_{13}^2),(s_8^1,s_{14}^2),(s_8^1,s_{15}^2),(s_9^1,s_{12}^2),(s_9^1,s_{13}^2),(s_9^1,s_{14}^2),(s_9^1,s_{15}^2),$$
$$(s_{10}^1,s_{12}^2),(s_{10}^1,s_{13}^2),(s_{10}^1,s_{14}^2),(s_{10}^1,s_{15}^2),(s_{11}^1,s_{12}^2),(s_{11}^1,s_{13}^2),(s_{11}^1,s_{14}^2),(s_{11}^1,s_{15}^2) \}$$

$$S^{30} = \{ (s_{12}^1,s_0^2),(s_{12}^1,s_1^2),(s_{12}^1,s_2^2),(s_{12}^1,s_3^2),(s_{13}^1,s_0^2),(s_{13}^1,s_1^2),(s_{13}^1,s_2^2),(s_{13}^1,s_3^2),$$
$$(s_{14}^1,s_0^2),(s_{14}^1,s_1^2),(s_{14}^1,s_2^2),(s_{14}^1,s_3^2),(s_{15}^1,s_0^2),(s_{15}^1,s_1^2),(s_{15}^1,s_2^2),(s_{15}^1,s_3^2) \}$$

$$S^{31} = \{ (s_{12}^1,s_4^2),(s_{12}^1,s_5^2),(s_{12}^1,s_6^2),(s_{12}^1,s_7^2),(s_{13}^1,s_4^2),(s_{13}^1,s_5^2),(s_{13}^1,s_6^2),(s_{13}^1,s_7^2),$$
$$(s_{14}^1,s_4^2),(s_{14}^1,s_5^2),(s_{14}^1,s_6^2),(s_{14}^1,s_7^2),(s_{15}^1,s_4^2),(s_{15}^1,s_5^2),(s_{15}^1,s_6^2),(s_{15}^1,s_7^2) \}$$

$$S^{32} = \{ (s_{12}^{1},s_{8}^{2}),(s_{12}^{1},s_{9}^{2}),(s_{12}^{1},s_{10}^{2}),(s_{12}^{1},s_{11}^{2}),(s_{13}^{1},s_{8}^{2}),(s_{13}^{1},s_{9}^{2}),(s_{13}^{1},s_{10}^{2}),(s_{13}^{1},s_{11}^{2}),$$
$$(s_{14}^{1},s_{8}^{2}),(s_{14}^{1},s_{9}^{2}),(s_{14}^{1},s_{10}^{2}),(s_{14}^{1},s_{11}^{2}),(s_{15}^{1},s_{8}^{2}),(s_{15}^{1},s_{9}^{2}),(s_{15}^{1},s_{10}^{2}),(s_{15}^{1},s_{11}^{2}) \}$$
$$S^{33} = \{ (s_{12}^{1},s_{12}^{2}),(s_{12}^{1},s_{13}^{2}),(s_{12}^{1},s_{14}^{2}),(s_{12}^{1},s_{15}^{2}),(s_{13}^{1},s_{12}^{2}),(s_{13}^{1},s_{13}^{2}),(s_{13}^{1},s_{14}^{2}),(s_{13}^{1},s_{15}^{2}),$$
$$(s_{14}^{1},s_{12}^{2}),(s_{14}^{1},s_{13}^{2}),(s_{14}^{1},s_{14}^{2}),(s_{14}^{1},s_{15}^{2}),(s_{15}^{1},s_{12}^{2}),(s_{15}^{1},s_{13}^{2}),(s_{15}^{1},s_{14}^{2}),(s_{15}^{1},s_{15}^{2}) \} \tag{3.7}$$

Now, the following 16 metrics are computed at the I-decoder before the trellis:

$$M_{lk} = \min_{(s^1,s^2)\in S^{lk}} \sum_{j=1}^{M} \left(r_I^j - \sum_{i=1}^{N} \alpha_{Iij} x^j + \sum_{i=1}^{N} \alpha_{Qij} y^j \right)^2$$
$$+ \left(r_Q^j - \sum_{i=1}^{N} \alpha_{Qij} x^j - \sum_{i=1}^{N} \alpha_{Iij} y^j \right)^2 \tag{3.8}$$

Where x^j and y^j are the in-phase and quadrature components of the 16-QAM signal s_j^i. In each M_{lk}, 16 metrics are compared and the minimum is found accordingly, ending with 16 different metrics. Each of them is associated with one of the 4-AM signal pairs that may be at the I-encoder's output. Since the encoder of this system has two input bits, there are four possible metrics to be compared at each state in the trellis.

The results of the I-Q ST codes show that the suboptimal decoding algorithm used does not give that good performance. This is due to the fact that the suboptimal decoder does nothing but comparing all metrics that have the same I components and all possible values of the Q components. So, it is trying to guess for the best Q components from the received signals. In the case of the QPSK case, there are four different combinations to check and compare their metrics and the performance is somehow degraded as will be explained in the next section. However, in the case of the 16-QAM constellation, there are 4^2=16 different combinations to compare their metrics. As the number of

combinations increases, the performance degrades more. On the other hand, as the SNR increases, the performance approaches that of the optimal decoding. The suboptimal decoding is called suboptimal because the I-decoder decodes the I components using sequence decoding by detecting the Q components symbol-by-symbol not in sequence. The same thing is done for the Q and I components in the Q-decoder, respectively. In order to get the maximum performance of the I-Q ST codes, an optimal but complex decoding algorithm is proposed in the following.

3.5 Optimal Decoding of I-Q ST Codes

3.5.1 The Super-Trellis Decoding

As mentioned above, the performance of the suboptimal decoding becomes worse as the number of signal combinations becomes higher. To mitigate for this phenomenon, especially with the 16-QAM case, the use of the super-trellis decoding is proposed to decode the I-Q ST codes. Its idea is summarized in the following. The I and Q components are decoded using one trellis whose size is the square of that of the individual I and Q trellises. So, in the case of the 4-state I-Q ST code, the super-trellis required to decode this code is of size 4^2=16 states. This means that a 16-state super-trellis is used to decode the 4-state I-Q ST code optimally.

For a given transition between two states in the I and Q encoders, the equivalent transition in the super-trellis is found as follows. The bit representation of the states of the super-trellis is found by concatenating all combinations of bit representation of the individual I and Q states. For example, consider a transition from state 0 to state 2 in the I encoder and

from state 3 to state 1 in the Q encoder is to be represented in the super-trellis notations. Concatenating the I-Q encoders' initial states gives state 03, whose bit representation is (0011) which is state 3 in the super-trellis. Repeating the same process for the final concatenated I-Q states gives state 9 in the super-trellis. So, the above transition can be represented in the super-trellis by a transition from state 3 to state 9. Also, the labels of transitions between super-trellis states are the concatenation of labels of the individual transitions between the equivalent I and Q states. So, each transition between super-trellis states has number of labels that is double the number of labels in single trellis. Figure 3.10 shows the equivalent super-trellis for the 4-state I-Q 16-QAM ST code. In the Figure, S_I and S_Q are the equivalent single-trellis states in the I-encoder and Q-encoder, respectively.

The super-trellis is used to decode I-Q ST codes optimally by decoding (not guessing) the I and Q components simultaneously using sequence decoding. So, the I and Q components are decoded in sequence fashion not as in the suboptimal decoding, which decodes the I components in sequence and the Q components on symbol-by-symbol base. Since the performance of I-Q QPSK ST codes is acceptable and the super-trellis results in an exponential increase in the decoding complexity, the super-trellis is not used to decode these codes. However, it is used to decode the 4-state I-Q QAM ST code only because the resultant super-trellis decoding complexity is $16^2/4=64$, which is the same as the complexities of the QAM1, QAM2 codes and the 32-state I-Q QAM code that uses suboptimal decoding algorithm.

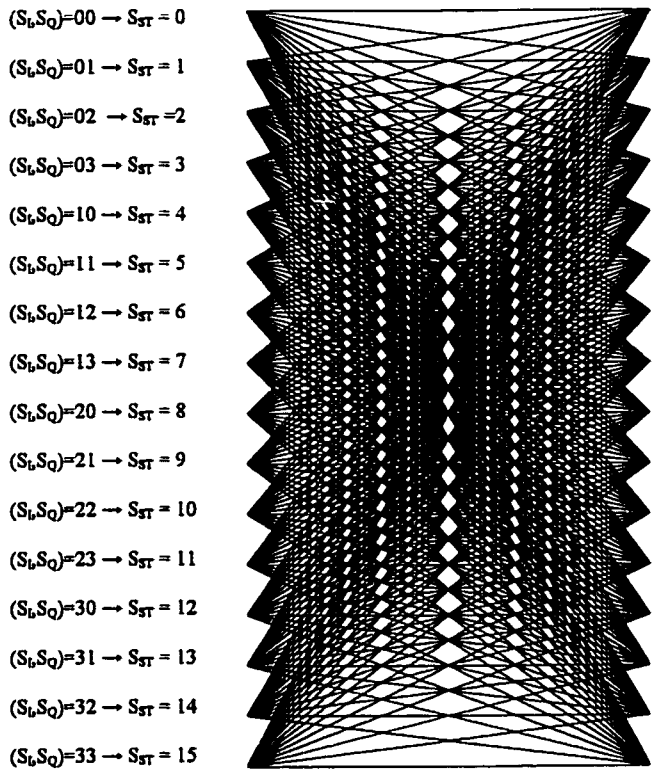

Figure 3.10: Super Trellis diagram used to decode the 4-state I-Q ST 16-QAM code (4 bit/s/Hz).

3.6 Comparisons of Codes

3.6.1 ST Codes Based on QPSK

The ST codes mentioned above were simulated over FNS rapid fading channels, which are characterized by samples from a complex Gaussian random process with zero mean and a total of unity variance in both dimensions for each of the transmit branches, i.e: the variance of each transmit branch is unity in both dimensions. These samples are independent from one sampling interval to the other. This means that the transmitted signals from each antenna at certain sampling time, are affected by independent fades from the next and previous transmitted signals over the same antenna.

Figure 3.11 shows the performance of the 4-state QPSK1, QPSK2 and I-Q codes for the cases in which the receiver is equipped with one or two receive antennas. It is clear from the Figure that the I-Q code is the best followed by QPSK2 and QPSK1. This is expected since the main controlling parameters of the code in rapid fading channels are the ST-MTD and ST-MSPD. Since the I-Q code has the largest ST-MTD and the QPSK1 has the minimum, the order was expected. The I-Q code provides a coding gain of more than 3 dBs over QPSK1 and more than 0.5 dB over QPSK2 at bit error rate (BER) of 10^{-3}. Also, the gain of QPSK2 over QPSK1 is almost 2.5 dBs. The I-Q code is decoded using the suboptimal decoding algorithm. From the tight performance bound on the bit error probability derived in Chapter 2, it is clear that the ST-MTD of the ST code is the controlling factor of the curve slope. By observing the slopes of the performance curves of the first two QPSK codes, it can be seen that they are the same since these codes have

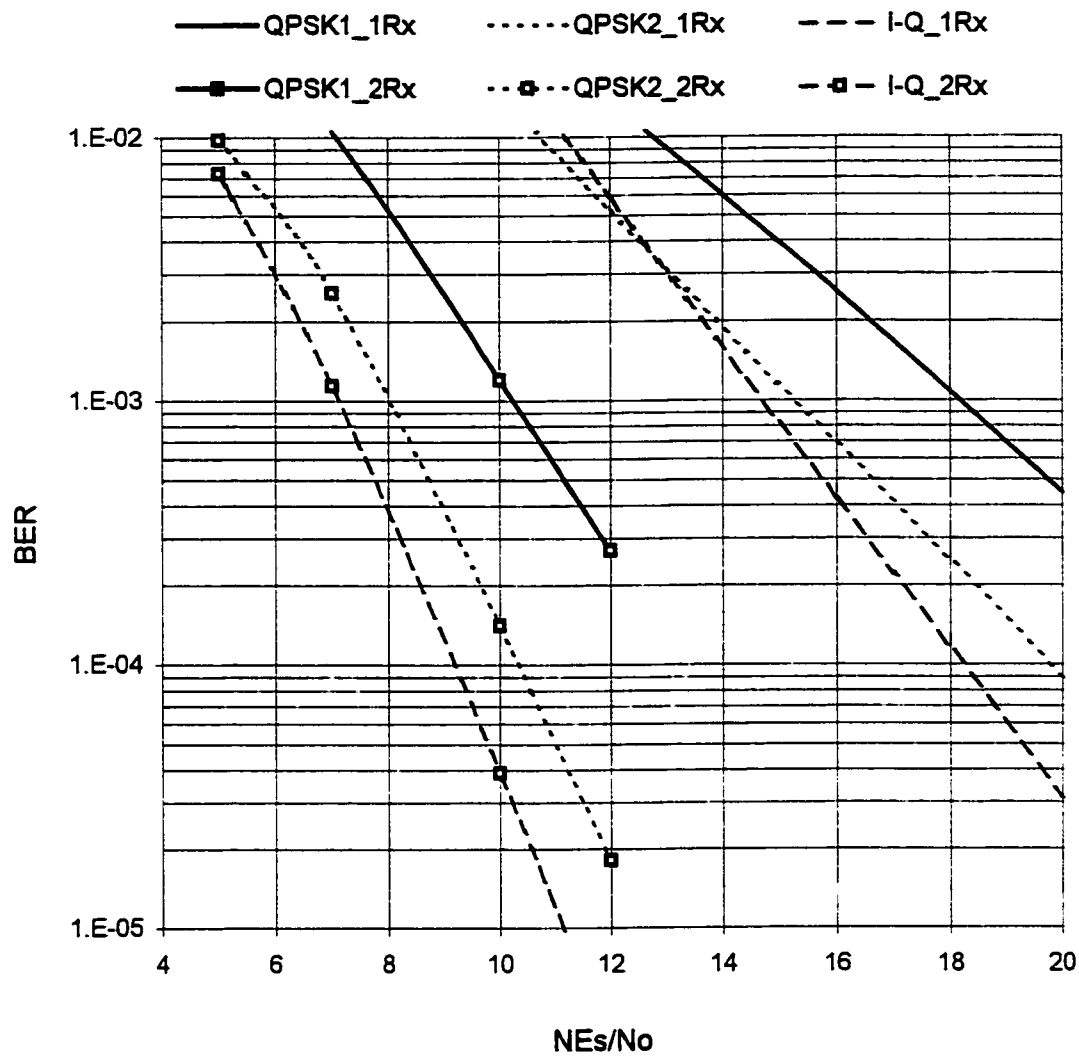

Figure 3.11: Performance of the 4-state QPSK codes for 1-Rx and 2-Rx antenna over rapid fading channel.

the same ST-MTD. However, the slope of the I-Q code is larger and hence the curve is steeper because of its higher ST-MTD.

The same trend is observed in the two-receive antenna case. The gain of the I-Q code over the other two codes increases compared to the one-receive antenna case. However, it is expected to decrease because using two receive antennas provides a form of diversity and hence, the diversity effect provided by the code becomes less important. The reason behind this trend is the sub-optimality of the detection scheme used to decode the I-Q code. The detection scheme discussed above tries to guess for the unknown Q components of the received signals. Since there are four possible combinations for the Q components, the decoder checks the nearest combination that gives the minimum metric M_{lk}. Therefore, the detection process passes to the decoder uncertain Q components, and hence the overall performance degrades compared to the optimum one. This degradation reduces in the case of two receive antennas because receiving two signals with the same Q components to be guessed for improves the probability of correct decisions on Q components. Also, the performance improves in the high SNR region. This is due to the fact that when the noise average power is decreased compared to the signal received average power, the detector decisions are associated with less noisy signals and hence, outputs better decisions. The gains of the I-Q code over QPSK1 and QPSK2 codes are more than 3 dBs and 1 dB, respectively. Of course, the gain of QPSK2 over QPSK1 is decreased to almost 2 dBs in the two receive antenna case.

The same information shown in Figure 3.11 is shown in Figure 3.12 for the 8-state codes. The addition of one memory element in the encoder has improved the performance of the three codes by 2, 1 and 0.5 dBs for QPSK1, QPSK2 and I-Q codes, respectively. Also,

this additional memory element reduced the gains of the I-Q code over the other two codes. This is due to the reduced number of multiplicities of the shortest error event path than in the 4-state codes. The same observation is noticed about the reduction in gain in one receive antenna case than the case of two antennas. In the one receive antenna case, the I-Q gains over QPSK1 and QPSK2 are 2 and 1 dBs, respectively. Conversely, they are slightly more at 10^{-4} BER and less at 10^{-3} BER. This is due to the variability in the detector's behavior in the cases of one and two receive antennas and in the high SNR region.

The same codes were tested for fading channels with slower fading rates, and hence smaller Doppler frequency (f_D). The most used parameter is the fade rate (f_DT) which is the rate at which the channels changes its response. For the previous channels, the fade rate was 1, meaning that the fade rate is the same as the transmission rate, which is the definition of the rapid fading channels. It is chosen in this case is chosen to be 0.01.

The transmitted symbols at each antenna are interleaved using a block interleaver with 25 rows (depth) and 16 columns (span). The interleaver is used in order to break the memory of the channels so that it approaches the behavior of rapid fading channels, and hence the diversity provided by the ST system is utilized fully. The transmitted symbols are filled row-wise in the interleaver and transmitted column-wise. The interleaver depth is chosen according to the rate of the channel so that any two consecutive symbols are faded by almost uncorrelated fade samples. It is shown that an interleaver depth of $1/(4f_DT)$ is enough to break the memory of the channel [26]. The span of the interleaver is chosen such that the signals that are faded by consecutive fade samples are separated in the decoder by a time intervals greater than the constraint length of the code.

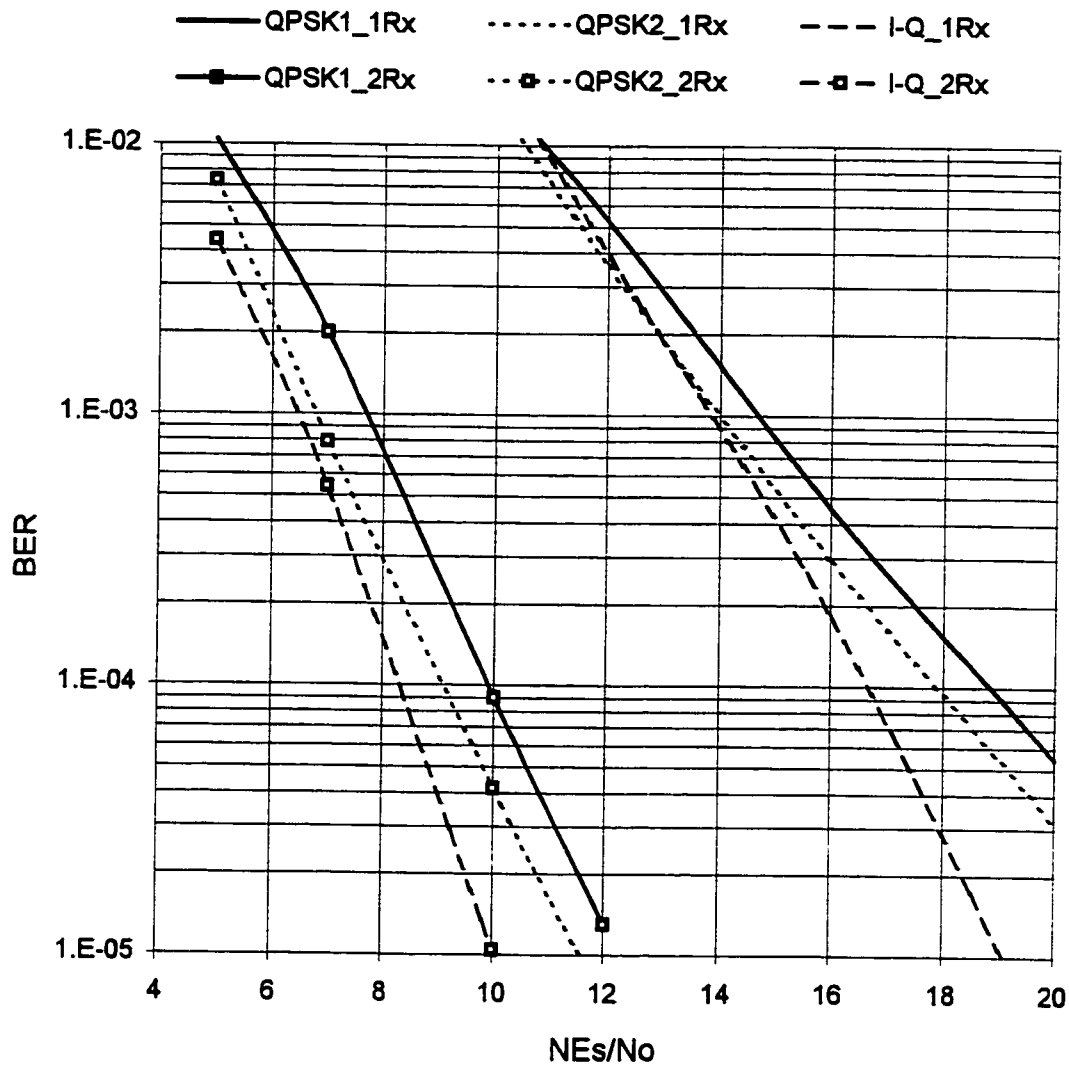

Figure 3.12: Performance of the 8-state QPSK codes for 1-Rx and 2-Rx antenna over rapid fading channel.

The performance of the 4 and 8-state QPSK ST codes over this channel is plotted in Figures 3.13 and 3.14, respectively. It is obvious that the I-Q coding scheme is still the best followed by QPSK2 and then QPSK1. The gains of the first two codes over the last one are slightly less than that for the independent fading channel. This reduction in gain is expected since the effect of the ST-MTD is reduced due to non-ideal interleaving.

Figures 3.15 and 3.16 show the performance of the same 4-state and 8-state QPSK codes, respectively, for a slower fading channel with fade rate f_DT of 0.005. The same interleaver, used in the case of f_DT=0.01, is used in this case. This interleaver size does not provide enough decorrelation for the channel's fades samples since the current channel has longer memory than the previous one, and hence it should be interleaved with an interleaver of larger depth. Therefore, the interleaver used for this channel is said to be an improper interleaver. The same trends observed in the independent fading channel are observed here but with less gains for the best code over the worse ones.

The existing and the tighter bounds developed in the previous chapter are applied to the QPSK2 code. The bit error rate is evaluated using the transfer function approach as in section 2.5. The bounds on the bit error rate for the 4-state and 8-state codes are plotted versus the received SNR, NE_s/N_o, where N is the number of transmit antenna, in Figure 3.17 and 3.18, respectively. It is clear that the new bound is very tight to the simulation curve of this code in addition to being so for the QPSK1 ST code as in Figures 2.1 and 2.2. It can be also seen from the Figure that the existing bound is very loose at almost all SNR regions.

3.6.2 ST Codes Based on 16-QAM

Existing and designed 16-QAM ST codes mentioned earlier are simulated over independent fading channels. Figure 3.19 shows the performance of the 16-state QAM1, QAM2 and I-Q codes for the cases in which the receiver is equipped with one and two receive antennas. It is clear from the Figure that the 4-state I-Q code with super-trellis decoding is the best followed by QAM2, QAM1 codes and the 32-state I-Q code with suboptimal decoding. This is expected for the 4-state I-Q code since the main controlling parameter of the code in rapid fading channels is the ST-MTD of the code that is highest in the I-Q code.

It can be seen that the 32-state I-Q code with suboptimal decoding performs very bad. The reason behind this was pointed out briefly in the suboptimal decoding section and the QPSK codes comparisons section. As the number of possible combinations of the Q components to be guessed for in the I-decoder increases, the performance degrades more. Since there are 16 combinations in the I-Q 16-QAM case, the degradation becomes more visible than the I-Q QPSK case. This degradation becomes less in the case of two receive antennas, where the 32-state I-Q with suboptimal decoding is the best in this case. Also, degradation decreases as the SNR in increased, because the guessing process is done in a less noisy environment.

In the case of one receive antenna, the gains of the I-Q code, decoded by the super-trellis method, over the QAM1 and QAM2 codes are 2.5 and 0.5 dBs, respectively. The performance of the 32-state I-Q code with suboptimal decoding improves in the high SNR region- above 23 dB. The gains are expected to be more than the QPSK case, since

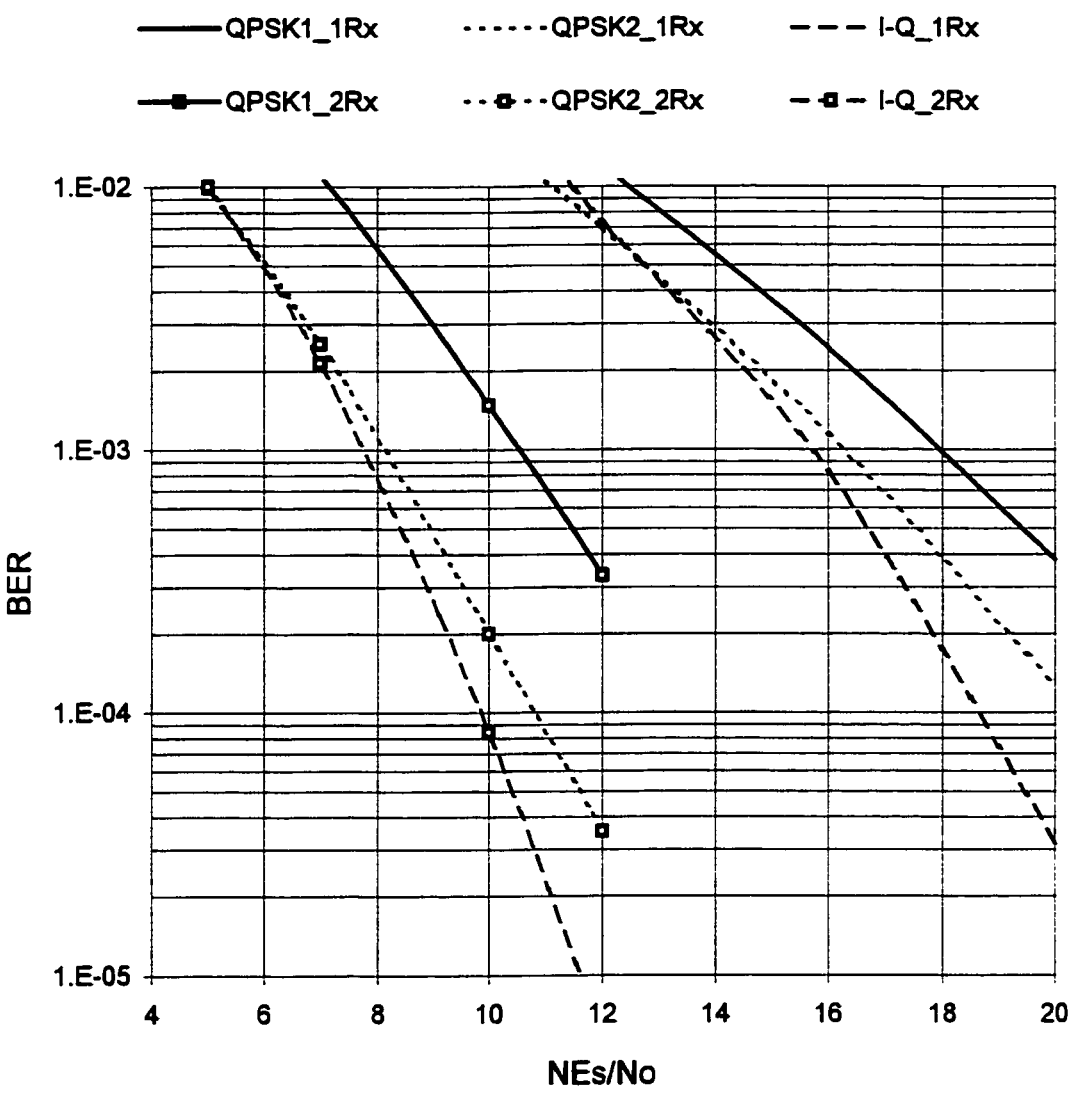

Figure 3.14: Performance of the 4-state QPSK codes for 1-Rx and 2-Rx antenna over correlated fading channel with $f_D T$=0.01.

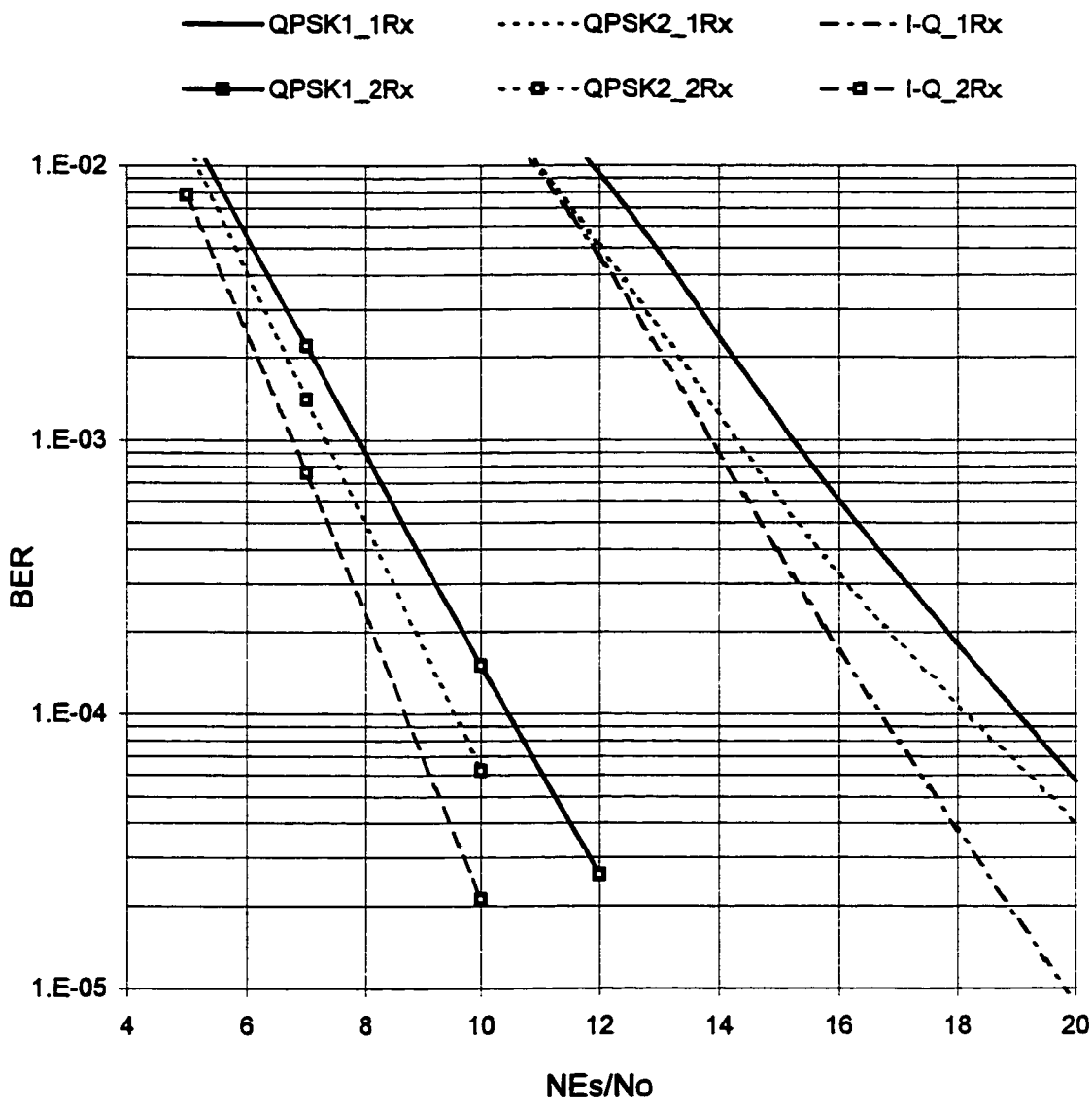

Figure 3.15: Performance of the 8-state QPSK codes for 1-Rx and 2-Rx antenna over correlated fading channel with $f_D T$=0.01.

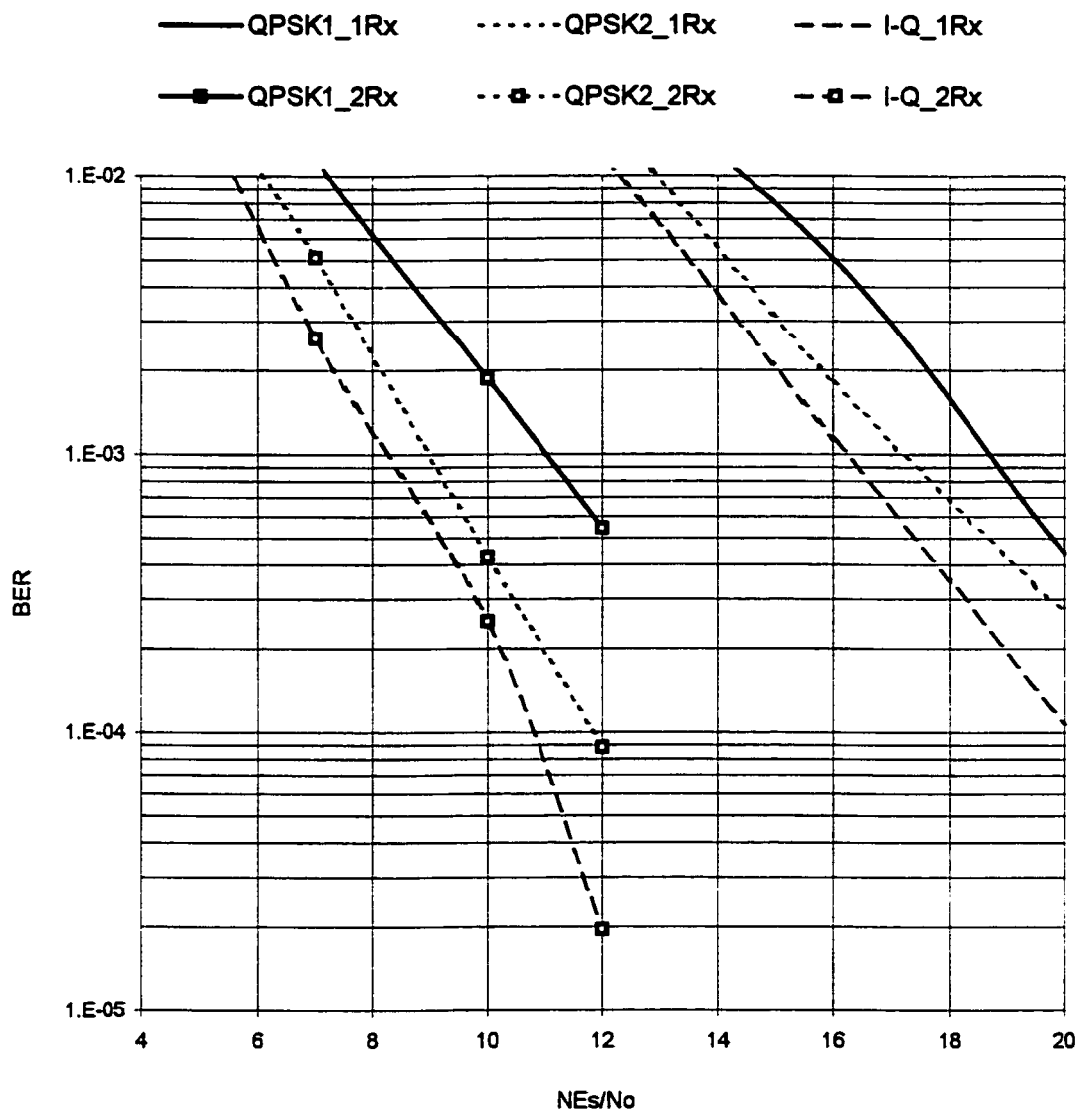

Figure 3.15: Performance of the 4-state QPSK codes for 1-Rx and 2-Rx antenna over correlated fading channel with $f_D T$=0.005.

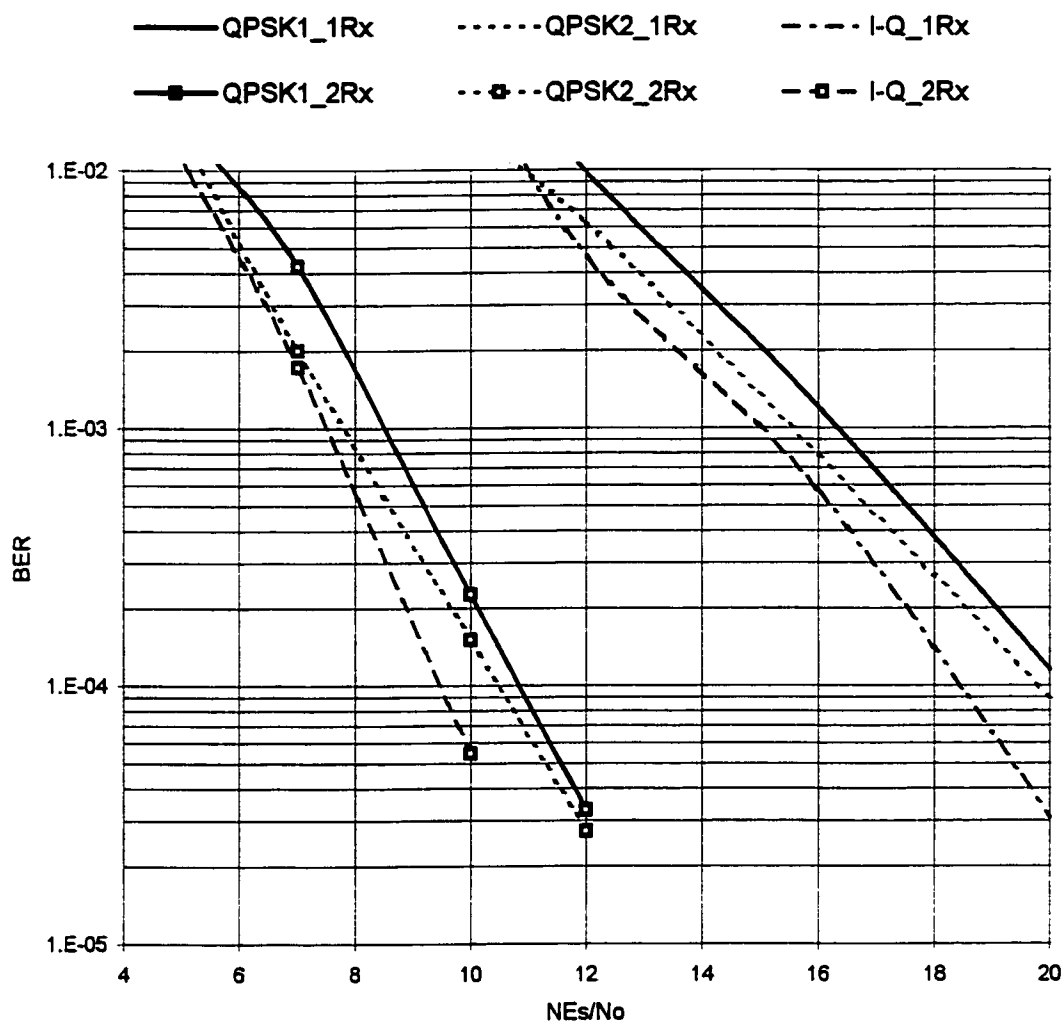

Figure 3.16: Performance of the 8-state QPSK codes for 1-Rx and 2-Rx antenna over correlated fading channel with $f_D T$=0.005.

the increase in ST-MTD and ST-MSPD in the I-Q QAM, having the same decoding complexity- 32-state, over the QAM1 and QAM2 is much higher than that in the QPSK case.

More gains are expected if a better decoding algorithm is devised and used. In the two receive antennas case, the above gains become around 2 and 0.3 dBs, respectively. On the other hand, gains of the 32-state I-Q code, using suboptimal decoding algorithm, over QAM1, QAM2 and the 4-state code with super-trellis decoding are 2.5, 1 and 0.5, respectively. Again, all these gains are observed at a BER of 10^{-3}.

The performance of the QAM codes over the correlated fading channel with a fade rate f_DT of 0.01 is shown in Figure 3.20, for the case of one and two receive antennas. Same trends observed in the independent fading channel case are observed in this case. The gains of the best code over worse codes are less in this case. In the one receive antenna case, gains of the 4-state I-Q code, using super-trellis decoding, over QAM1, QAM2 and the 32-state code with suboptimal decoding are 2, 0.2 and 1.5, respectively. All these gains are observed at a BER of 10^{-3}. In the two receive antennas case, they do not change much because the presence of two receive antennas makes it less dependent on the codes' parameters. All these gains are observed at a BER of 10^{-3}.

Figure 3.21 shows the performance of the same codes for slower rate fading channel, with fade rate f_DT of 0.005. The same interleaver used in the case of f_DT=0.01 is used in this case, which is improper for this channel. The performance trends for the codes are the same as the previous two channels with decreased gains.

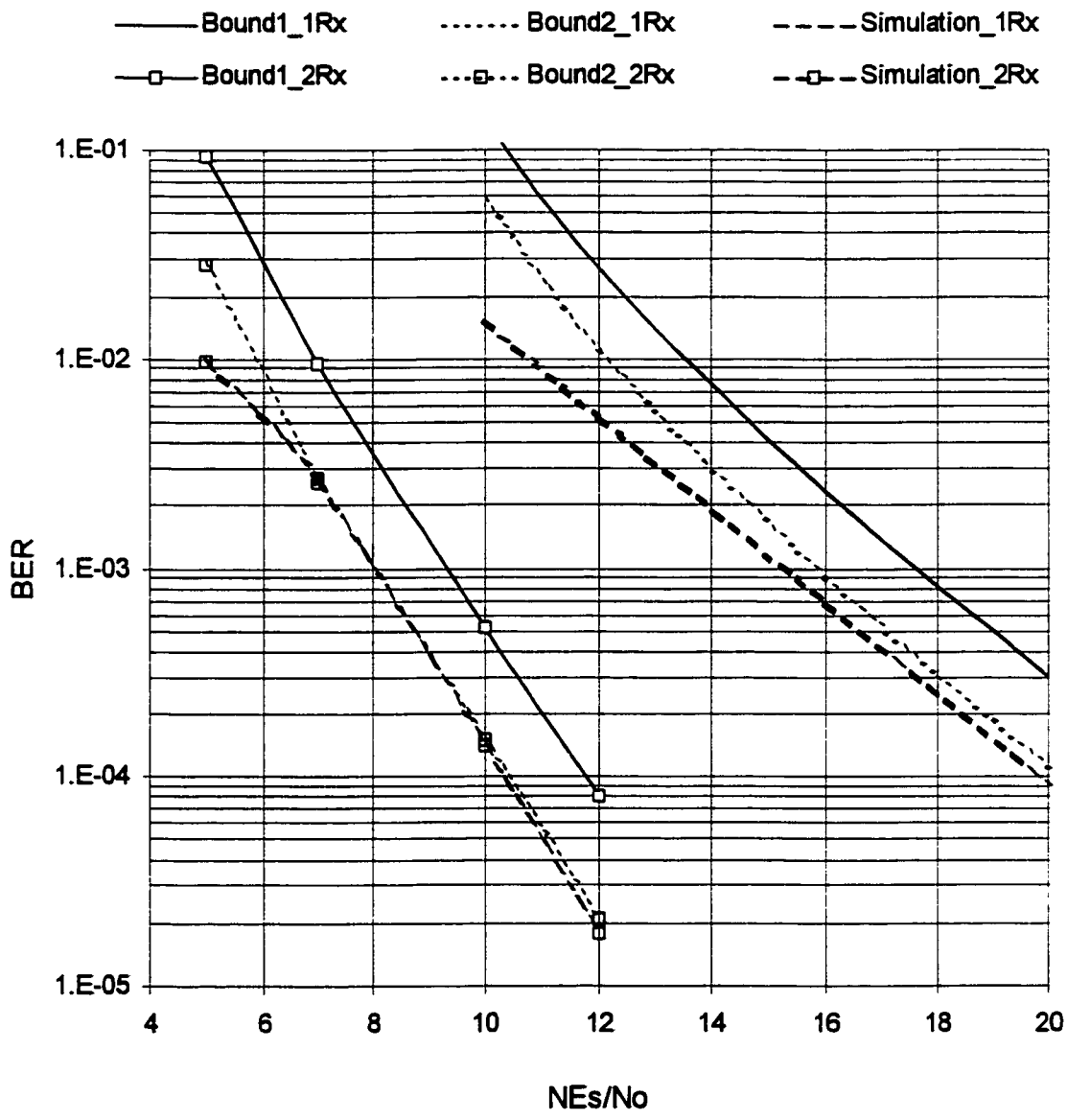

Figure 3.17: Performance of the 4-state QPSK2 ST code for one and two receive antennas.

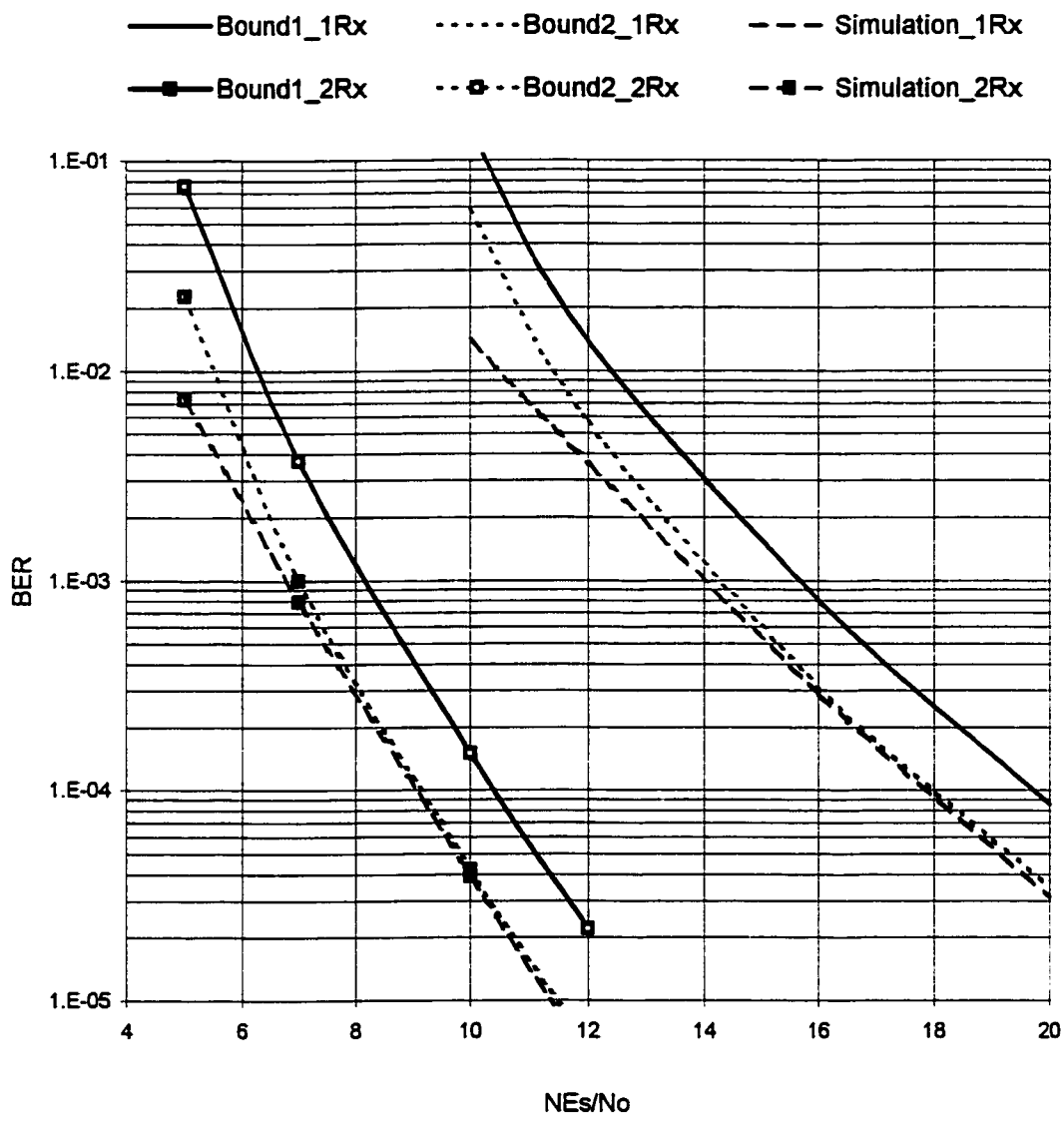

Figure 3.18: Performance of the 8-state QPSK2 ST code for one and two receive antennas.

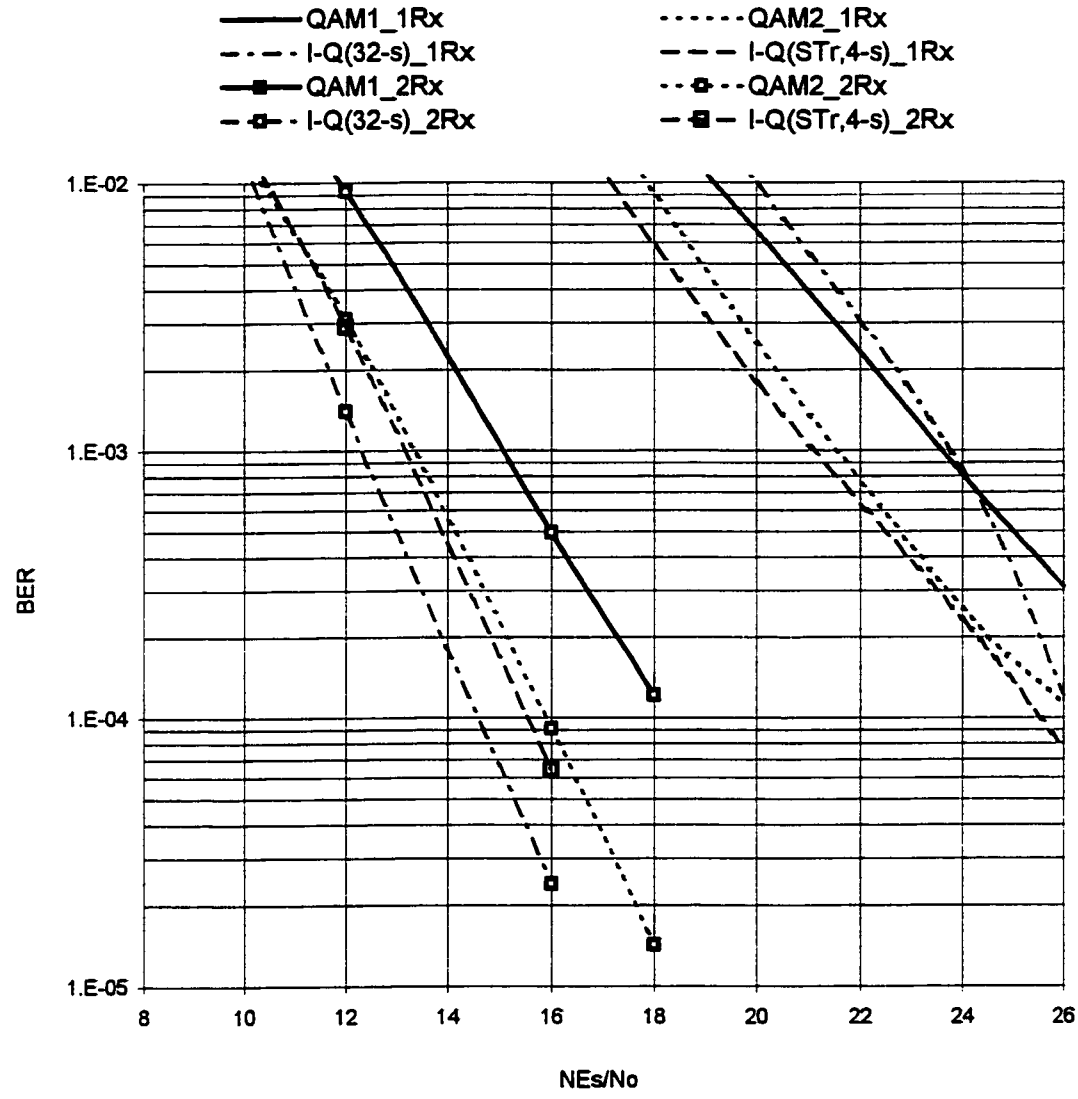

Figure 3.19: Performance of the 16-QAM codes for 1-Rx and 2-Rx antenna over rapid fading channel.

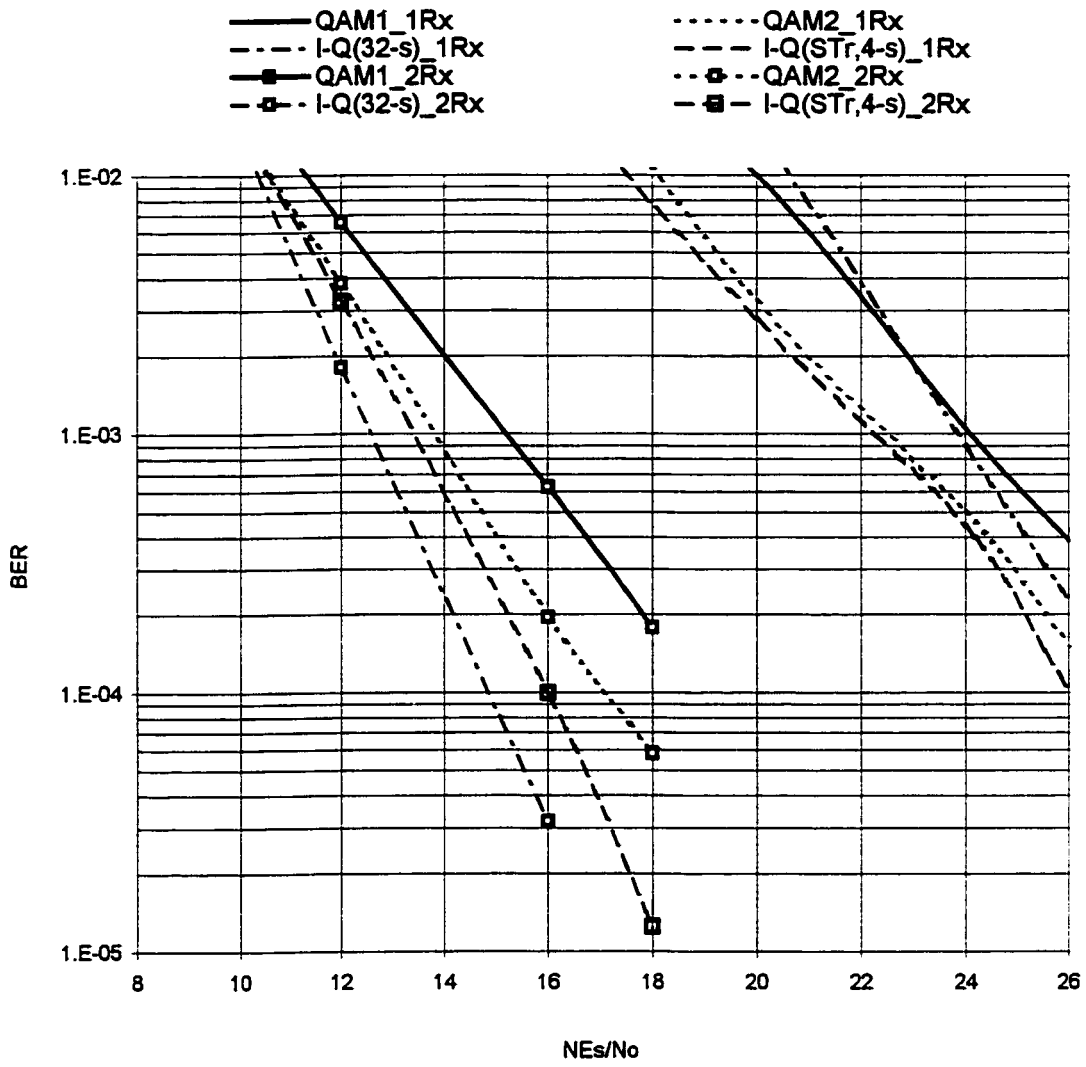

Figure 3.20: Performance of the 16-QAM codes for 1-Rx and 2-Rx antenna over correlated fading channel with $f_D T$=0.01.

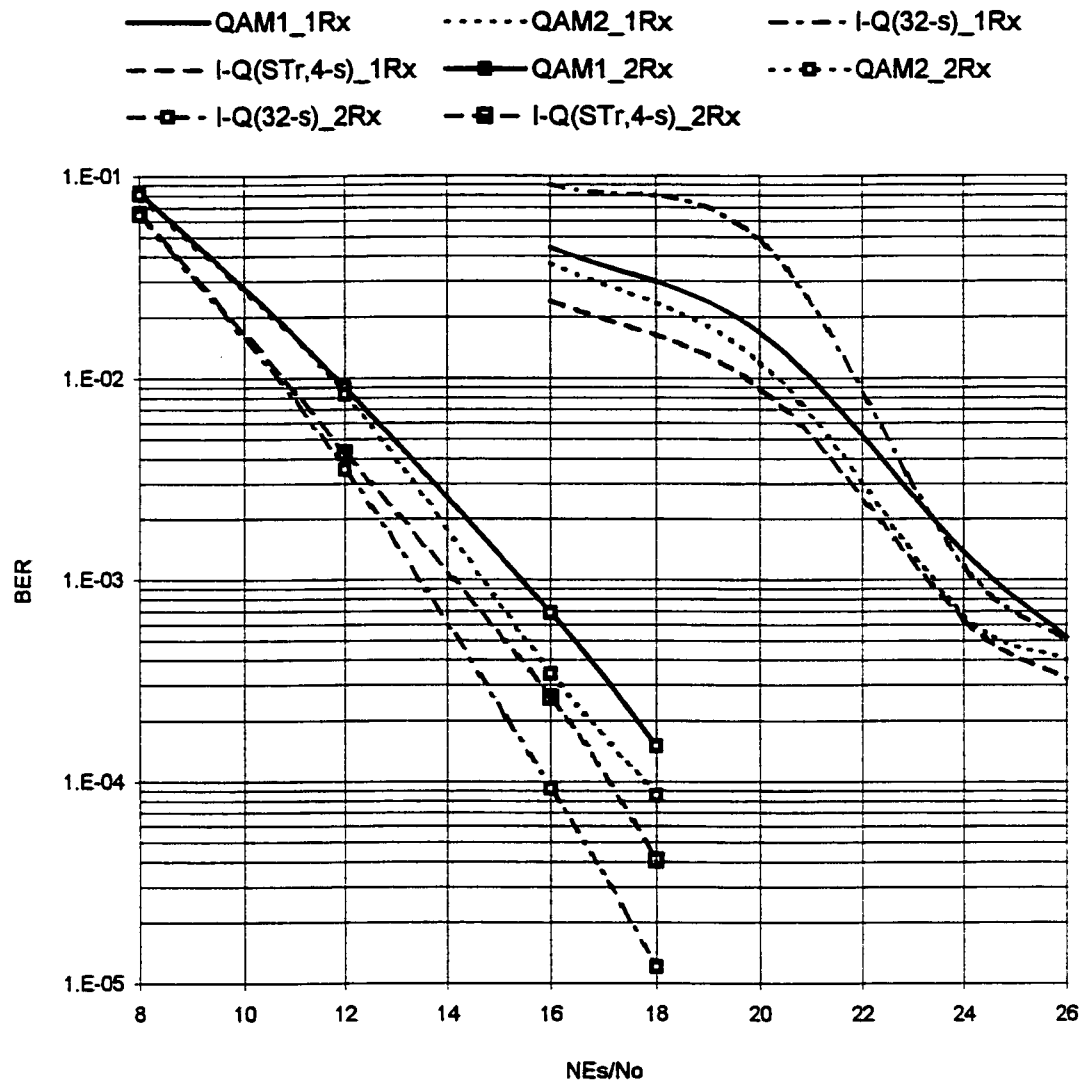

Figure 3.21: Performance of the 16-QAM codes for 1-Rx and 2-Rx antenna over correlated fading channel with $f_D T$=0.005.

CHAPTER 4

PERFORMANCE OF ST CODES IN IMPERFECT CSI ESTIMATION

4.1 Introduction:

In previous chapters, the channel state information (CSI) is assumed to be perfectly estimated at the receiver. In practical cases, CSI is estimated using an estimation technique that generally results in an estimation error. The problem of CSI estimation involves two important parts: the training algorithm used to get enough samples of the channel, and the interpolation filter used to average out the estimation noise from the samples of the channel. It is required to get enough samples of the channels so that it can

be estimated based on some of its stochastic properties. In the literature, there are different channel training methods and interpolation filters that were applied to estimate complex Gaussian fading channels. The most common CSI estimation techniques are previewed in the next section along with a detailed description of the pilot symbol assisted modulation (PSAM) technique. Then, the estimation technique used in ST coded systems is discussed. Finally, simulation results are presented.

4.2 CSI Estimation System

4.2.1 Pilot Symbol Assisted Modulation (PSAM)

An important method used in CSI estimation is the pilot tone [31]. It is transmitting a tone every a predefined period, that depends on the fading rate, receive it and interpolate it with other pilot tones using a filter to average the noise. This method was good in estimating both the fade's amplitude and phase explicitly but has a problem in deciding the location the pilot tone within the transmission spectrum. In flat fading channels, this problem does not have that significant importance since the channel response is the same for the whole spectrum. Many solutions to this problem were proposed in the literature but the most important solution is the transparent tone-in-band (TTIB) [31]. Unfortunately, this solution requires relatively complex signal processing algorithms and causes an increased peak-to-average power ratio. To overcome such problems, the use of PSAM was proposed in [32].

The use of PSAM to estimate fading channels was proposed in [33] and [34]. It is based on inserting a known pilot symbol every certain duration, that depends on the fading rate,

and transmitting it within the data transmission. At the receiver, the pilot symbol will be corrupted by an AWGN and hence the fade's amplitude and phase can not be estimated correctly. Therefore, the received pilot symbols are interpolated, using an interpolation filter, so that the noise on top of the received pilot symbols is averaged out and good estimators of the amplitude and the phase of the fade are found. The performance analysis of a general PSAM system was derived in [32]. Also, the performance of PSAM when used with 16-QAM and QPSK signal constellations is evaluated in [35] and [36], respectively.

The general diagram of the PSAM transmitter/receiver is shown in Figure 4.1. The transmitter consists of an encoder, a modulator and a pilot insertion block. The pilot insertion block inserts the pilot symbol in the data stream and the modified data stream is transmitted. The receiver consists of a demodulator, splitter, delay buffer, interpolation filter and a decoding stage. The received symbol stream is split into a data stream and a pilot symbols stream. The second stream is fed into an interpolation filter and the decision is made to estimate the channel state. The delay buffer is used to store the received data stream until enough pilot symbols are received and interpolated.

The transmitted frame is composed of one pilot symbol that is inserted every m data symbols to end up with a frame size of $(m+1)$. There are K pilot symbols used in the interpolation filter. The interpolation filter estimates the CSI of the date symbols that lie in the middle of the K pilot symbols. In this case, the wasted bandwidth in pilot symbols is $1/(m+1)$ of the allocated bandwidth since there is one pilot symbol every m data symbols. Also, the delay required is $m\lfloor K/2 \rfloor$ since the receiver should wait for the

reception of $\lfloor K/2 \rfloor$ pilot symbols to be used in the filter to get good estimators of the amplitude and the phase of the CSI at the middle of the pilot symbol buffer. The received data signal is modeled by:

$$r_d(k) = c(k)s(k) + n(k) \tag{4.1}$$

Where $n(k)$ is the k^{th} AWGN sample drawn from a complex Gaussian process with variance $N_o/2$ per dimension. Also, $c(k)$ is the fading channel gain that consists of a complex Gaussian fading process $g(k)$ and a frequency offset f_o as follows [31]:

$$c(k) = exp(j2\pi f_o k)\, g(k) \tag{4.2}$$

The frequency offset is assumed to be zero throughout this study. It is a valid assumption if automatic frequency control (AFC) is used in the system [32]. The correlated fading complex Gaussian channel $c(k)$ has the following autocorrelation function:

$$R(\tau) = exp(j2\pi f_o \tau)\, J_o(2\pi f_D \tau) \tag{4.3}$$

Where $J_o(2\pi f_D \tau)$ is the Bessel function of first kind with zero order. This autocorrelation function is important in finding the optimum filter coefficients as will be discussed in the next section. The pilot symbol, inserted in each frame, is known at both transmitter and receiver and is denoted by $b(k)$. So, the received pilot signal is:

$$r(k) = u(k)b(k) + n(k) \tag{4.4}$$

where $u(k)$ is the channel gain that affected the pilot symbol. The channel gains affecting the pilot signals are differentiated from those affecting the data because the former are used as the measurements in the estimator. Also, different notations of received data signals and pilot signals are used to differentiate between the known pilot symbols and the unknown data symbols.

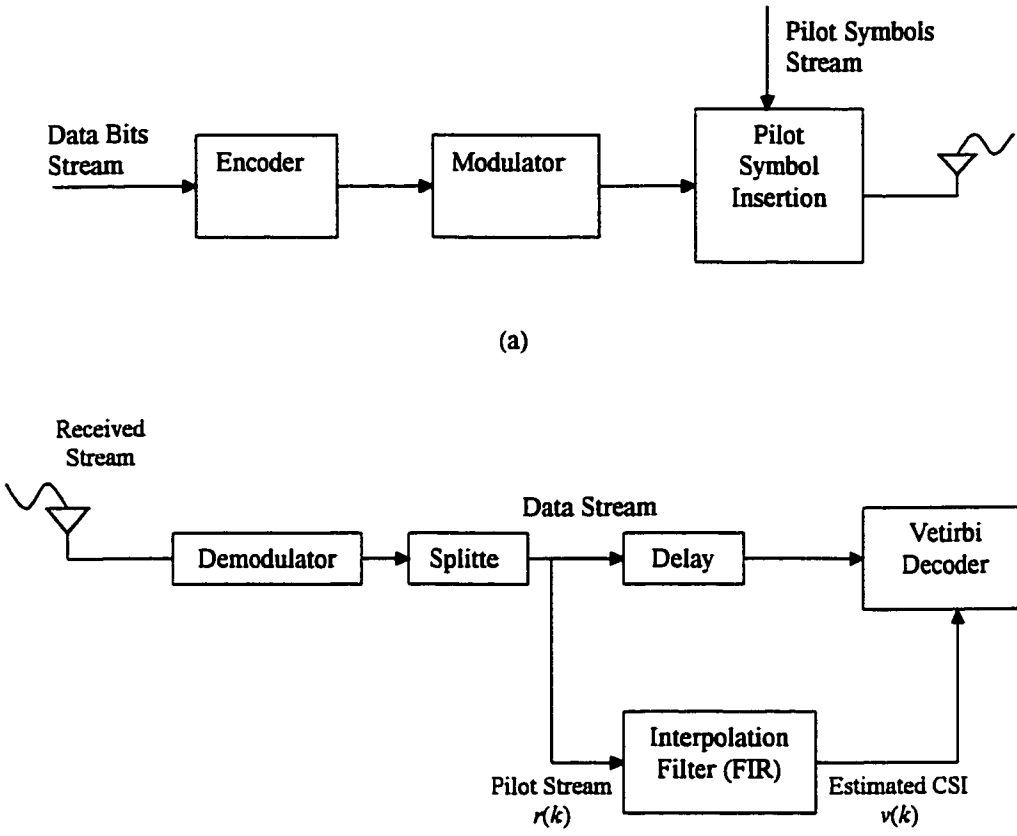

Figure 4.1: The structure of the PSAM for CSI estimation system (a) Transmitter, (b) Receiver.

The interpolation filter uses the nearest K received pilot signals to estimate the channel state at the middle of the available pilot sequence via a finite impulse response (FIR) filter. The k^{th} coefficient of the FIR filter used to estimate the i^{th} symbol, of the frame in the middle, is denoted by $h(k,i)$. Hence, the estimated channel state at the i^{th} position in each frame is found from [31]:

$$v(i) = \sum_{k=-\lfloor K/2 \rfloor}^{\lfloor K/2 \rfloor} h(k,i)\, r(km) \qquad , i = \lfloor -m/2 \rfloor, .., 0, .., \lfloor m/2 \rfloor \tag{4.5}$$

Where $v(i)$ is the estimated channel state at the i^{th} data position in each frame. The problem now is how to find the optimum filter coefficients so that the MSE in the estimated CSI, $v(i)$'s, is minimized. The estimated channel state is the true one with an estimation error that is to be minimized, $e(k)$, where:

$$u(k) = v(k) + e(k) \tag{4.6}$$

The optimum solution to the filter coefficients is found by using the Wiener filter.

4.2.2 Wiener Interpolation Filter

Many different filters were used at the beginning of PSAM systems such as the Lowpass and the Gaussian filters. In [32], the Wiener filter was proposed to have optimum estimations of both amplitude and phase of the channel state. It provides the optimum solution of any time-invariant estimation problem in AWGN environment [37]. If the channel's fading rate is changing from time to time, which is expected in many applications, an adaptive Wiener filter is used to adapt the filter coefficients as the channel rate varies. The Wiener filter is based on the MMSE estimation criterion. This

criterion requires the minimization of the MSE in the estimated parameters. It minimizes the following cost function [31]:

$$I = E\{[u(k)-v(k)]^2\} \tag{4.7}$$

By substituting (4.5) into (4.7), we get:

$$I = E\{[u(k) - \sum_{k=-\lfloor K/2 \rfloor}^{\lfloor K/2 \rfloor} h(k,i)\, r(km)]^2\} \tag{4.8}$$

Solving (4.8) for the unknown filter coefficients $h(k,i)$, we get [31]:

$$\sum_{k=-\lfloor K/2 \rfloor}^{\lfloor K/2 \rfloor} h(k,i)\, \phi_r(k-i) = \phi_{ru}(i), \quad \text{for } i=\lfloor -m/2 \rfloor,..,0,..,\lfloor m/2 \rfloor \tag{4.9}$$

Equation (4.9) can be squeezed in matrix form to be:

$$\phi_r\, \underline{h}(i) = \phi_{ru}(i), \qquad \text{for } i = \lfloor -m/2 \rfloor,..,0,..,\lfloor m/2 \rfloor \tag{4.10}$$

Where ϕ_r is the autocorrelation function of the received pilot signals $\underline{r}$, $\underline{h}(i)$ is the filter coefficients of the channel state in the i^{th} position in the frame and $\phi_{ru}(i)$ is the cross-correlation function between the K received pilot signals and the i^{th} position in the frame. So, there are m cross-correlation functions to be found since there are m channel gains to be estimated in each frame. The correlation functions defined above can be found automatically from the autocorrelation function of the channel itself as follows:

$$\phi_r(i,k) = R[(i-k)(m+1)T],$$

$$\phi_{ru,k}(i) = R[(k(m+1)-i)T] \tag{4.11}$$

Where T is the symbol duration. The first equation in (4.11) is found by finding the correlation between pilot symbols by finding the spacing between them in terms of symbol duration. Since each pilot symbol was faded with a fade whose autocorrelation

function is $R(\tau)$ as in (4.3), then the autocorrelation of the faded pilot symbols is derived from $R(\tau)$, taking into account the correct symbol spacing. Also, it is valid to assume that the receiver noise is uncorrelated with the fading process since there is no relation between them. The second equation, the m cross-correlation functions, are found from the autocorrelation function of the fade process by observing the time spacing between each position in the frame and each of the pilot symbols.

Thus, the filter coefficients can be found from (4.10) at each position in the frame and they can be computed offline for a certain SNR and fading rate values. This is considered as a problem in the Wiener filter. However, adaptive filtering can be used in the case of varying SNR or fading rate so that the new filter coefficients are adapted each time the conditions are changed and they are optimized for the new conditions. Since the coefficients computations requires a matrix inversion that is not easy to do online, fast adaptive algorithms should be used. Of course, this requires estimation algorithms of the received SNR and the channel's fade rate.

4.2.3 Orthogonal Pilot Symbol Insertion (OPSI)

The idea of OPSI was proposed in [12] and [13] to estimate channel state for ST coded systems. It exploits the same idea as the PSAM with a little modification. Since the received signal in the ST system is the superposition of all transmitted signals from all transmit antennas, then transmitting one pilot symbol in each frame will give no information about the channel states in all transmit branches. This is because all pilot symbols transmitted from all antennas will overlap at the receiver giving no information about the state of any of the transmit branches.

To overcome this problem, OPSI idea proposes that each of the transmit antennas transmits a sequence of pilot symbols in the same time interval, instead of transmitting one pilot signal from each transmit antenna. The transmitter block diagram is shown in Figure 4.2-a. The pilot sequence at each transmit antenna is orthogonal to sequences allowed to the other antennas.

$$P^i = [P^i_1, P^i_2, \ldots, P^i_N],$$

$$P^i P^j = 0, \qquad \text{for } i \neq j \tag{4.12}$$

Where P^i_1 is the pilot symbol transmitted at time t from the i^{th} transmit antenna. The length of each pilot sequence should be at least equal to the number of transmit antennas in order to insure the orthogonality property of the pilot sequences. The orthogonal sequences at the transmit antennas are obtained from a constant-envelop signal constellations such as MPSK. The symbols in each sequence are chosen such that they are orthogonal to all other sequences at the other transmit antennas. At the beginning of the pilot sequence duration in each frame, the i^{th} transmit antenna transmits the pilot symbol P^i_1. At the t^{th} time interval of the allowed duration for the pilot sequence, the i^{th} antenna transmit the pilot symbol P^i_t. The transmitted stream including the orthogonal pilot symbols is shown in Figure 4.2-b for the case of two transmit antennas. The received signal is:

$$r^j_t = \sum_{i=1}^{N} \alpha^j_i P^i_t + \eta^j_t, \tag{4.13}$$

The orthogonality property of the pilot sequences at each transmit antenna is utilized at the receiver to decouple the CSI for each branch. In order to decouple the CSI of branches

from the i^{th} transmit antenna to the j^{th} receive antenna, the received signal is multiplied by the i^{th} pilot sequence as follows:

$$r^j.P^j = \alpha_i^j(P^j.P^j) + P^j.\eta^j, \tag{4.14}$$

Hence, the CSI of that branch can be obtained in addition to the AWGN after being scaled by a factor of $(P^j/(P^j.P^j))$. The fade process is assumed to be constant for the transmission duration of the pilot sequence in each frame. This assumption is valid for small number of transmit antennas, N=2, which is the case here.

4.2.4 Properties of CSI Estimator

The main parameter that affects the performance of the estimator is the number of symbols between the insertion of each pilot sequence or the frame size, $(m+N)$. The length of each pilot sequence is assumed to be equal to the number of transmit antennas. In general, as the frame size increases, the samples of the fading channel taken from the pilot sequence transmitted becomes less and may not be enough to sample the channel. Hence, the performance degrades substantially when the spacing between pilot sequences exceeds the Nyquist sampling rate of the channel, i.e: $m<1/(2f_DT)$. Also, the frame size should not be very small because this reduces the throughput of the system substantially. An efficient tradeoff between the wasted bandwidth in transmitting pilot sequences and the estimation accuracy should be taken into account. As a rule of thumb, the pilot sequences spacing should not be below m=8 so that the wasted bandwidth is fifth the actual one, which may be a reasonable value. For the channels that are studied, the used value of the frame size is chosen to be m=8.

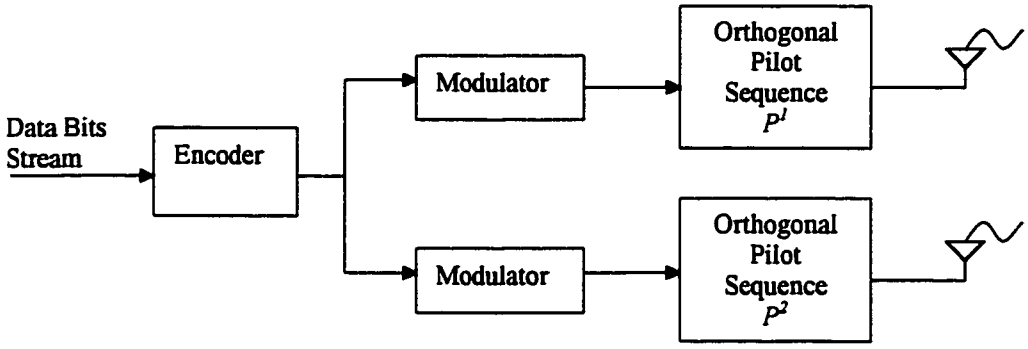

(a)

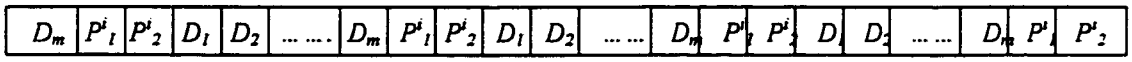

(b)

Figure 4.2: (a) The transmitter structure of the OPSI for CSI estimation in a ST system.

(b) The frame structure of OPSI system in a 2-Tx antenna ST system.

The second parameter the affects the estimator performance is the number of filter coefficients used in the interpolation, or the length of the interpolation filter K. As the filter size increases, the performance improves because the estimation noise is averaged better because the number of interpolated samples of the channel is increased. Also, the delay involved in the estimation process increases as the filter size increases. Again, a tradeoff between the more accurate estimation and the less delay required should be done. The performance improvement decreases when the filter size is increased beyond K=8. For the channels studied here, the interpolation filter is taken to be of length K=10. The first parameter of the estimator used is more critical than the second one and should be optimized first.

4.3 Simulation Results

The CSI estimation is applied to test the performance of ST systems that uses QPSK codes. In the following, the results of the 4-state QPSK1, QPSK2 and I-Q codes are presented and discussed. Figure 4.3 shows the performance of the 4-state QPSK codes over a correlated fading channel with 1% fading rate, (i.e: $f_D T$=0.01), using one and two receive antennas. An interleaver was used with depth of 25 and span of 16 so that the channel in hands is interleaved enough. The CSI is estimated using OPSI with a frame size of 10, hence m=8, and an interpolation filter of length K=10.

For one receive antenna, the QPSK1 code shows the worst performance, where the QPSK2 and I-Q codes have very close performances. Comparing Figure 4.3 and 3.13, it

can be seen that both QPSK1 and QPSK2 degraded with almost equal amount, about 5 dBs at 0.005 BER. The I-Q code degraded more, almost 6dBs at 0.002 BER.

However, the degradation of the I-Q code due to the inaccurate CSI decreases at high SNR region. It can be concluded that the degradation of the I-Q code is due to the unreliable suboptimal decoding used whose effect becomes more severe when combined with the imperfect CSI estimation.

In the two receive antenna case, the superiority of the I-Q code over the other two codes for most of the SNR regions can be seen clearly. This is due to the reduced effect of the suboptimal decoding for the two receive antenna case, as was concluded in the results when perfect CSI exists at the decoder, in Chapter 3. Also, the degradation in the performance of the three codes is less than the case of one receive antenna because having more receive antennas increases the decoding reliability because of diversity effect on the CSI estimation accuracy. For example, if the signal at the first receive antenna is faded but the channel state was not accurately estimated, and the channel state at the second receive antenna was estimated more accurately. In such case, using two receive antenna increases the reliability of the overall decoding metric and hence, reduces the performance degradation due inaccurate CSI estimation. The degradation due to inaccurate CSI at the receiver for the three codes are approximately 4 for the QPSK1 and QPSK2 and 1.5 dB for the I-Q code.

Figure 4.4 shows the same information as Figure 4.3 when the three codes are tested over a correlated fading channel with $f_D T$=0.005 and using the same interleaver used in the first case. Also, the same CSI estimator parameters are used (i.e: m=8 and K=10). Since this channel is slower than the previous channel, it is sampled more often and hence the

degradation due to inaccurate CSI is reduced as compared to the previous case. In order to view the amount of degradation due to the imperfect CSI, the reader is referred to Figure 3.14. In case of one receive antenna, the degradation in the QPSK1 and QPSK2 codes is 2 dBs, where it is about 2.5 dBs in the I-Q code.

However, the degradation of the I-Q code decreases as the SNR increases to a medium value of about 16 dB. One can see that when the CSI estimation becomes more reliable, as sampling rate of the channel is increased compared to the channel rate, the degradation in the I-Q code performance becomes less critical than the other two codes. The same observations about the degradation in performance in the two receive antennas case of the previous channel are valid for this channel. However, the degradation in the three codes is reduced to almost 1 dB at 10^{-3} BER due to better CSI estimation.

The same estimation problem can be posed to the case of 16-QAM ST coded system designed in Chapter 3. The pilot signals sequences in this case can be chosen from a constant-envelop signal constellations such as MPSK or Differential QPSK [14]. This requires the modulator at each transmit antenna to modulate two types of signals: the 16-QAM for the data stream and the constant-envelop signals for the pilot sequence. Moreover, the signal energy of the pilot and data signals should be adjusted to the required SNR at the receiver.

To overcome this problem, the use of orthogonal sequences designed in [23] for general number of transmit antennas and signal constellation, is proposed to be used as the orthogonal pilot sequences. This idea makes the modulators at the transmit antennas work with one type of signal constellation and one signal energy. This is left for further research in the future.

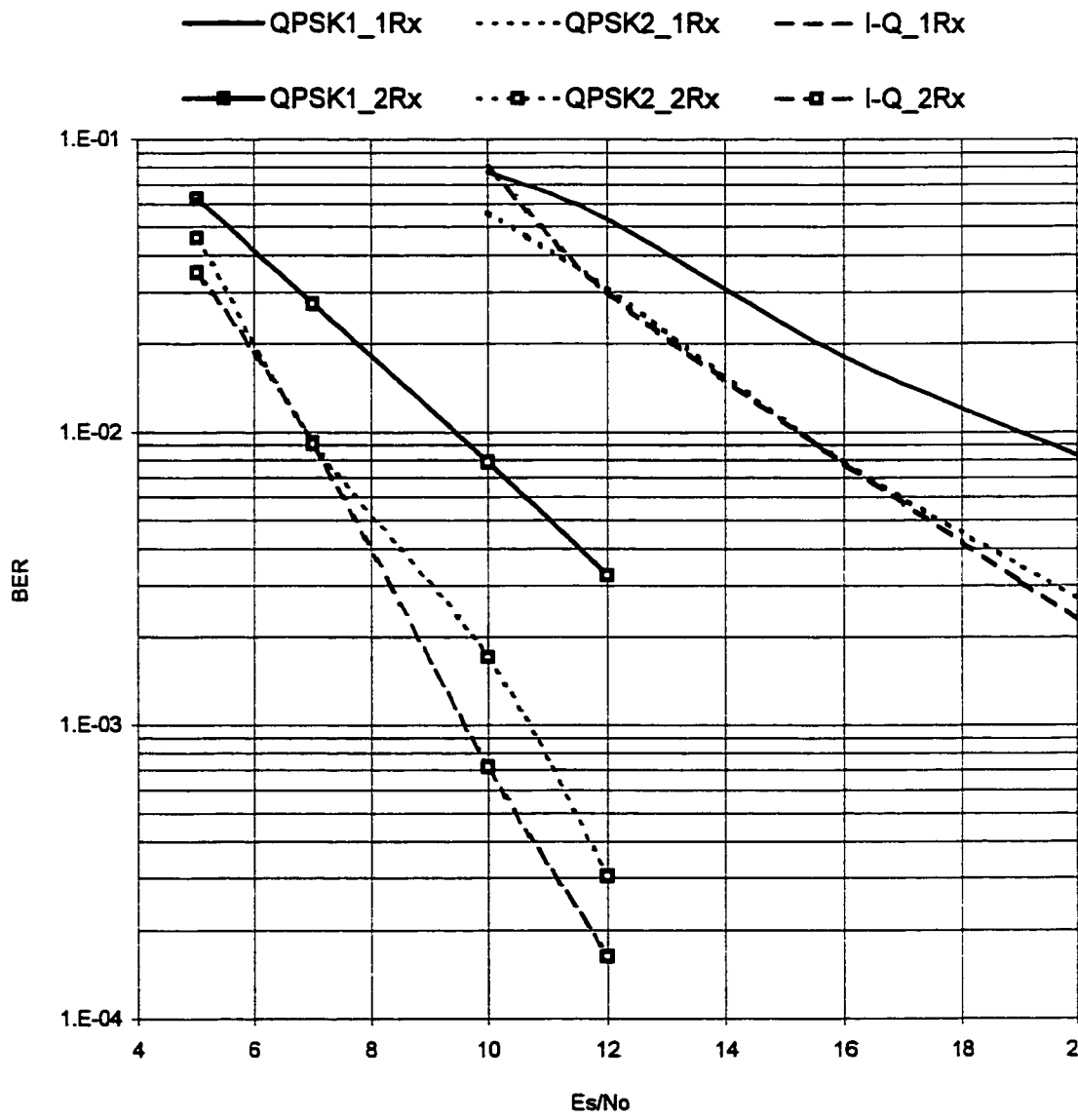

Figure 4.3: Performance of 4-state QPSK codes for 1-Rx and 2-Rx antenna over correlated fading channel with $f_D T$=0.01, and with CSI estimation using m=8, K=10.

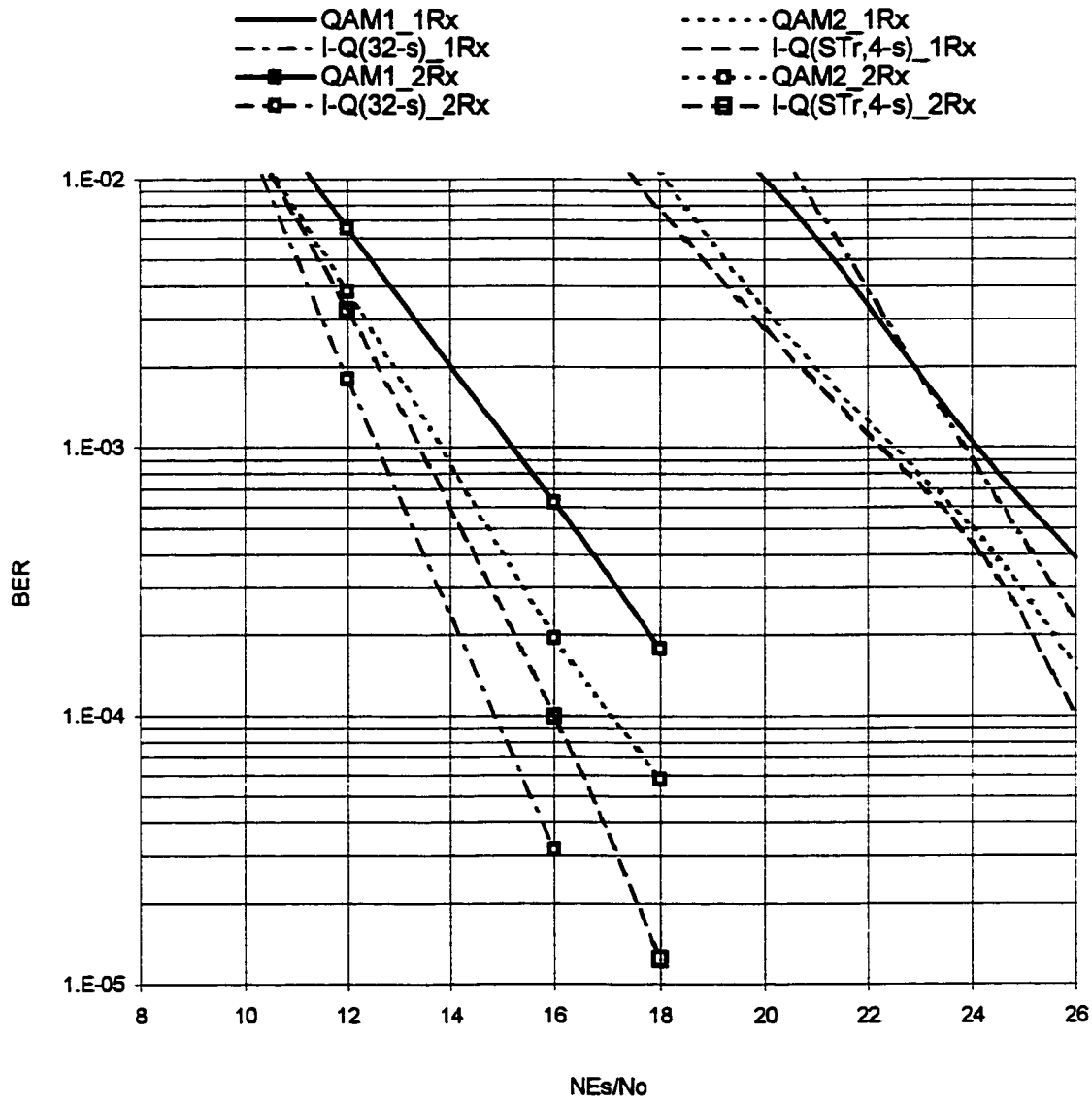

Figure 4.4: Performance of 4-state QPSK codes for 1-Rx and 2-Rx antenna over correlated fading channel with $f_D T$=0.005, and with CSI estimation using m=8, K=10.

CHAPTER 5

CONCLUSIONS AND FUTURE RESEARCH

5.1 Conclusions and Summary

In this thesis, we have studied the performance and the design of ST codes over rapid Rayleigh fading channels. The performance analysis carried out was based on the derivation used in [1] to obtain an existing upper bound on the pairwise error probability. An upper bound on the bit error probability derived from the existing pairwise probability was evaluated for the QPSK codes presented in chapter 3 as QPSK1 and QPSK2 ST codes. The existing bound was shown to be very loose to the simulation results. A tighter

upper bound on the bit error probability was derived and compared to the existing bound. It was shown to be very tight to the simulation results.

Two QPSK ST codes were proposed for rapid fading channels. The first one was designed based on the set partitioning approach leading to subsets with maximized ST-MTD and ST-MSPD. The code was simulated and compared with the QPSK code in [1]. Also, the existing and the tighter bounds were applied to this code and the tighter bound was also found to be very tight.

The second code was the I-Q QPSK ST code. It is based on the I-Q encoding technique and provides higher ST-MTD and ST-MSPD than codes with one encoder such as QPSK1 and QPSK2 ST codes. A suboptimal decoding algorithm was used to decode this code. For one receive antenna, suboptimal decoding results in a loss in gains over the QPSK1 and QPSK2 ST codes. This is due to the uncertainty in the decision taken on the Q and I components in the I and Q decoders, respectively. In the two receive antennas systems, the I-Q code provides more gains because of the more reliable decisions on the Q and I components in the I and Q decoders, respectively.

Two more codes based on the 16-QAM signal constellation were designed. These codes were compared to the 16-QAM ST code presented in [1]. The first code uses one encoder and is designed based on maximizing the ST-MTD and ST-MSPD of the code. The design approach was explained and the code was simulated over rapid fading channels. Results showed that this code outperforms the 16-QAM ST code in [1].

The second code uses the I-Q encoding scheme. This code was designed to provide the maximum ST-MTD and ST-MSPD among the other 16-QAM based ST codes. Two decoding strategies were used for this code. The first one is the suboptimal decoding

algorithm and the second on is the optimal decoding algorithm using the super-trellis of the overall code. The suboptimal decoding algorithm results in a very bad performance for the case of one receive antenna. This is expected because the number of combinations among which the I/Q decoder should take the decision on the Q/I component was increased by a square of that in the I-Q QPSK ST code. The degradation in the performance becomes less as the received SNR increase because this reduces the confusion in deciding among the available combinations of the I or Q components. In the case of two receive antennas, the suboptimal decoding provides substantially better performance.

The optimal decoding technique was used to decode the I-Q 16-QAM ST code whose encoder's memory is much less than that of the code with suboptimal decoding. This is to provide the same decoding complexity and to compare the two decoding approaches based on this parameter. The optimal decoding of this code results in a performance that is better than the QAM1, QAM2 and the I-Q ST code with suboptimal decoding. This concludes that the I-Q 16-QAM ST code is able to give high coding and diversity gains to the ST system provided that good decoding algorithms are used to decode it.

All the designed codes were tested in channels whose characteristics are different from the channel for which they were designed, rapid fading channels. The first channel was a correlated fading channel with proper interleaving. The performance of all the designed codes was degraded slightly. The gains of the better codes over the worst codes were decreased slightly. This shows that the designed codes can operate under slower fading channels not only under rapid fading channel.

The proposed codes were also tested for correlated fading channels with improper interleaving. The performance was degraded more than the previous case but with the same performance order. Again, the designed codes are robust to the channel environment and can operate, with slightly degraded performance, on different channels.

The practical case that incorporates the process of estimating the CSI at the receiver was also considered. In this case, the CSI were estimated using the OPSI method along with a Wiener interpolation filter to give reasonable CSI estimates. This test was applied to the QPSK codes over correlated fading channels, with proper and improper interleaving. The same order in the performance was noticed with a more degradation in the I-Q QPSK ST code. This is because of the increased unreliability of the suboptimal decoding algorithm used when CSI estimation is not exact.

5.2 Future Research

- The performance of ST codes over rapid and Quasi-static fading channels was evaluated. A tighter upper bound on the bit error probability over quasi-static channels can be derived and evaluated.
- As was proved, the performance of the I-Q ST codes can be improved if a better decoding algorithm is devised. So, a more reliable decoding algorithm to estimate the Q/I components in the I/Q decoders is essential to the use of I-Q ST codes, especially with systems that have one receive antenna.
- The design of ST codes that output symbols at the transmit antennas, where these symbols are from a subset of the N-dimensional signal space. This can be applied to

QPSK codes with a 2/3 encoder is used to output one of 2^3 symbols of the 2-dimensional QPSK signal space. Also, a 4/5 encoder can be used instead of the 4/8 encoder in the 16-QAM ST code. This approach is expected to increase the Euclidean distance of the code and hence improves the ST-MTD and ST-MSPD of the new ST code.

- The designed codes may be tested over frequency-selective channels and their performance can be evaluated for this case. The use of equalization techniques to reduce the effect of multipath reception may be considered.
- Also, the generalization of ST block codes (STBC) for any transmit antenna proposed in [23] may be used in the generation of the orthogonal pilot sequences to be used to estimate the CSI of the ST system at the receiver. By using this method, orthogonal sequences can be generated for any number of transmit antennas and not constrained to the constant-envelop constellations as proposed in [14] and [15].
- The geometrically uniform trellis codes can be used to design ST codes with less complicated decoding algorithms and easier expressions to evaluate their performance.

Appendix

The performance criteria of ST codes over rapid fading channels derived in [1] is derived in details in this Appendix. The squared Euclidean distance in (2.8) can be expressed in matrix notation as:

$$d^2_E(C_l,\hat{C}_l) = E_s \sum_{t=1}^{l} \sum_{j=1}^{M} \Omega_{j,t} A_t \Omega_{j,t}^T \qquad (A.1)$$

Where $\Omega_{j,t} = [\alpha_{1j,t}\ \alpha_{2j,t} \ldots\ldots \alpha_{Nj,t}]_{1xN}$. The matrix A_t is an NxN matrix with $A_t = \underline{c}_t \cdot \underline{c}_t^{T^*}$, and $\underline{c}_t^T = [(c^1_t - \hat{c}^1_t)\ (c^2_t - \hat{c}^2_t) \ldots (c^N_t - \hat{c}^N_t)]$, and $\underline{c}_t^{T^*}$ is the conjugate transpose of $\underline{c}_t$, i.e:

$$A_{pq,t} = (c^p_t - \hat{c}^p_t).(c^q_t - \hat{c}^q_t) \qquad (A.2)$$

Using similarity transformation to convert A_t into diagonal matrix D_t with diagonal elements as its eigenvalues and a unitary matrix containing the set of orthonormal eigenvectors of the matrix A_t as,

$$V_t A_t V_t^{T^*} = D_t, \qquad (A.3)$$

With $D_t = \text{diag}\{\lambda_{1,t}, \lambda_{2,t}, \ldots\ldots, \lambda_{N,t}\}_{NxN}$ and $V_t = [v_{1,t}\ v_{2,t} \ldots\ldots v_{N,t}]^T_{NxN}$

Where $v_{i,t}$ is a Nx1 vector indicating the i^{th} orthonormal eigenvector of the matrix A_t, i.e: the mean square of the N elements of $v_{i,t}$ is normalized to one. Since V_t is a unitary matrix, it is a full-rank matrix and its inverse is its transpose, i.e: $V_t^{-1} = V_t^{T^*}$. Using this property of V_t and using Equation (A.3), Equation (A.1) can be written as:

$$d^2_E(C_l,\hat{C}_l) = E_s \sum_{t=1}^{l} \sum_{j=1}^{M} \Omega_{j,t} V_t^{T^*} D_t V_t \Omega_{j,t}^{T^*} \qquad (A.4)$$

By defining: $B_{j,t} = [\beta_{1j,t}\ \beta_{2j,t}\ \ldots\ldots \beta_{Nj,t}] = \Omega_{j,t}.V_t^{T^*}$

$= [\alpha_{1j,t}\ \alpha_{2j,t}\ \ldots\ldots \alpha_{Nj,t}] \times [v_{1,t}\ v_{2,t}\ \ldots\ldots\ v_{N,t}]^{T^*}$, Equation (A.4) becomes:

$$d^2_E(C_l,\hat{C}_l) = E_s \sum_{t=1}^{l} \sum_{j=1}^{M} B_{j,t} D_t B_{j,t}^{T^*} \tag{A.5}$$

Since $D_t = \mathrm{diag}\{\lambda_{1,t}, \lambda_{2,t}, \ldots\ldots, \lambda_{N,t}\}$, then (A.5) simplifies to:

$$d^2_E(C_l,\hat{C}_l) = E_s \sum_{t=1}^{l} \sum_{j=1}^{M} \sum_{i=1}^{N} |\beta_{ij,t}|^2 \lambda_{i,t} \tag{A.6}$$

The $|\beta_{ij,t}|$'s represent the channel coefficients from the i^{th} transmit antenna to the j^{th} receive antenna multiplied by the orthonormal set of eigenvectors of A_t. So, the probability distribution of $\beta_{ij,t}$'s is the same as that of the $\alpha_{ij,t}$'s. When the channel is assumed to be independent Rayleigh fading channel, $\alpha_{ij,t}$'s are samples of complex Gaussian random process with $E(|\alpha_{ij,t}|)=0$, and $E(|\alpha_{ij,t}|^2)=E(|\beta_{ij,t}|^2)=1$ in both dimensions. Hence, the pdf of each of the $|\beta_{ij,t}|$'s is:

$$f_\beta(|\beta_{ij,t}|) = 2|\beta_{ij,t}| \exp(-|\beta_{ij,t}|^2) \tag{A.7}$$

Substituting (A.7) in the expression of the conditional pairwise error probability, $P(C_l,\hat{C}_l)$ yields:

$$P(C_l,\hat{C}_l\,|\beta_{ij,t}) \le \prod_{t=1}^{l} \prod_{j=1}^{M} \exp\left(-(E_s/4N_o) \sum_{i=1}^{N} \lambda_{i,t} |\beta_{ij,t}|^2\right) \tag{A.8}$$

In order to find an upper bound on $P(C_l,\hat{C}_l)$, it should be averaged with respect to $f(|\beta_{ij,t}|)$ as follows[1]:

$$P(C_l,\hat{C}_l) \le \prod_{t=1}^{l} \prod_{j=1}^{M} f_\beta(|\beta_{ij,t}|) \exp\left(-(E_s/4N_o) \sum_{i=1}^{N} \lambda_{i,t} |\beta_{ij,t}|^2\right) \tag{A.9}$$

Doing this for independent Rayleigh channels results in the following expression:

$$P(C_l,\hat{C}_l) \le \prod_{t=1}^{l}\prod_{i=1}^{N} \left(1+\lambda_{i,t}\,(E_s/4N_o)\right)^{-M} \qquad (A.10)$$

Since the matrix A_t is the product of two vectors, and since the rank of each vector is one, then A_t has a unity rank if $c_t \neq \hat{c}_t$ and rank zero otherwise, where $c_t = (c^1{}_t\, c^2{}_t \ldots c^N{}_t)$. Hence, the eigenvalues of A_t are all zero except one which is the summation of the diagonal terms of A_t, $|c_t - \hat{c}_t|^2$. The pairwise error probability can be written as:

$$P(C_l,\hat{C}_l) \le \prod_{t\in\eta} \left(1+ |c_t - \hat{c}_t|^2\,(E_s/4N_o)\right)^{-M} \qquad (A.11)$$

With: $$|c_t - \hat{c}_t|^2 = \sum_{i=1}^{N} |c^i{}_t - \hat{c}^i{}_t|^2 \qquad (A.12)$$

Where $\eta = \{t: c_t \neq \hat{c}_t\}$, which is the set of time instances $1<t<l$ in which $|c_t - \hat{c}_t| \neq 0$.

Nomenclature

Abbreviations

ISI	Inter-Symbol Interference
SNR	Signal-to-Noise Ratio
ST	Space-Time
I-Q	Inphase-Quadrature
FF	Fast Fading
SF	Slow Fading
FS	Frequency Selective
FNS	Frequency Non-Selective
pdf	Probability Density Function
CSI	Channels State Information
DFE	Decision Feedback Equalizer
MLSE	Maximum Likelihood Sequence Equalizer
EGC	Equal Gain Combining
MRC	Maximal Ratio Combining
SC	Selective Combining
AWGN	Additive White Gaussian Noise
FDM	Frequency Division Multiplexed

TDM	Time Division Multiplexed
MTD	Minimum Time Diversity
MSPD	Minimum Squared Product Distance
HD	Hamming Distance
SPD	Squared Product Distance
ST-MTD	ST Minimum Time Diversity
ST-MSPD	ST Minimum Squared Product Distance
ST-SPD	ST Squared Product Distance
erfc	Complementary Error Function
MTCM	Multiple Trellis Coded Modulation
RS	Reed-Solomn
BER	Bit Error Rate
FER	Frame Error Rate
OPSI	Orthogonal Pilot Signal Insertion
PSAM	Pilot Signal Assisted Modulation
PSK	Phase Shift Keying
MPSK	Multiple Phase Shift Keying
QPSK	Quadrature Phase Shift Keying
AM	Amplitude Modulation
16-QAM	Quadrature Amplitude Modulation with 16 signals
OFDM	Orthogonal Frequency Division Multiplexed
LST	Layered Space-Time
STBC	Space-Time Block Codes

MAP	Maximum A posteriori Probability
MSE	Mean Squared Error
MMSE	Minimum Mean Squared Error
Rx	Receive
STr	Super-Trellis
AFC	Automatic Frequency Control
FIR	Finite Impulse Response
S/P	Serial-to-Parallel converter

Symbols

E_s	Signal energy
N_o	noise power at one receive antenna
N	number of transmit antennas
M	number of receive antennas
$(\Delta t)_c$	Coherence time
$(\Delta f)_c$	Coherence frequency
T_m	Multi-path spread
f_D	Doppler spread
d^2_E	squared Euclidean Distance
d^2_P	squared Product Distance
L	shortest error event length
η	the set of time instance having different signals in an error event

l_η	length of en error event
v	number of memory elements in the trellis encoder
E[x]	expected value of randome variable x
$E[x^2]$	mean square of random variable x
P_b	bit error probability
P_e	error event probability
$f_a(a)$	probability density function of variable a
S_i	state i in a trellis encoder
S_I	state of the I-encoder in I-Q systems
S_Q	state of the Q-encoder in I-Q systems
J_o	Bessel function of zero order of the first kind
P_t^i	orthogonal pilot sequence at the i^{th} transmit antenna
S^{lk}	set of possible signals at an I-Q ST decoder when I-encoder outputs lk
M_{lk}	surviving metric of signals in the set S^{lk}
$\alpha_{ij,t}$	fade sample from the i^{th} transmit to the j^{th} receive antennas at time t
$\alpha_{Iij,t}$	in-phase companent of $\alpha_{ij,t}$
$\alpha_{Qij,t}$	Quadrature companent of $\alpha_{ij,t}$
η_t^j	noise added at the j^{th} receive antenna at time t
λ_i	i^{th} eigenvalue of the matrix A
c_t^i	transmitted symbol over i^{th} tranmit antenna at time t
d_t^j	received signal at j^{th} receive antenna at time t
H	transition matrix of a trellis code

b_i	i^{th} bit at the output of the encoder
$\underline{b}^i$	i^{th} m-bit word at the output of the encoder transmitted at the i^{th} antenna
g_j	j^{th} k-bit input sequence to an encoder
$\underline{b}_j$	j^{th} n-bit output word corresponding to g_j
$\underline{e}_j$	j^{th} n-bit error word
$F(\underline{e}_j,D)$	error weight profile due to error word $\underline{e}_j$
$P(C_l,\hat{C}_l)$	pairwise error probability between sequences C_l and $\hat{C}_l$ of length l

Bibiliography

[1] V. Tarokh, N. Seshadri and A.R. Calderbank, "Space-Time Codes For High Data Rate Wireless Communication: Performance Criterion and Code Construction," *IEEE Trans. Info. Theory*, March 98.

[2] N. Seshadri, V. Tarokh and A.R. Calderbank, "Space-Time Codes For High Data Rate Wireless Communication: Code Construction," *Proc. IEEE VTC'97.*

[3] Sklar, "Rayleigh Fading Channels in Mobile Digital Communication Systems Part II: Mitigation," *IEEE Comm. Magazine*, Sep. 1997.

[4] J. Poakis, *Digital Communications.* New York: McGraw-Hill, Inc., 1989.

[5] W. Kuo and M. Fitz, "Design and Analysis of Transmitter Diversity Using Intentional Frequency Offset for Wireless Communications," *IEEE Trans. on Veh. Tech.*, Nov. 1997.

[6] S. H. Jamali and T. Le-Ngoc, *Coded-Modulation Techniques for Fading Channels.* Massachusetts: Kluwer Academic Publisher, 1994.

[7] G. Femenias and R. Agust, "Combined Space Diversity Reception and Trellis Coding for Rayleigh Fading Channels," *Wireless Personal Communications*, vol. 4, pp. 299-314, 1997.

[8] S. Al-Semari and T. Fuja, "Performance Analysis of Coherent TCM Systems with Diversity Reception in Slow Rayleigh Fading," *IEEE Trans. on Veh. Tech.*, Jan. 1999.

[9] A. Wittneben, "A New Bandwidth Efficient Transmit Antenna Modulation Diversity Scheme for Linear Digital Modulation," *Proc. IEEE ICC'93.*

[10] V. Tarokh, N. Seshadri and A.R. Calderbank, "Space-Time Codes For High Data Rate Wireless Communication: Performance Criterion," *Proc. IEEE ICC'97.*

[11] V. Tarokh, A. Naguib, N. Seshadri and A.R. Calderbank, "Low-rate Multi-dimensional Space-Time Codes For Both Slow and Rapid Fading Channels," *Proc. IEEE PIMRC'97.*

[12] A. Naguib, V. Tarokh, N. Seshadri and A.R. Calderbank, "A Space-Time Coding for High-Data-Rate Wireless Communications," *IEEE JSAC,* Oct. 98.

[13] A. Naguib, V. Tarokh, N. Seshadri and A.R. Calderbank, "Space-Time Coded Modulation for High Data Rate Wireless Communications," *Proc. IEEE GLOBECOM'97.*

[14] V. Tarokh, A. Naguib, N. Seshadri and A.R. Calderbank, "Space-Time Codes for High Data Rate Wireless Communication: Mismatch Analysis," *Proc. IEEE ICC' 97.*

[15] D. Agrawal, V. Tarokh, A. Naguib and N. Seshadri, "Space-Time Coded OFDM for High Data-Rate Wireless Communication Over Wideband Channels," *Proc. IEEE VTC'98.*

[16] V. Tarokh, A. Naguib, N. Seshadri and A.R. Calderbank, "Combined Array Processing and Space-Time Coding," *IEEE Trans. On Info. Theory,* May 99.

[17] V. Tarokh, A. Naguib, N. Seshadri and A.R. Calderbank, "Space-Time Codes for High Data Rate Wireless Communication: Performance Criteria in the Presence of Channel Estimation Errors, Mobility and Multiple Paths," *IEEE Trans. On Comm.,* Feb. 99.

[18] D. Shiu and J. Kahn, "Layered Space-Time for Wireless Communications Using Multiple Transmit Antennas," *Proc. IEEE ICC'99.*

[19] Gerhard Bauch, "Concatenation of Space-Time Block Codes and "Tubo"-TCM," *Proc. IEEE ICC'99.*

[20] Siavash Alamouti, "A Simple Transmit Diversity Technique for Wireless Communications," *IEEE JSAC,* Oct. 98.

[21] V. Tarokh, S. Alamouti and P. Poon, "New Detection Schemes for Transmit Diversity with no Channel Estimation," *Proc. IEEE Int. Conf. On Universal Personal Comm. '98.*

[22] S. Alamouti, V. Tarokh and P. Poon, "Trellis-Coded Modulation and Transmit Diversity: Design Criteria and Performane Evaluation," *Proc. IEEE Int. Conf. On Universal Personal Comm. '98.*

[23] V. Tarokh, H. Jafarkhani and A. Calderbank, "Space-Time Block Codes from Orthogonal Designs," *IEEE Trans. On Infor Theory,* July 1999.

[24] V. Tarokh, H. Jafarkhani and A. Calderbank, "Space-Time Block Codes for Wireless Communications: Perfromance Results," *IEEE JSAC,* March 1999.

[25] A. Nahuib, N. Seshadri and A. Calderbank, "Applications of Space-Time Block Coded and Interference Suppression for High Capacity and High Data Rate Wireless Systems," *The 32nd Asilomar Conf. On Signal, Systems and Computers'1998.*

[26] S. Al-Semari and T. Fuja, "I-Q TCm: Reliable Communication Over Rayleigh Fading Channel Close to the Cutoff Rate," *IEEE Trans. On Infor Theory,* Jan 1997.

[27] E. Zehavi and J. Wolf, "On the Performance Evaluation of Trellis Codes," *IEEE Trans. On Infor Theory,* March 1987.

[28] E. Dougherty, *Probability & Statistics for the Engineering, Computing & Physical Sciences.* New Jersy: Prentice Hall, Inc., 1990.

[29] E. Leonardo, L. Zhang and B.Vucetic, "Multidimensional M-PSK Trellis Codes for Fading Channels," *IEEE Trans. On Infor Theory,* July 1996.

[30] D. Divsalar and M. Simon, "The Design of Trellis Coded MPSK for Fading Channels: Set Partitioning for Optimum Code Design," *IEEE Trans. On Comm.,* Sep. 1988.

[31] J. McGreehan and A. Bateman, "Phase Locked Transparent Tone-in-Band (TTIB): A New Spectrum Configuration Particularly Suited to the Transmission of Data Over SSB Mobile Radio Networks," *IEEE Trans. On Comm.,* Jan. 1984.

[32] J. Cavers, "An Analysis of Pilot Symbol Assisted Modulation for Rayleigh Fading Channels," *IEEE Trans. On Vehicular Tech.,* Nov. 1991.

[33] J. Lodge and M. Moher, "Time Diversity for Mobile Satellite Channels using Trellis Coded Modulation," *IEEE Global Telecomm. Conf.,* 1987.

[34] S. Sampei and T. Sunaga, "Rayleigh Fading Compensation Method for 16QAM in Digital Land Mobile Radio Channels," in *Proc. IEEE Vech. Tech. Conf.*, May 1989.

[35] J. Cavers, "An Analysis of Pilot Symbol Assisted 16QAM for Digital Mobile Communications," *Proc. GLOBECOM'90.*

[36] J. Cavers, "An Analysis of Pilot Symbol Assisted QPSK for Digital Mobile Communications," *Proc. IEEE Vech. Tech. Conf.*, 1991.

[37] M. Srinath, P. Rajasekaran and R. Viswanathan, *Introduction to Statistical Signal Processing with Applications.* New Jersy: Prentice Hall, Inc., 1996.